AWARD NUMBER: W81XWH-14-1-0479

TITLE: ING4 Loss in Prostate Cancer Progression

PRINCIPAL INVESTIGATOR: Cynthia K Miranti

CONTRACTING ORGANIZATION: University of Arizona
Tucson, AZ 85724-5024

REPORT DATE: October 2018

TYPE OF REPORT: Annual

PREPARED FOR: U.S. Army Medical Research and Materiel Command
Fort Detrick, Maryland 21702-5012

REPORT DOCUMENTATION PAGE

Form Approved
OMB No. 0704-0188

1. REPORT DATE	2. REPORT TYPE	3. DATES COVERED
October 2018	Annual	9/23/2017 to 9/22/2018

4. TITLE AND SUBTITLE

ING4 Loss in Prostate Cancer Progression

5a. CONTRACT NUMBER

5b. GRANT NUMBER
W81XWH-14-1-0479

5c. PROGRAM ELEMENT NUMBER

6. AUTHOR(S)

Cynthia Miranti, PhD

E-Mail: cmiranti@email.arizona.edu

5d. PROJECT NUMBER

5e. TASK NUMBER

5f. WORK UNIT NUMBER

7. PERFORMING ORGANIZATION NAME(S) AND ADDRESS(ES)

UNIVERSITY OF ARIZONA
ARIZONA BOARD OF REGENTS
888 N EUCLID AVE RM 510
TUCSON AZ 85719-4824

8. PERFORMING ORGANIZATION REPORT NUMBER

9. SPONSORING / MONITORING AGENCY NAME(S) AND ADDRESS(ES)

U.S. Army Medical Research and Materiel Command
Fort Detrick, Maryland 21702-5012

10. SPONSOR/MONITOR'S ACRONYM(S)

11. SPONSOR/MONITOR'S REPORT NUMBER(S)

12. DISTRIBUTION / AVAILABILITY STATEMENT

Approved for Public Release; Distribution Unlimited

13. SUPPLEMENTARY NOTES

14. ABSTRACT

The goal of this project is to identify specific differentiation events controlled by ING4, whose disruption by combined Myc/PTEN loss leads to aggressive PCa. Our three Aims are to 1) determine how ING4 controls prostate epithelial differentiation, 2) determine how loss of ING4 impacts tumorigenesis, and 3) determine how loss of ING4 in patients relates to tumor progression. To date we have published 4 papers as a result of these studies that address these aims. In those papers we demonstrate: 1) ING4, downstream of Myc is required for luminal cell differentiation, ING4 loss is required for Myc-dependent oncogenesis, and ING4 expression is lost in ~60% of primary PCa tumors. This is the first time ING4 has been linked to differentiation and its loss reported in prostate cancer. 2) Myc, via p38-MAPK, drives luminal cell differentiation by inducing Notch3 mRNA transcription and stability. This is the first study to demonstrate the importance and mechanisms of Notch3 induction in luminal cell differentiation. 3) Miz1, which is absent in tumor cells, is an ING4 target that is required to suppress integrin a6b1 in normal luminal cells, which explains how integrin a6b1 can be retained in tumor cells when ING4/Miz1 is lost. 4) We developed more robust Tet-inducible shRNA vectors, which are available to the entire research community. Additional major findings not yet published include 1) JFK, an E3-ligase for ING4, is transcriptionally controlled by ING4 itself, 2) PTEN sets the timing for ING4 expression and 3) ING4 loss is highly correlated with PTEN loss and Gleason grade in human tissues.

15. SUBJECT TERMS

Prostate epithelial differentiation, Myc, ING4, chromatin, integrins, Erg, Pten, Miz1, JFK, CREB, Notch, p38, prostate cancer oncogenesis, TMA, mouse model, human model.

16. SECURITY CLASSIFICATION OF:			17. LIMITATION OF ABSTRACT	18. NUMBER OF PAGES	19a. NAME OF RESPONSIBLE PERSON
a. REPORT	b. ABSTRACT	c. THIS PAGE			USAMRMC
Unclassified	Unclassified	Unclassified	Unclassified	86	19b. TELEPHONE NUMBER *(include area code)*

Table of Contents

Page

INTRODUCTION: Being able to determine which PCa patients have indolent disease and require minimal treatment, versus those who will die unless aggressively treated, remains a major challenge. The goal of this project is to test the **hypothesis** that Myc normally promotes prostate epithelial differentiation through chromatin remodeling mediated by ING4, such that loss of ING4 is required for Myc oncogenesis, which leads to aggressive disease through suppression of differentiation. Our specific aims are: Aim 1: Determine how ING4 controls prostate epithelial differentiation. We hypothesize that Myc normally promotes prostate epithelial differentiation through chromatin remodeling mediated by ING4. Aim 2: Determine how loss of ING4 impacts tumorigenesis. We hypothesize that loss of ING4 cooperates with specific oncogenes to disrupt terminal differentiation, which is required for aggressive tumorigenesis. Aim 3: Determine how loss of ING4 in patients relates to tumor progression. Our hypothesis is that ING4 loss will predictive of aggressive/lethal disease. Our objectives are to 1) establish if there is a correlation between ING4 loss and over expression of Myc, Erg fusions, or Pten loss, and the relationship to disease recurrence in patients; and 2) determine how ING4 expression correlates with the expression of known differentiation markers in the tumors.

KEYWORDS: Prostate epithelial differentiation, Myc, ING4, chromatin, integrins, Erg, Pten, Miz1, CREB, Notch, p38, prostate cancer oncogenesis, TMA, mouse model, human model.

ACCOMPLISHMENTS:

What were the major goals of the project?

Goals	**Percent Complete**
Aim 1: Determine how ING4 controls prostate epithelial differentiation	
Milestones:	
Task 1: Identify ING4 and Myc Targets (6 months)	100%
Task 2: Determine relationship between ING4 and EZH1/2 (12 months)	100%
Prepare manuscript for publication	100%
Task 3: Identify Global ING4 targets by RNA-Seq and ChIP-Seq (36 months)	50%
Prepare manuscript for publication	100%
Aim 2: Determine how loss of ING4 impacts tumorigenesis	
Milestones:	
Task 4: Demonstrate Blocking ING4 Promotes Tumorigenesis (15 months)	100%
Task 5: Measure Oncogenic Control of ING4 Expression (15 months)	100%
Prepare manuscript for publication	50%
Task 6: ING4 Loss and Myc Cooperation in Tumorigenesis (30 months)	50%
Prepare manuscript for publication	50%
Aim 3: Determine how loss of ING4 in patients relates to tumor progression	
Milestones:	
Task 7: Regulatory processes (3 months)	100%
Task 8: ING4 Loss vs Outcome and Oncogenic Events (18 months)	30%
Task 9: ING4 Loss and Tumor Differentiation (36 months)	10%
Prepare manuscript for publication	0%

What was accomplished under these goals?

Aim 1: Determine how ING4 controls prostate epithelial differentiation

Myc and ING4 do not work together to regulate the expression of Myc targets, EZH1, EZH2, ODC, and cyclin D during luminal cell differentiation. We initially hypothesized that Myc and ING4 promote differentiation by cooperatively binding to the same gene targets. In our first approach, we found that although ING4 binds to and suppresses two known Myc targets, ODC and cyclin D1, Myc was not bound to these targets in differentiating cells. Similarly, we found that two other predicted Myc targets, EZH1 and EZH2, were not regulated by ING4 or Myc in differentiating cells. Thus, we ruled out our original hypothesis. However, we were much more successful at identifying ING4 and Myc targets using the data we obtained from our RNA-Seq studies.

Myc controls Notch3 induction during luminal cell differentiation via p38-MAPK, but independent of ING4. In the first RNA-Seq approach we investigated the relationship between p38-MAPK, Myc, and differentiation. Using an RNA-Seq technique which measures newly synthesized RNA, called Bru-Seq, we compared untreated to 7-hour doxycycline-treated cells expressing a constitutive active form of the p38 activator MKK6. From our analysis we identified Notch3 as one of our top 6 targets. In our published paper from these studies (**Frank, 2017, J Cell Sci, Appendix**), we demonstrate that blocking p38α, p38δ, Notch1, or Notch3 greatly impairs differentiation and causes luminal cell death. Constitutive p38-MAPK activation by MKK6 increases NOTCH3 (but not NOTCH1) mRNA/protein levels and is diminished upon MYC inhibition. Furthermore, we validated two NOTCH3 enhancer elements by a combination of eRNA detection (BruUV-seq) and luciferase reporter assay. Lastly, we found that NOTCH3 mRNA half-life increases during differentiation or upon acute p38-MAPK activation. These results reveal a new connection between p38-MAPK, MYC, and NOTCH3 signaling, demonstrate two new mechanisms of NOTCH3 regulation, and provide evidence for NOTCH3 involvement in prostate luminal cell differentiation via Myc. We also found that Myc-induction of Notch3 does not dependent on ING4, suggesting these are two independent but necessary pathways for luminal cell differentiation. **Based on these studies, we conclude that even though Myc is required for ING4 and Notch3 induction, Myc is not required for the downstream functions of ING4 or Notch3.** Our current model suggests that loss of Myc-induced targets, such as ING4 and Notch3 are likely required for oncogenesis driven my Myc. Our data demonstrate this is true for ING4 (**Berger, 2014, Cancer Res, Appendix**), but future studies will be required to determine if loss of Notch3 is also required for oncogenesis.

Miz1, a direct target of ING4 induced during luminal cell differentiation, can suppress integrin α6 and β1 expression in luminal cells. In the second RNA-Seq approach, we compared the gene expression changes over time during normal luminal cell differentiation using RNA-Seq. First, we saw many of the same regulated genes in the normal cells as we saw in the BruUV-Seq data we obtained above, helping to assure us of the validity of the targets. From the RNA-Seq data we identified Miz1, a Myc repressor, as another ING4 target. Miz1 was previously shown to suppress integrin α6 and β1 transcription in supra-basal cells (Gebhardt et al., 2006). We measured integrin mRNA during differentiation and found that integrin α3 and β4 were turned off 4 days before integrin α6 or β1 (**Fig. 1**). This supported our previous data based on immunostaining (Lamb et al., 2010).

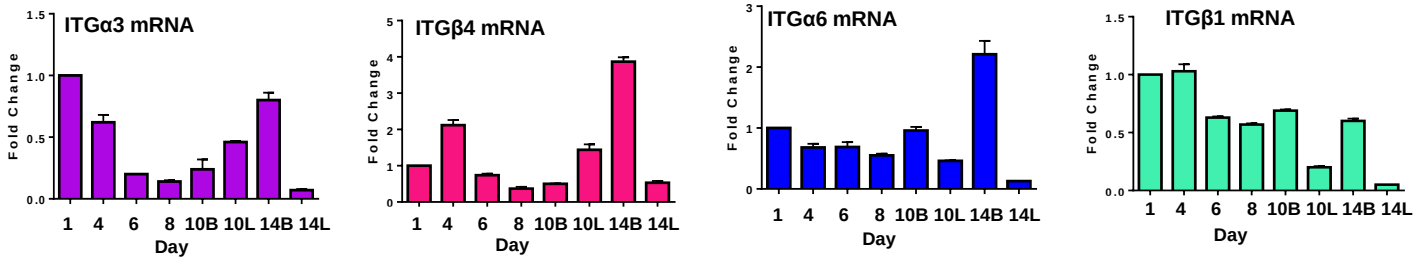

Fig. 1: Integrin mRNA expression during differentiation. PrECs were differentiated in vitro for indicated number of days, mRNA isolated from basal (B) or luminal (L) cells, and levels of integrins α3, β4, α6, and β4 assessed by qRT-PCR. Two distinct patterns emerged, integrin α3 and β4 mRNAs were lost within the first 6 days of differentiation, while integrin α6 and β1 mRNAs did not decrease until day 10 in the luminal cells.

Loss of integrin α3 and β4 coincides with Myc and Notch3 induction, while loss of integrin α6 and β1 coincides with ING4 expression. We hypothesized that Miz1, induced by ING4 is required to suppress integrin α6 and β1 in luminal cells. In our published paper from these studies (**Berger, 2017, Prostate, Appendix**), we demonstrate that ING4 directly binds the Miz1 promoter and is required to induce Miz1 mRNA and protein expression during luminal cell differentiation. Miz1 mRNA is not induced in shING4 expressing cells, or in tumorigenic cells which fail to express ING4. Miz1 dependency on ING4 was unique to differentiating luminal cells; Miz1 mRNA expression was not induced in basal cells. Although Miz1 is a direct target of ING4, and its overexpression drives luminal cell differentiation, by suppressing integrin α6 and β1, Miz1 was not absolutely required for differentiation. **Based on these studies, we conclude that Miz1/ING4 cooperative work together to suppress integrin α6 and β1 expression, but there are other mechanisms that cooperate with ING4 to suppress integrin α6 and β1.** These findings can in part explain why loss of ING4 in tumor causes the retention of integrin α6β1 and contributes to prostate cancer pathogenesis (Lamb et al., 2011).

CREB1/ATF1, and their potential targets Blimp1, Claudin1, are elevated specifically in luminal cells. In a third RNA-Seq analysis, we took all the significant hits (those which changed by 2x or more in the time course of luminal cell differentiation) and passed them through Gene-Go to determine which transcription factors could be responsible for driving the expression of those genes. In addition to finding Myc, p53, Sp1, and AR targets as expected, the factor that regulated the most genes was CREB1 (**Fig. 2A**). To validate these findings, we monitored CREB1 and ATF1 (CREB1-related) activation during differentiation. CREB1/ATF1 activity is induced during normal differentiation exclusively in the luminal cells (**Fig. 2B,C**). CREB1 activation peaks when ING4 is highest, while ATF1 activation is transient and peaks a few days earlier when ING4 is induced (**Fig. 2B**). ATF1 goes down when CREB1 activation peaks. These data suggest a sequential role for CREB1 and ATF1 specifically in luminal cells. We validated some of the predicted CREB targets, demonstrating that BLIMP1 and CLDN1 mRNA are dramatically induced at the same time CREB1 is activated in normal PrECs (**Fig. 2D**). We further validated protein expression, demonstrating PLK2 and Claudin1 kinetics mimic CREB1, while BLIMP1 kinetics mirrored ATF1 (**Fig. 2E**). Interestingly, of some these CREB1-induced genes, Claudin 1, are absent in the tumorigenic EMP cells, further supporting our overriding hypothesis that tumorigenic cells are defective in differentiation.

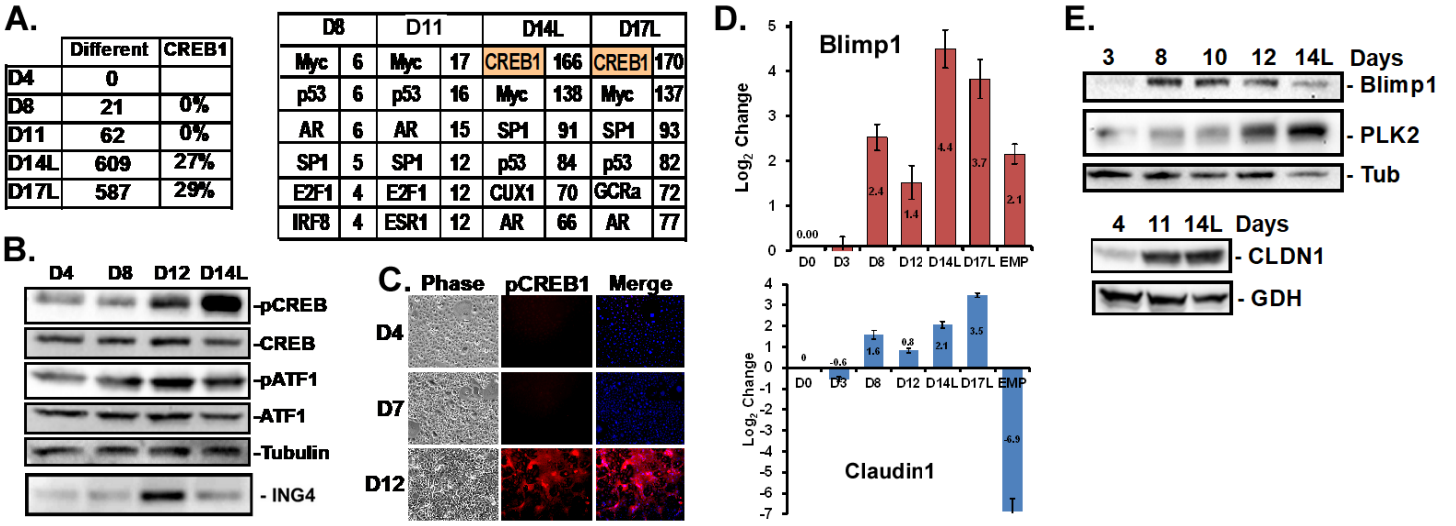

Fig. 2: CREB1 and ATF1 activation and their targets, including ING4, are specifically elevated in luminal cells during differentiation. A) Number of genes that are differentially expressed during indicated days (D) of luminal (L) cell differentiation. The transcription factors that regulate the expression of these genes. CREB1 is predicted to regulate the expression of ~30% of these genes. **B)** CREB1 and ATF1 activation (pCREB, pATF1) as measured by phospho-immunoblotting at different times during luminal cell differentiation compared to ING4 expression. **C)** Levels of active CREB1 (pCREB1) in iPrECs differentiated for indicated number of days detected by immuno-staining. CREB1 is only activated in the nuclei of differentiating luminal cells, starting at Day 12. **D)** Predicted CREB1 targets, Blimp1 and Claudin1 mRNA levels, measured by qRT-PCR during normal PrEC luminal cell

differentiation and in tumorigenic EMP cells. **E)** Expression of BLIMP1, PLK2, and Claudin1 (CLDN1) as measured by immunoblotting at indicated days of differentiation. D = days, L = luminal cells.

CREB1 suppresses, while ATF1 induces, ING4 expression. To determine whether CREB1 or ATF1 control ING4 expression, we engineered PrECs to express Tet-inducible shRNAs targeting CREB1 or ATF1 (**Fig. 3B,D**). Knocking down CREB1 upon doxycycline treatment, appeared to initially accelerate differentiation, i.e. supra-basal cells appear earlier (**Fig. 3A**), but closer examination revealed that these supra-basal cells were dying based on caspase 3 immunostaining. Knock-down of ATF1, on the other hand, prevented differentiation, resulting in cells that contain both basal (integrin α6) and luminal markers (AR) (**Fig. 3C**). This latter phenotype is exactly what happens when oncogenes, such as loss of PTEN and overexpression of Myc, (i.e. EMP cells), suggesting that disruption of ATF1 may also be important in oncogenesis since its loss prevents differentiation.

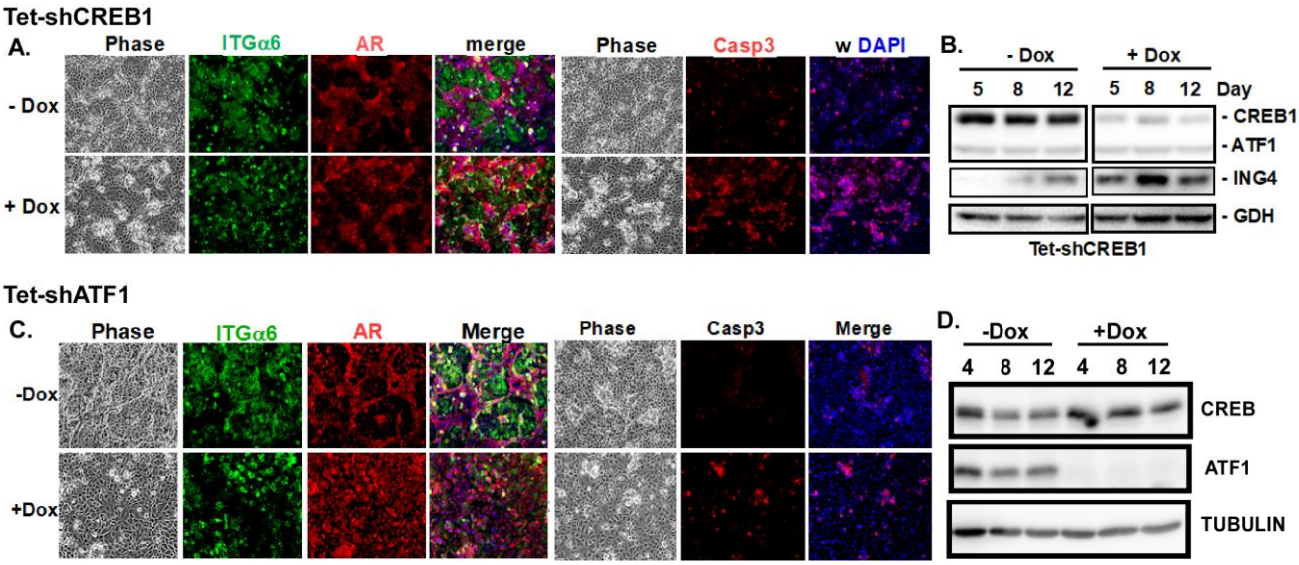

Fig. 3: CREB1 and ATF1 have opposing functions. Normal iPrEC were engineered to express Tet-inducible (Dox) shRNA to either CREB1 (A,B) or ATF1 (C,B). **A)** Tet-shCREB1 cells were differentiated for 10 days in the absence of presence of Doxycycline to induce CREB1 shRNA expression. **B)** Validation that the shRNA inhibits CREB1 and not ATF1 by immunoblotting. **C)** Tet-shATF1 cells were differentiated for 10 days in the absence of presence of Doxycycline to induce ATF1 shRNA expression. **D)** Validation that the shRNA inhibits ATF1 and not CREB1 by immunoblotting

The phenotype observed upon loss of CREB1, i.e. enhanced supra-basal cell formation accompanied by cell death, phenocopies that seen when ING4 is overexpressed (**Berger, Cancer Research, 2014, Appendix**), and the ATF1 knocked down phenocopies loss of ING4. This led us to investigate the effect of CREB1/ATF1 loss on ING4 expression. Loss of CREB1 resulted in early induction and enhanced expression of ING4, relative to normal iPrECs, and loss of ATF1 prevented ING4 induction (**Fig. 4A**). Promoter analysis of ING4 revealed the presence of a canonical CREB1 binding site (CRE), and we were able chromatin immunoprecipitated (ChIP) CREB1/ATF1 (antibody recognizes both, so we can't distinguish which one) on the ING4 promoter (**Fig. 4B**) at Day 10 (when ING4 is induced), but not Day 3 (when ING4 is not expressed). In cells constitutively expressing ING4, CREB could be detected bound to the ING4 promoter at Day 3. This latter finding suggests that ING4 itself may control/permit CREB1 binding to its promoter. Our working model on how ATF1 and CREB1 control the Myc/ING4 differentiation switch is depicted in **Figure 4C**. **Altogether these data indicate that ATF1 and CREB1 have opposing functions in regulating ING4, with ATF1 being required for ING4 expression, while CREB1 is required to suppress ING4 expression**.

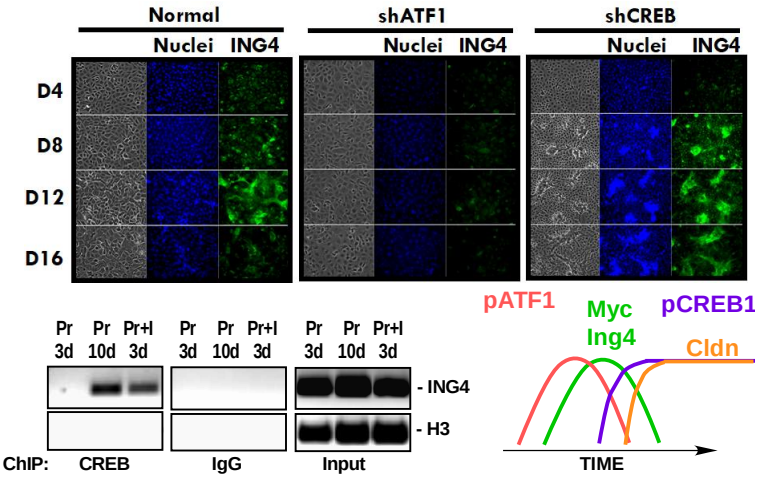

Fig. 4: CREB1 negatively regulates ING4, ATF1 positively regulates ING4. A) Normal PrECs or PrECs expressing Tet-inducible shATF1 or shCREB were differentiated for the indicated number of days (D) in the absence (Normal) or presence of doxycycline (shATF1, shCREB1) and levels of ING4 expression measured by immunostaining. Phase and nuclear staining shown for comparisons. **B)** ChIP of CREB bound to the ING4 promoter in normal PrECs (Pr) and PrECs overexpressing ING4 (Pr+I) at days 3 and 10 (3d, 10d) of differentiation. **C)** Proposed model, whereby ATF1 is required for Myc/ING4 expression, and CREB1 is required to turn off ING4 and induce Claudin (Cldn) and other terminal differentiation genes.

ING4 suppresses its own expression by activating its own E3-ligase, JFK. To identify other mechanisms for how ING4 expression can be regulated, we scanned our RNA-Seq data for expression of a known ING4 E3-ligase JFK (Yan *et al.*, 2015). The kinetics of JFK mRNA induction mirrored that of ING4, rising at Day 8 and peaking in luminal cells. Interestingly, JFK was not induced in the tumorigenic EMP cells, ruling out JFK induction as a mechanism for how ING4 loss could occur in tumors (**Fig. 5A,B**). We found both ING4 and CREB1/ATF1 bound to the JFK transcriptional start site and CREB-binding element (CRE) in the JFK promoter respectively (**Fig. 5C,D**). CREB1 was constitutively bound to JFK at Day 3, and decreased some around Day 10, while ING4 binding did not occur until ING4 was induced at Day 10. Overexpression of ING4 resulted in increased ING4 binding to the JFK start site as is expected for a direct target (**Fig. 5D**), and of course knocking down ING4 prevents its binding. However, ING4 over expression suppressed CREB1/ATF1 binding at the JFK promoter, suggesting ING4 limits the ability of CREB1/ATF1 to induce JFK or change how JFK is induced (**Fig. 5C**). From these data we propose a model (**Fig. 5E**), whereby **ING4 is initially transcriptionally induced by ATF1, and ING4 feeds back on itself to limit its own expression by two mechanisms: 1) enhancing CREB1 binding to the ING4 promoter to suppress its transcription, and 2) enhancing CREB1 binding to induce JFK to activate its own E3-ligase to degrade ING4 protein.**

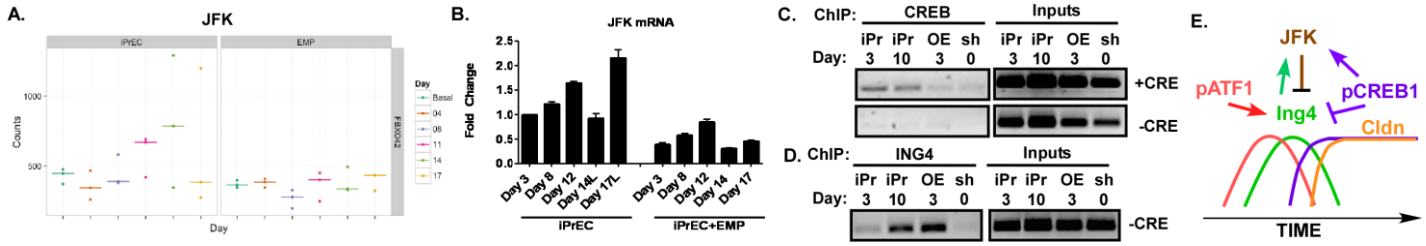

Figure 5: CREB binds the ING4 promoter, and CREB and ING4 bind the promoter of ING4's own E3 ligase, JFK. A) RNA-Seq reads in triplicate demonstrating increased JFK expression at Day 11 and 14 in normal differentiating cells (iPrEC), but not in tumorigenic EMP cells. **B)** JKF mRNA levels in differentiating PrECs over time (D = days) and in tumorigenic EMP cells. L = luminal cells as measured by qRT-PCR. **C)** ChIP of CREB bound to the CRE element (CRE) and not bound to non-CRE element (-CRE) in the JFK promoter of normal PrECs (Pr) and PrECs overexpressing ING4 (Pr+I) at days 3 and 10 (3d, 10d) of differentiation. **D)** ChIP of ING4 bound to a non-CRE element in the JFK promoter of normal PrECs (Pr), PrECs overexpressing ING4 (Pr+I), or PrECs expressing ING4 shRNA (sh) at days 0, 3, and 10 (0, 3d, 10d) of differentiation. **E)** Model for CREB/ATF1 regulation of ING4 via JFK.

PTEN protein phosphatase activity controls the timing of CREB1 activation. During differentiation, PTEN is elevated early (**Fig. 6A**), but decreases after ING4 is induced and CREB1 becomes active (after day 10). A decrease in PTEN results in elevated Akt activity due to loss of lipid phosphatase activity, and Akt is a potent activator of CREB1 (Caravatta et al., 2008). However, PTEN can also use its protein phosphatase activity to dephosphorylate and inactivate CREB1 (Gu et al., 2011; Lyu et al., 2015). To decipher which mechanisms are involved in differentiation, we obtained 2 PTEN dominant acting mutants, one which

inactivates the lipid phosphatase activity (G129E) and one that inactivates both the lipid and protein phosphatase (C124S) activity. When we overexpress these mutants during differentiation (**Fig. 6B**), we find that blocking only the protein phosphatase activity (C124S), but not the lipid phosphatase (G129E), unexpectedly results in constitutive CREB1/ATF1 activation as early as 4 days after differentiation, before it is detectable in normal PrECs (**Fig. 6C**). Somewhat contradictory to our model, we also observed an increase in ING4 expression when "CREB1" is active (**Fig. 6C**) and these cells still differentiate (**Fig. 6D**). In fact, they differentiate more rapidly in 4x less differentiation medium (**Fig. 6D**). Our interpretation of these apparent conflicting data is that PTEN dephosphorylates CREB1, but not ATF1 (which we cannot distinguish with this antibody), which remains active to drive ING4 expression, and it is not countered by CREB1-mediated down regulation. Additional experiments are required to fully test this idea. A model depicting the intersection of PTEN with ING4 is shown (**Fig. 6E**). **The the protein phosphatase activity of PTEN is critical for the timing of when CREB1 and ATF1 becomes activated to induce, yet limit, ING4 expression.**

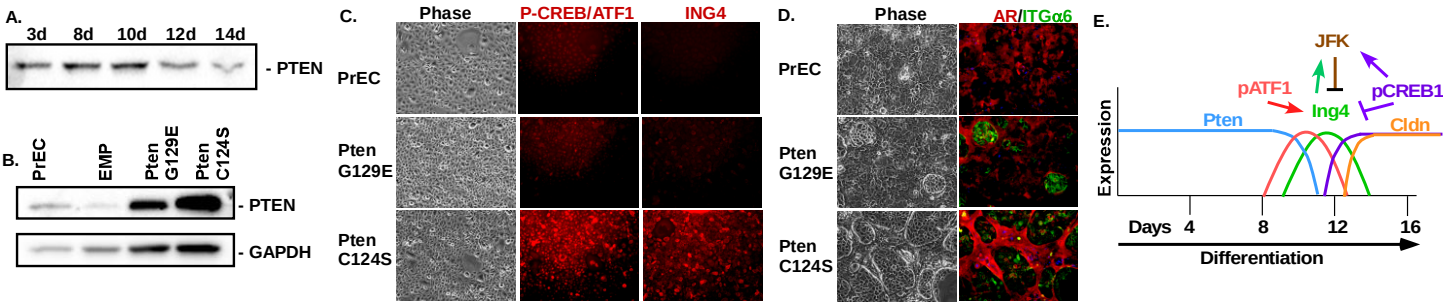

Figure 6: PTEN protein phosphatase activity sets the timing of differentiation, CREB activation, and induction of ING4. A) Pten expression was measured by immunoblotting of PrECs differentiated for 3, 8, 10, 12 or 14 days (d). **B)** PTEN expression was measured by immunoblotting of normal PrECs, EMPs, or PrECs overexpressing Pten mutants G129E or C124S. **C)** Activated CREB/ATF1 (P-CREB) and ING4 levels were measured by immunostaining normal PrECs and PTEN mutant cell lines differentiated for 4 days. **D**) Differentiation is accelerated in the lipid/protein phosphatase mutant (C124S) under suboptimal levels of differentiation factors. Differentiation was measured by immunostaining for AR in the luminal layer (red) and integrin α6 (green) in the basal layer. Many more luminal cells with more robust AR staining was observed in the C124S mutant cells. **E)** Model for how PTEN sets the timing for ATF1/CREB1 activation at the ING4 chromatin switch.

One incomplete task. One of the original goals for this Aim (Task3) was to use ChIP-Seq to globally identify the genes that ING4 interacts with to better understand the extent and mechanisms by which ING4 drives differentiation. We collaborated with Dr. Suwon Kim at TGEN who has expertise in ING4 ChIP. Unfortunately, we were unable to interpret any of the sequencing data. We are not sure what caused the problem. We initially blamed the ING4 antibody, but since we were able to ChIP ING4 on single genes, we don't think this was the primary problem. We suspect it had something to do with the sequencing, where we encountered poor communication and direction from the sequencing core at TGEN. We will revisit this approach in the future when more resources become available.

More efficient Tet-shRNA vectors. To analyze the requirement of a specific gene for luminal cell development in a human model that transfects poorly and takes over 2 weeks to develop, requires that we generate stable shRNA approaches using lentivirus. Because we are interested in genes that function at different stages of differentiation, we thought it prudent to use conditional shRNA expression to control when the protein is suppressed. At the time we initiated the studies the existing Tet-inducible shRNA lentiviral system, pLKO, had many limitations. Therefore, we put considerable effort into optimizing both the vector and its use. In our published paper on these vectors (**Frank, 2017, BMC Biotechnology, Appendix**), we describe the improvements, which include removal of the large stuffer that reduces cloning efficiency, use of an odd number of base pairs, 7 or 9, in the shRNA loop to prevent loop collapse, engineering plasmids with blast or hygro resistance, in addition to the puromycin, to be able to target several genes at once in the same cells, and use of immunoblotting to quickly screen expression of the Repressor in cells. The vector plasmids, as well those expressing specific shRNAs were deposited with Addgene to make them available to all researchers.

Aim 2: Determine how loss of ING4 impacts tumorigenesis

Loss of PTEN is responsible for ING4 loss in tumors. In our first publication from these studies (**Berger, Cancer Res, 2014, Appendix**), we showed that overexpression of Myc + Erg + PTEN loss (EMP) generates tumorigenic cells that lose ING4 expression and fail to differentiate *in vitro*. Of the three possible combinations of genes (Erg, Myc, PTEN loss), only combined constitutive Myc overexpression and PTEN loss (MP) produced tumors in mice. In these tumors, ING4 was also lost. Furthermore, preliminary studies outlined in Aim 3 below, demonstrated a high correlation between ING4 loss and PTEN loss in primary prostate cancer tissues. Thus, defining exactly how Myc overexpression and PTEN loss work together to suppress ING4 is a high priority.

Erg expression specifically in AR+ cells is crucial for its tumorigenic functions. We were disappointed that constitutive expression of Erg did not seem to effect proliferation or differentiation of the cells in vitro or in vivo. However, when we re-engineered Erg to be expressed under the control of the PSA ARE enhancer such that it is only expressed in the AR+ cells (**Fig. 7a**), as it occurs in prostate cancer, luminal cells initially appear, but then disappear (**Fig. 7b**). These Erg+ cells had a high level of cell death based on active caspase 3 immunostaining (**Fig 7c**). Thus, we propose there is something about the need to restrict Erg expression to luminal-destined AR+ cells, and not in basal cells, that is critical for its oncogenic properties. However, in the RNA-Seq data, one of the striking findings is an increase in 2 ETV family members associated with Ets gene fusions in cancer, ETV1 and ETV4, but not other ETV or Ets genes in EMP cells relative to basal cells (**Table 1**). This was not observed in normal luminal cell differentiation. This suggests there is a fundamental relationship between lack of Ets factors in normal luminal cells and its retention specifically in tumorigenic cells that may drive PCa development. This finding is fundamentally important because it changes our thinking about how Erg functions as an oncogene.

TABLE 1: ETV Expression

Gene	Log2 Increase
ETV1	4.742699
ETV4	2.012325
ETV6	1.002061

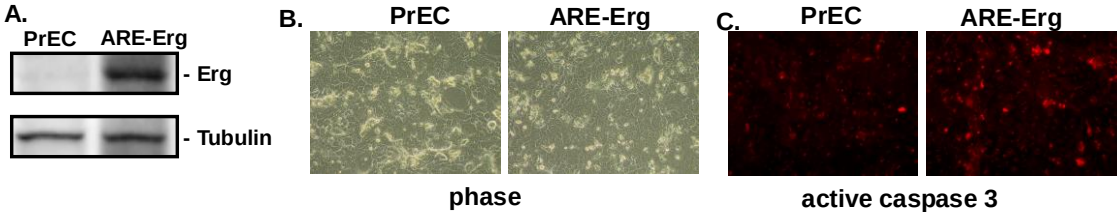

Figure 7: Erg under Control of Androgen Negatively Impacts Differentiation. A. Level of Erg and tubulin expression measured by immunoblotting in normal PrECs and PrECs expressing ARE-Erg after 21 days of differentiation. **B.** PrECs and PrECs with ARE-Erg differentiated for 16 days and viewed by phase contrast. Piles of luminal cells are appearing in the PrEC culture, but only single cells are appearing in ARE-Erg cells. **C.** PrECs and PrECs with ARE-Erg differentiated for 21 days and immunostained for cleaved/active caspase 3. More dead cells appear in the ARE-Erg cultures.

ARE-Erg cells are more tumorigenic and metastatic in combination with Myc and shPTEN than constitutive Erg cells. To determine if this cell-specific effect of Erg on differentiation, translates into tumorigenic potential, we tested the tumorigenicity of the ARE-Erg cell lines in various combinations with Myc overexpression and/or PTEN loss. As previously noted, loss of PTEN alone rarely generates tumors, and we saw a few prostate nodules with just ARE-Erg expression (**Table 2**). These ended up being PIN-like lesions in both cases. But all the different combinations gave much more robust tumor phenotypes then we saw previously with constitutive Erg; and most striking the triple combination produced visible metastasis in 1 mouse. **Thus, ARE-Erg in the context of the Myc and/or Pten was much more aggressive and tumorigenic than constitutive Erg.**

TABLE 2: Tumor Production

Cell Line Injected	# Tumors
iPEC37.ARE-Erg cl.3	4/10
iPEC37.ARE-Erg+Myc	9/10
iPEC37.ARE-Erg+shPten(B)	7/10
iPEC37.ARE-Erg+Myc+shPten(B)	7/10 1/10 mets
iPEC37+Myc+shPten(B)	7/10
iPEC37+shPten(B)	1/10

Development of additional immortalized iPrEC/EMP lines. The original iPrEC lines we developed for these studies (iPrEC37 and iPrEC36) were immortalized using HPV E6/E7 and hTert. Since disruption of Rb and p53 are not common events early in prostate cancer development, we wanted to design a set of cell lines that were immortalized with just hTert. To that end we infected primary PrEC36 cells with hTert, hTert+Myc, and hTert+Myc+shPten and selected a pool of cells from each infection. Of these, only two cell lines, hTert and hTert+Myc, grew past the crisis period and have now been maintained for 30 passages. Validation of Myc overexpression and intact Pten was demonstrated, as well as retention of the p53 response after doxorubicin treatment (**Fig. 8**). As expected the hTert+Myc line is much more prolific than the hTert line, but both are now available for us to determine how the different immortalization scheme impacts differentiation and tumorigenesis.

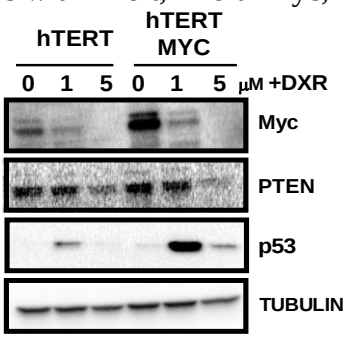

Fig. 8: hTert immortalized lines still retain p53 function. Primary PrEC36 line was immortalized with either hTert alone, or combined hTert and Myc. At passage 28 they were treated with 0-5 μM doxorubicin (DXR) for 24 hours and the levels of Myc, PTEN, p53 and tubulin assessed by immunoblotting. Note induction of p53 with treatment at low dose and loss of viability at higher dose.

CREB1/ATF1 activation and gene targets are altered in tumorigenic EMP cells versus normal luminal cells. Because CREB1/ATF1 activity was only present in differentiated luminal cells, we expected that in the tumorigenic EMP cells, which don't form supra-basal terminally differentiated luminal cells, CREB1/ATF1 would be inactive. Surprisingly, we found that CREB1/ATF1 are highly activated in the nuclei of EMP cells compared to basal iPrECs as measured by immunostaining, and loss of PTEN alone is sufficient to induce CREB1/ATF1 activation (**Fig. 9A**). Constitutive CREB1/ATF1 activation in EMP cells was further confirmed by immunoblotting (**Fig. 9B**). RNA-Seq of the EMP cells further revealed differential expression of over 1200 genes relative to basal cells. Interestingly, only a few of these genes were altered by the differentiation conditions, compared to normal iPrECs where clear differential expression over time was observed. These data add support out contention that oncogenic conversion drastically suppresses the ability of iPrECs to differentiate (**Fig. 9C**). Furthermore, over a third of the genes that are differentially expressed in EMP cells, relative to normal cells, are potential CREB1 targets (**Fig. 9D**). However, there is very little overlap between the CREB target genes in EMP cells versus normal PrECs (**Fig. 9E**).

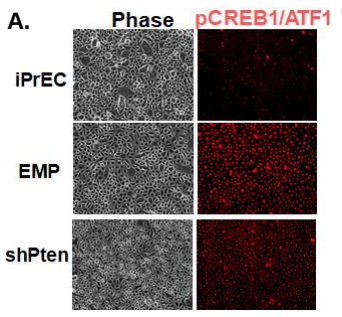

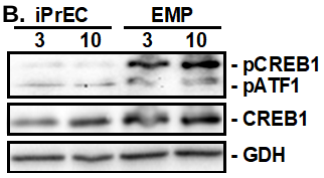

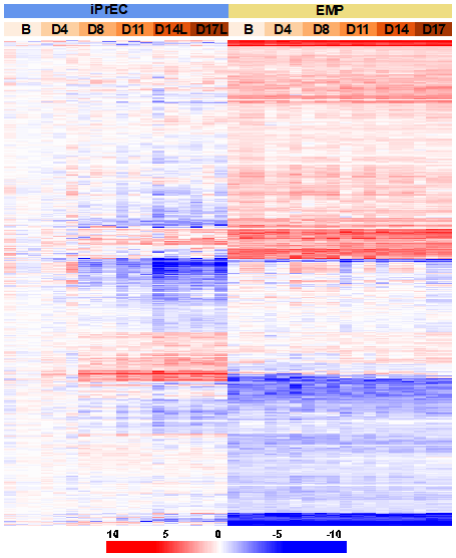

D.

B		D8		D11		D14		D17	
CREB1	388	CREB1	458	CREB1	336	CREB1	364	CREB1	533
Myc	188	Myc	247	Myc	169	Myc	185	Myc	266
SP1	165	SP1	195	SP1	141	SP1	152	SP1	198
GCRa	116	p53	153	GCRa	103	p53	105	p53	148
p53	113	ESR1	146	ESR1	99	ESR1	101	ESR1	148

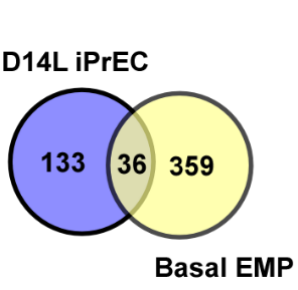

Fig. 9: CREB1/ATF1 activity in EMP cells. A) Levels of CREB1/ATF1 activation (pCREB1/ATF1) in basal iPrEC, EMP, and basal iPrEC expressing a constitutive shRNA to PTEN measured by immunostaining. Note heavy nuclear staining of activated CREB1/ATF1. **B)** Levels of CREB1/ATF1 activation (pCREB1/ATF1) in iPrEC and EMP cells differentiated for 3 or 10 days measured by immunoblotting. Note higher constitutive activity in EMP cells compared to normal iPrECs – note CREB is not activate until day 14 in iPrECs. **C)** RNA-Seq results comparing differentially regulated genes predicted to be CREB1 targets during different

times of differentiation in iPrEC and EMP cells. **D)** Gene-go analysis of transcription factors predicted to drive expression of the differentially expressed genes in EMP cells. **E)** Venn diagram of overlapping predicted CREB1 targets in luminal iPrEC (D14L) versus basal EMP cells.

Several of the predicted CREB1 targets in the EMP cells, not see in the iPrEC luminal cells, included genes known to be associated with prostate cancer progression and progenitor cell programming, such as Sox, Hox, GATA, and Twist genes. We validated that the expression of Twist1 and GATA2 mRNA and protein is specifically elevated in the tumorigenic EMP cells compared to normal luminal cells (**Fig. 10A,B**).

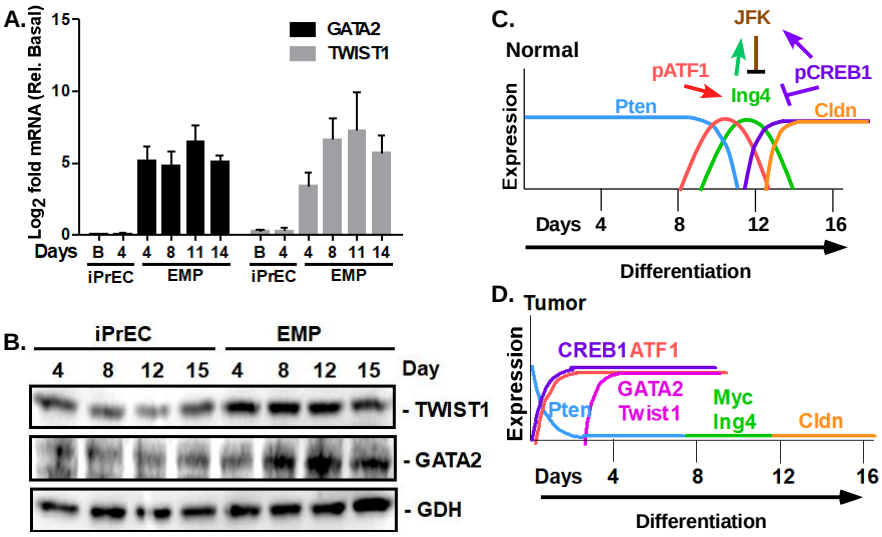

Fig. 10: CREB1 Targets in EMP Cells. A) Levels of GATA2 and Twist1 mRNA in iPrEC and EMP cells at different times of differentiation as assessed by qRT-PCR. **B)** Levels of GATA2 and Twist1 protein in iPrEC and EMP cells at different times of differentiation as assessed by immunoblotting. **C)** Model for how PTEN, CREB1/ATF1, and ING4 are coordinated to set the terminal commitment of normal luminal cell differentiation. **D)** Model for how loss of PTEN leads to premature activation of CREB1/ATF1 leading to up-regulation and retention of progenitor transcription factors and failure to induce ING4 and terminal differentiation. This then allows Myc to become oncogenic when ING4 is lost.

Working Model: Based on our findings in Aim 1, that CREB1 is a negative regulator of ING4, we propose that the aberrant activation of CREB1 by loss of PTEN, too early in differentiation prevents induction of ING4 and prevents terminal luminal cell differentiation (**Fig. 10C,D**). We further predict that the reason there are different CREB1 targets in EMP cells compared to luminal cells, is that loss of the ING4 chromatin switch prevents the chromatin remodeling required to 'open' the genes required for terminal differentiation and CREB1 cannot bind to the promoter of those genes. Further studies are required to fully test this hypothesis. **Thus, we have identified a new tumorigenic event in prostate cancer induced by PTEN loss, which deregulates the CREB1/ING4 differentiation control switch necessary for prostate cancer oncogenesis.** However, it is not PTEN loss alone that deregulates CREB1/ING4, as disrupting PTEN alone does not suppress ING4 (see Fig. 6C). It is only when we have combined Myc overexpression and PTEN loss that we see this deregulation. We still don't know how Myc contributes to this deregulation of CREB1/ING4. Once we more fully understand how CREB1 functions, then we can assess the role of Myc. We are in the process of writing up out findings on CREB for publication.

Cross ING null mice to Pb-Cre Myc transgenic mice. We are hypothesizing that tumors which lose ING4 expression are more aggressive, and that loss of ING4 cooperates with Myc overexpression to drive aggressive disease. To genetically test this hypothesis, our goal is to cross the Pb-Cre Myc transgenic mouse, which forms prostate tumors after a long latency period of 6 months, to ING4 null mice. Our expectation is that the tumors will appear sooner and be larger. We originally proposed to use an ING4 null mouse that was generated by insertional mutagenesis and deposited at JAX labs (Coles et al, 2010). However, despite extensive characterization of the F3 and F4 mice generated from the sperm we received, we never detected loss of ING4 in any of the tissues of those mice.

To rectify this problem, we generated our own global ING4 null mice using CRISPR. We generated four lines with varying lengths of deletions (em1Δ88, em3Δ133, em4Δ333, and em2Δ510 bp) of exon 3 or exon 3 plus exon 4 using a dual guide RNA approach (**Fig. 11A, B**). We found these deletions lead to exon skipping, such that the two smallest deletions both result in total loss of exon3 in the mRNA, which puts the protein out of

frame and truncates it (**Fig. 11C**). The two largest deletions result in loss of both exon 3 and 4, and for Δ333 the protein is out of frame and truncated, similar to the two smaller deletions. The Δ510 is an in-frame deletion of both exon 3 and 4, which removes the HBO1 binding site and the nuclear localization signal. All mice are viable and fertile, and we confirmed loss of both mRNA and protein in several tissues, including prostate (**Fig. 11C,D**). Prostate histology appears to be normal indicating that loss of ING4 in a mouse does not lead to a defect in luminal cell development. We still need to validate secretory function and AR expression in these glands. Mice kept for up to 1 year did not display any signs of overt tumor development in any tissue examined. The Δ88 (em1) ING4 mice are being crossed to the Pb-Cre Myc Tg mice, which we obtained from NIH and have re-derived and validated their genotype.

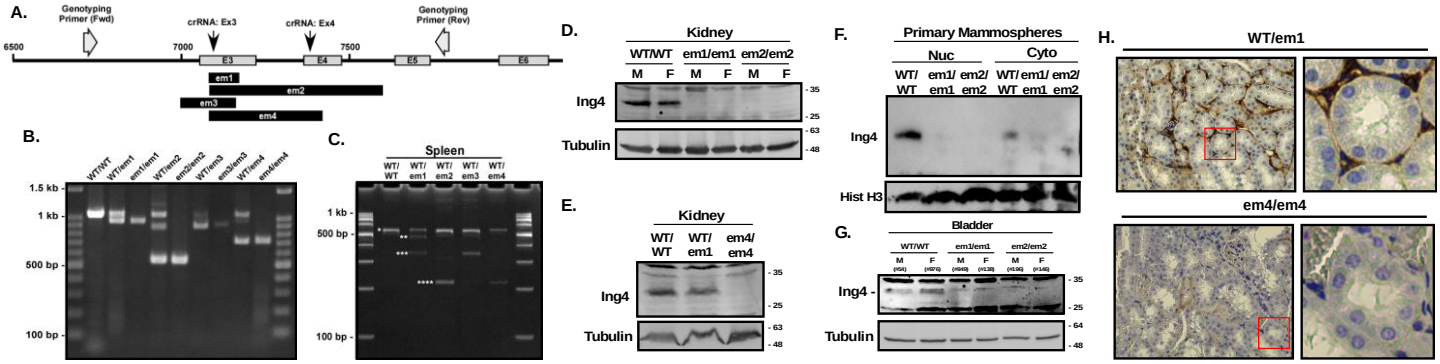

Fig. 11: CRISPR ING4 null mice. A) Map of the ING4 locus spanning Exons 3 through 6. The guide RNA sites are indicated (crRNA), the genotyping primers, and the different deletions generated by CRISPR. **B)** PCR Genotype validation of the four CRISPR lines. **C)** RT-PCR of ING4 mRNA in heterozygotes of the four lines. * indicates predicted full length ING4 mRNA. ** is expected truncated mRNA in em1, but all alleles also produced mRNAs representing exon skipping of exon 3 *** and exon 3+4 ****. These transcripts were confirmed by Sanger sequencing. **D, E)** ING4 expression in kidneys of male (M) and female (F) WT, em1, em2, and em4 KO mice by immunoblotting. **F)** ING4 expression in nuclear (Nuc) and cytoplasmic (Cyto) fractions of WT, em1, or em2 mammospheres developed in vitro from isolated mammary fat pads of WT, em1, or em2 female mice. **G)** ING4 expression in bladders of male (M) and female (F) WT, em1, em2, and em4 KO mice by immunoblotting. **H)** ING4 expression in em1 Het and em4 KO kidneys detected by IHC.

Aim 3: Determine how loss of ING4 in patients relates to tumor progression.

High correlation between PTEN loss and ING4 loss, supports our findings that loss of PTEN leads to loss of ING4. Our goal is to use TMAs of primary human prostate cancer samples to determine if there is a correlation between ING4 loss and over expression of oncogenes Myc, Erg fusions, and PTEN loss, differentiation markers and Gleason grade, and the relationship to disease recurrence. We successfully applied for and obtained IRB approval and a TMA from VARI that lacked any clinical information. We used that TMA to stain for ING4, pCREB, and PTEN. Statistical analysis of these data indicate 1) ~60% of the AR-positive tumors have elevated nuclear pCREB (**Fig. 12Ai**), 2) 65% of the samples with low ING4, have high pCREB (**Fig. 12Aii**), 3) strikingly 85% of those samples with low ING4 also have low PTEN (**Fig. 12Aiii**), and although it didn't quite reach significance 4) 65% of the samples with low ING4 also had low PTEN and high pCREB (**Fig. 12Aiv**). Representative image of double negative PTEN/ING4 tumors is shown (**Fig. 12B**). Further validation of the findings will be required on the PCBN TMAs and the link between ING4 and other oncogenic events as well as outcomes is still required and in the process of being evaluated.

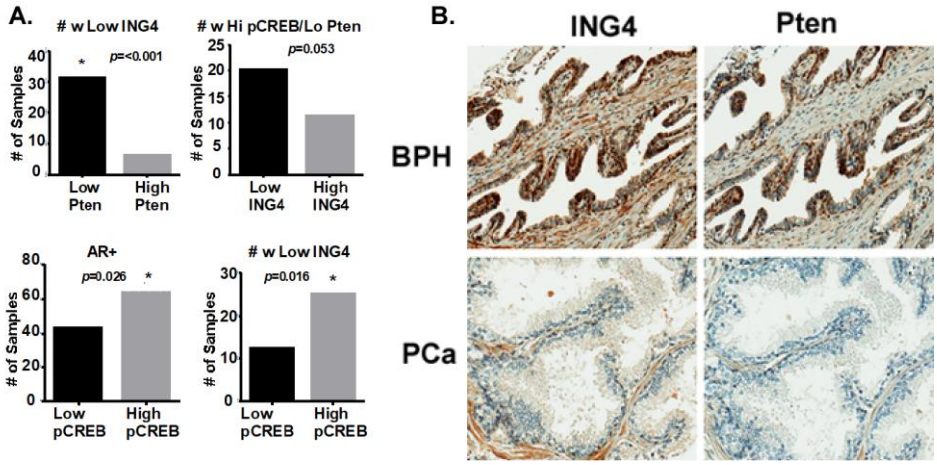

Figure 11: IHC staining of patient samples indicates a strong relationship between loss of PTEN, increased pCREB, and suppression of ING4. A) Consecutive slices from a TMA of 100 primary prostate cancer samples and 12 normal samples were immunochemically stained with antibodies to ING4, pCREB, and PTEN. Intensity of staining was graded from 0 to 3, with 0-1 being no or low staining and 2-3 being moderate to strong staining. Chi square z test was used to compare correlations between the different proteins. **B)** Representative image of dual ING4 negative and PTEN negative tumors. Note normal ING4 and PTEN staining in the stroma, but its absence in the tumor epithelium.

Delays due to lab relocation. At the time we started the above studies at VARI, we submitted an application to PCBN to obtain a 200+ case TMA at Johns Hopkins with clinical data, so that we can compare expression of ING4 relative to clinical stage and oncogene status of Erg, Myc, and PTEN. During the exchange with PCBN, we were contacted by Dr. DeMarzo about collaborating on this project, as he has already stained this TMA antibodies to the Erg, Myc, and PTEN. We agreed this would be a great collaboration and save on tissues. After reviewing our application, they requested better validation of our antibodies. We further demonstrated its specificity by lack of staining in shING4 cells, and elevated staining when ING4 was over expressed. The staining was nuclear as anticipated. PCBN sent a tester array to make sure the antibody works in their array system. It worked well and we were ready to begin, but the move to Arizona disrupted this work flow. The person who was working on the IHC did not relocate with me and the during the process we could not recover the staining program that was being used on the Ventana machine at VARI. Unfortunately, U of AZ had no automated machine available at the time we needed it to start these studies again. Therefore, we started from scratch with new personnel, developing our own staining protocols using several different antibodies. The upside is that because we successfully generated the ING4 KO mice during this time, we were able to validate the antibodies much better.

Loss of nuclear ING4 correlates with Gleason Grade. We validated the specificity of the ING4 antibody by immunoblotting and IHC of tissues from ING4 mice (**Fig. 12A**). Preliminary staining of an 80 sample TMA, which has clinical data, from the University of Arizona with a much better antibody demonstrates at least three different staining patterns in the tissues. Preliminary scoring indicate that a strong nuclear staining

is associated with normal and low Gleason grade 6 tumors, reduced nuclear staining and strong cytoplasmic staining with Gleason grade 7, and significant loss of nuclear staining with Gleason ≥8 (**Fig. 12B**). **Thus, our preliminary results indicate increased nuclear ING4 loss with increased aggressiveness/decreased differentiation as assessed by Gleason Score.**

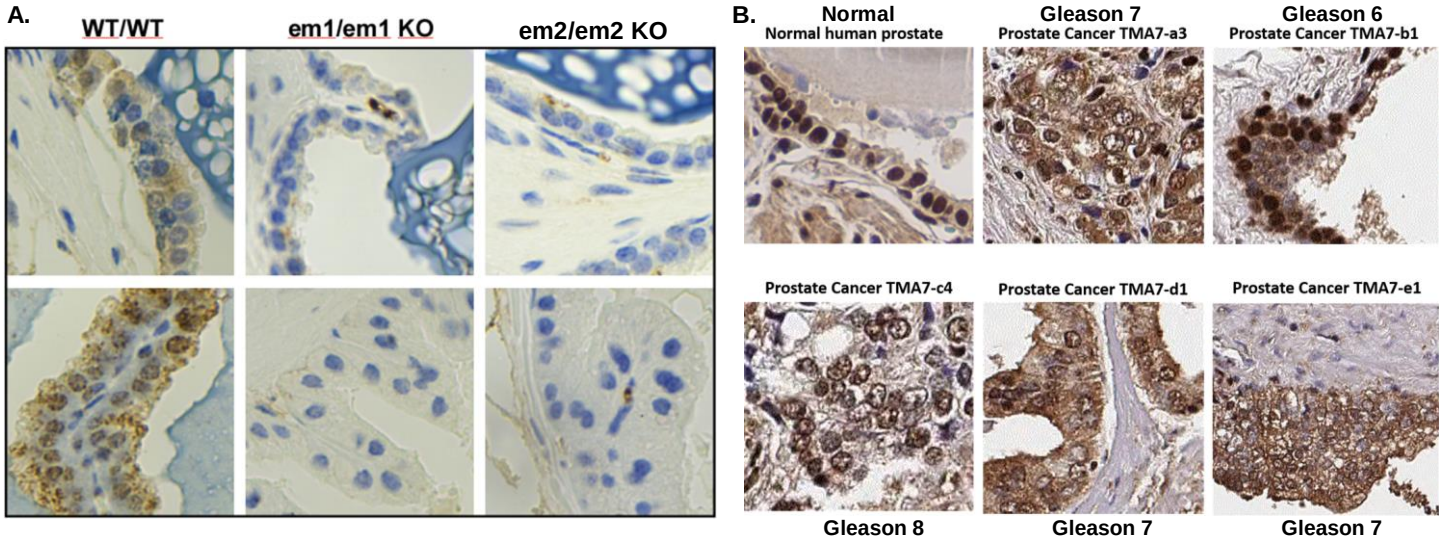

Fig. 12: ING4 IHC validation and TMA staining. A) IHC of mouse prostate tissues from WT and em1 (Δ88) and em2 (Δ510) ING4 KO mice. **B)** IHC of 80 samples from a TMA of primary prostate cancer samples with pathology grading. Note loss of nuclear ING4 with increased Gleason Grade.

Using this data, we re-applied to PCBN for the 200+ case Johns Hopkins TMA and received approval. The TMA was shipped and we are setting up the staining. Dr. DeMarzo has re-agreed to the collaboration and we look forward to the final analysis. Once this is completed, we will apply for another TMA at PCBN that has clinical outcomes and additionally assess differentiation targets such as Notch3, and several CREB targets identified in the EMP cells relative to ING4 and PTEN.

What opportunities for training and professional development has the project provided?

Nothing to report.

How were the results disseminated to communities of interest?

Nothing to report.

What do you plan to do during the next reporting period to accomplish the goals?

Aim 2: Task 6: ING4 Loss and Myc Cooperation in Tumorigenesis. Cross Pb-Cre Myc transgenic mice to ING4 null mice to determine if loss of ING generates more aggressive tumors.

Aim 3: Task 8 & 9: Correlation of ING4 Loss with Outcome and Oncogenic Events, ING4 Loss and Tumor Differentiation. Stain human prostate cancer tissue arrays for ING4, oncogenes, and differentiation markers and then assess the relationship between ING4 loss, oncogene status, differentiation status, clinical stage, and clinical outcome.

IMPACT:

What was the impact on the development of the principal discipline(s) of the project?

The principal disciplines of our project are cancer biology, prostate cancer, oncogenesis, and differentiation.

1) We are the only lab working with this prostate differentiation model and the first to show the involvement of ING4 in prostate epithelial differentiation – and indeed the first to show ING4 has anything to do with differentiation in any model. We were also the first to demonstrate ING4 is lost in PCa, and to define its relationship to Myc, a well-established oncogene in PCa.

2) We identified Miz1 and JFK as direct targets of ING4 in normal luminal cell differentiation, and find that the loss of ING4 in tumors, also leads to their loss in prostate cancer. They control the commitment of luminal cells to terminal differentiation, and by losing ING4, tumor cells remain proliferative and cannot move into a post-mitotic differentiation state.

3) We are the first to identify Notch3 as a crucial Myc target, independent of ING4, and a driver of luminal cell differentiation. Notch dysregulation is known to be associated with advanced PCa; thus, it will be important to determine if Notch3 is specifically altered in aggressive tumors and how it works with ING4 to promote differentiation.

4) We identified the link between PTEN loss and ING4 loss. Half the tumors that loose ING4 also loose PTEN and genetic loss of PTEN in the differentiation model prevents ING4 expression. We tentatively identified CREB1 as the mechanism by which PTEN loss leads to loss of ING4. This is highly novel, as almost no studies have investigated the role of CREB1 in prostate cancer.

5) We are the first to begin to decipher the exact mechanisms by which several known PCa onocgenes i.e. Myc, Erg, and loss of Pten, contribute to PCa development through dysregulation of differentiation. In addition to the above results, our finding that AR-specific expression of the Erg fusion gene is crucial for its ability to disrupt differentiation is a fundamental advancement. How Erg functions as an oncogene is poorly understood. Our studies indicate that its specific expression within a luminal-like population (and its absence from basal cells), is important. Thus, analysis of potential oncogenic Erg targets has to take this into consideration and calls into question some of the target data and models using constitutive overexpression of Erg.

6) This work will contribute to defining the cell of origin in PCa. Moreover, because these studies use human cells, the mechanisms that are specifically important in human disease, as opposed to mice, will be better defined.

What was the impact on other disciplines?

Development of improved techniques and plasmids for conditional expression of shRNAs in mammalian cells using lentivirus. Improvements included removing the large stuffer that reduced efficiency of cloning, use of an odd number of base pairs, 7 or 9, in the shRNA loop to prevent loop collapse, engineering plasmids with blast or hygro resistance, in addition to the puromycin, to be able to target several genes at once in the same cells, and use of immunoblotting to quickly screen expression of repressor in clones/pools. The vector plasmids, as well those expressing specific shRNAs were deposited with Addgene to make them available to all researchers. To date, over 100 requests have come in for those plasmids, demonstrating the demand and utility of the technology.

Generation of ING4 KO mice will be of interest to others in cancer research, such as glioblastoma and breast cancer, where ING4 has also been reported to be dysregulated. Researchers interested in ING4 role in the brain, liver, and spleen will also be interested in these mice, as these are the tissues where ING4 is most highly expressed. We have already shared this line with a breast cancer researcher who is crossing it with other genetically modified mouse that develops breast cancer. Their research shows that ING4 loss is associated with increased aggressiveness and inflammation in breast cancer.

What was the impact on technology transfer?

Nothing to report.

What was the impact on society beyond science and technology?

Nothing to report.

CHANGES/PROBLEMS:

Changes in approach and reasons for change

We encountered problems with being able to validate the ING4 KO mice we obtained from JAX labs as actually being KO mice. The mouse supposedly was generated with a gene trap; however, we were unable to 1) validate the site of insertion, 2) demonstrate any loss in ING4 protein expression in several tissues even after 3 generation crosses, and 3) did not detect any changes in ING4 mRNA. Upon consultation with another PI, who also tried to work with the mice, we both concluded they are not ING4 KO mice. Since the Vivarium Core at VARI had developed efficient and effective techniques for using CRISPR in mice, we generated ING4 KO mice using CRISPR at our own expense. We successfully generated 6 different lines, which are viable and fertile. We are now back on track to finish the Pb-Myc x ING4-/- model.

Actual or anticipated problems or delays and actions or plans to resolve them

1) The move from VAI to University of Arizona and loss of personnel with the expertise required to conduct many aspects of the work significantly delayed and ultimately prevented us from identifying additional ING4 targets as hoped. Nonetheless, we did identify three.
2) Prior to the move, we had optimized an ING4 antibody for the TMA studies, but after the move we lost the automated stainer and had to redo all the IHC optimization by hand. But the upside of this is that we now have a more specific antibody and the ING4 KO mice with which we validated it.
3) Because we had to generate the ING4 KO mice from scratch, it took time to get that mouse colony established at Arizona, re-derive the PB-Myc mice, and set up the crosses. We have some funds left over for the NCE that will allow us to be able to complete the human TMA and ING4xMyc mouse studies.

Changes that had a significant impact on expenditures

Changes had no impact on expenditures

Significant changes in use or care of human subjects, vertebrate animals, biohazards, and/or select agents

Nothing to report

PRODUCTS:

Journal publications

The following publications relevant to this project were published. Copies are in the **appendix** and all acknowledged DOD support.

Berger PL, Frank SB, Schulz VV, Nollet EA, Edick MJ, Holly B, Chang TA, Hostetter G, Kim S and Miranti CK. 2014. Transient induction of ING4 by MYC drives prostate epithelial cell differentiation and its disruption drives prostate tumorigenesis. **Cancer Res** 74:3357-68.

Berger PL, Winn ME, and Miranti CK. 2017. Miz1, a novel target of ING4, can drive prostate luminal epithelial cell differentiation. **The Prostate**, 77:49-59.

Frank SB, Schultz VV, and Miranti CK. 2017. A streamlined method for the design and cloning of shRNAs into an optimized Dox-inducible lentiviral vector. **BMC Biotechnology**, 17:24

Frank SB, Berger PL, Ljungman M and Miranti CK. 2017. Prostate luminal cell differentiation requires Notch3 induction via p38α-MAPK and Myc. **J Cell Sci**, 130:1952-1964.

The following are manuscripts under preparation.

Watson MJ, Berger PL, Frank SB, and Miranti CK. 2018. PTEN loss in prostate cancer disrupts a CREB-dependent differentiation pathway. In preparation for Cancer Research.

Frank SB, Kim S, and Miranti CK. 2018. CRISPR mutagenesis of the mouse ING4 locus. In preparation for J of Cell Science.

Conference posters and oral presentations

Posters:

Frank SB and Miranti CK. 2014. p38-MAPK Regulation of Notch via Myc is Required for Prostate Epithelial Cell Differentiation. **Society for Basic Urologic Research**. Dallas, TX, November 13-16.

Frank SB, Berger PL and Miranti CK. 2015. Myc Governs a Prostate Epithelial Differentiation Program involving Chromatin Remodeling Protein ING4 and Notch3: Disruption of Which is Necessary for Human Prostate Cancer Development. **AACR: MYC: From Biology to Therapy**, San Diego, CA, Jan 7-10.

Berger PL, Watson M, Winn ME and Miranti CK. 2015. Key Intermediate Progenitor in Luminal Prostate Epithelial Differentiation Dictates Susceptibility to Myc Overexpression and Pten Loss in Prostate Cancer Cell of Origin. **AACR: Developmental Biology and Cancer**, Boston, MA, Nov 30-Dec 3.

Frank SB, Berger PL, Ljungman M and Miranti CK. 2016. Human Prostate Luminal Cell Differentiation requires NOTCH3 Induction by p38-MAPK and MYC. **Society for Basic Urologic Research**. Phoenix, AZ November 10-14.

Watson MJ, Burger P, Frank SB, Winn M, and Miranti CK. 2017. CREB1 and ATF1 Differentially Regulate Terminal Prostate Luminal Cell Differentiation by Controlling the Timing of ING4 Expression, while CREB1 Prevents ING4 Expression upon PTEN Loss in Prostate Cancer. **Society for Basic Urologic Research**, Tampa, FL, Nov 9-12.

Am J Clin Exp Urol 2017;5(Suppl 1):1-92 Poster P51, p60. www.ajceu.us

Watson MJ, Burger P, Frank SB, Winn M, and Miranti CK. 2017. CREB1 and ATF1 Differentially Regulate Terminal Prostate Luminal Cell Differentiation by Controlling the Timing of ING4 Expression, while CREB1 Prevents ING4 Expression upon PTEN Loss in Prostate Cancer. **AACR Special Conference on Prostate Cancer**, Orlando, FL, Dec 2-5, 2017.

Oral Presentations:

Berger PL, Watson M, Winn ME and Miranti CK. 2015. Elucidating ING4 Targets Important in Prostate Epithelial Cell Differentiation and Examining CREB as a Key Regulator of ING4 Expression. **Society for Basic Urologic Research: Environment-Gene Interface in Urologic Disease**, Fort Lauderdale, FL, Nov 12-15.

Miranti, CK. 2015. SwitchING4 Prostate Cancer: A Differentiation Control Switch that Defines the Cell of Origin for Prostate Cancer, **University of AZ**, Tucson, AZ, Dec 7.

Miranti, CK. 2016. PTEN and CREB Cooperativity during Prostate Luminal Epithelial Differentiation is Disrupted in Prostate Cancer. **11th Prostate Cancer Symposium at Clark Atlanta University**, Atlanta, GA, Sep 26-28.

Miranti, CK. 2017. Pten Loss Promotes Prostate Cancer Tumorigenesis through Disruption of a CREB-Dependent Differentiation Pathway. **University of Arizona Cancer Center Retreat**, Tucson, AZ, Apr 21.

Miranti, CK. 2017. Pten Loss Promotes Prostate Cancer Tumorigenesis through Disruption of a CREB-Dependent Differentiation Pathway. **SBUR Annual Meeting: Multiple Genetic and Epigenetic Mechanisms of Urologic Disease**, Tampa, FL, Nov 9-12.

Miranti, CK. 2017. Pten Loss Disrupts a CREB-Dependent Differentiation Pathway during Prostate Cancer Oncogenesis, **Ventana Medical Systems,** Oro Valley, AZ, Nov 13.

Miranti, CK. 2018. How and Why Integrin α6β1 Drives Prostate Cancer. **Dana Farber Cancer Institute, Harvard Medical School**, Boston, MA Jun 12.

Technologies or techniques

1) Techniques: Development of a HUMAN in vitro differentiation model. This model utilizes primary or immortalized basal epithelial cells isolated from patients. Cells are grown to confluency in defined medium and then treated with DHT and KGF. Over a period of 14-20 days, a subset of basal cells differentiate into functional secretory luminal cells (Lamb et al., 2010). This model was initially developed using primary cells by a graduate student, Dr. Laura Lamb, who received a DOD Predoctoral Award for this work. We have since generated 4 immortalized cell lines, two using HPV E6/E7 immortalization, and two using only hTert. All four immortal cell lines behave similarly to the primary cells. These lines have now been stably modified to express a host of different genes or shRNA, either constitutively or under control of Tet-R or an ARE. These cell lines and model greatly expand the HUMAN repertoire of tools available for PCa research and are readily available upon request.

2) Techniques: Development of improved techniques and plasmids for conditional expression of shRNA in mammalian cells using lentivirus. See Accomplishments. The vector plasmids, as well those expressing specific shRNAs were deposited with Addgene to make them available to all researchers. Within 1 year of publishing, over 100 requests have come in for the vector plasmids, demonstrating the demand and utility of the technology.

3) Mouse model: Generation of global loss of ING4 expression in the mouse using CRISPR. See Accomplishments. Once we publish the paper, the ING4 KO mice will be made available to anyone who asks for them.

4) RNA-Seq: We generated 3 sets of RNA-Seq data. This data defines the mRNA transcriptional program of normal HUMAN prostate epithelial differentiation from basal cells into luminal cells, from luminal cells to tumor cells, and defines those genes targeted by ING4, Myc, and p38-MAPK during differentiation. Two of the three datasets are now publicly available at GEO.

Inventions, patent applications, and/or licenses
Nothing to report.

PARTICIPANTS & OTHER COLLABORATING ORGANIZATIONS

What individuals have worked on the project in Year 3?

Name:	Cynthia Miranti
Project Role:	PI
Researcher Identifier (e.g. ORCID ID):	0000-0003-0668-6106
Nearest person month worked:	2.4
Contribution to Project:	Supervised and directed the project. Obtained necessary IACUC and IRB approvals. Managed, analyzed, and interpreted data. Submitted and presented posters/talks at meetings and seminars. Wrote and submitted papers for publication.
Funding Support:	Startup funds from University of Arizona

Name:	Sander Frank
Project Role:	Postdoctoral Fellow
Researcher Identifier (e.g. ORCID ID):	
Nearest person month worked:	12
Contribution to Project:	Conducted the studies and published the paper on Myc/Notch3; Made the ING4 CRISPR KO mouse; Worked on the CREB/ING4 interactions; Presented posters at meetings; Developed and published the Tet-shRNA plasmids. Helped with writing of the papers.
Funding Support:	

Name:	Jack Tran

Project Role:	Research Specialist
Researcher Identifier (e.g. ORCID ID):	
Nearest person month worked:	2.4
Contribution to Project:	Help with characterization of ING4 mouse tissues; optimized ING4 antibody IHC for the TMA for the PCBN application. Quantifying ING4 IHC staining on in-house TMA and assessing expression relative to Gleason grade.
Funding Support:	

Name:	Lin Tang
Project Role:	Assistant Research Scientist
Researcher Identifier (e.g. ORCID ID):	
Nearest person month worked:	6
Contribution to Project:	Responsible for maintaining the ING4 and Pb-Cre Myc mice, their genotyping, and supervising the breeding/crosses. Helped write the IACUC protocol.
Funding Support:	

Has there been a change in the active other support of the PD/PI(s) or senior/key personnel since the last reporting period?

W81XWH-17-1-0570 (Miranti, PI) 09/01/17-08/31/20
DoD Prostate Cancer Research Program
CREB Activation: A Gene Signature and Control Switch in Prostate Cancer
The goal is to define how CREB1 dysregulated gene expression promotes prostate cancer development.
Specific Aims:
1) Determine the role of CREB1/ATF1 in differentiation and oncogenesis
2) Identify the CREB1/ATF1 targets necessary for prostate cancer oncogenesis
3) Define the CREB1/ATF1 signature in clinical human prostate cancer samples

Accelerate for Success (Miranti, PI) 01/01/17-12/31/18
University of Arizona
Targeting Castration-Resistant Prostate Cancer
Project aimed towards enhancing multi-PI co funded grants through interdisciplinary collaborations.

What other organizations were involved as partners?

Nothing to report.

SPECIAL REPORTING REQUIREMENTS

Nothing to report.

CITATIONS

Berger, P.L., Frank, S.B., Schulz, V.V., Nollet, E.A., Edick, M.J., Holly, B., Chang, T.T., Hostetter, G., Kim, S., and Miranti, C.K. (2014). Transient induction of ING4 by Myc drives prostate epithelial cell differentiation and its disruption drives prostate tumorigenesis. Cancer Res 74, 3357-3368.

Berger, P.L., Winn, M.E., and Miranti, C.K. (2016). Miz1, a Novel Target of ING4, Can Drive Prostate Luminal Epithelial Cell Differentiation. The Prostate 77, 49-59.

Caravatta, L., Sancilio, S., di Giacomo, V., Rana, R., Cataldi, A., and Di Pietro, R. (2008). PI3-K/Akt-dependent activation of cAMP-response element-binding (CREB) protein in Jurkat T leukemia cells treated with TRAIL. J Cell Physiol 214, 192-200.

Coles, A.H., Gannona, H., Cerny, A, Kurt-Jones, E., and Jones, S.N. (2014) Inhibitor of growth-4 promotes IκB promoter activation to suppress NF-κB signaling and innate immunity. PNAS 107:11423–11428.

Frank, S.B., Schultz, V.V., and Miranti, C.K. (2017). A streamlined method for the design and cloning of shRNAs into an optimized Dox-inducible lentiviral vector. BMC Biotechnology 17,24

Frank, S.B., Berger, P.L., Ljungman, M., and Miranti, C.K. (2017). Prostate luminal cell differentiation requires Notch3 induction via p38α-MAPK and Myc. J Cell Sci 130, 1952-1964.

Gebhardt, A., Frye, M., Herold, S., Benitah, S.A., Braun, K., Samans, B., Watt, F.M., Elsasser, H.P., and Eilers, M. (2006). Myc regulates keratinocyte adhesion and differentiation via complex formation with Miz1. J Cell Biol 172, 139-149.

Gu, T., Zhang, Z., Wang, J., Guo, J., Shen, W.H., and Yin, Y. (2011). CREB is a novel nuclear target of PTEN phosphatase. Cancer Res 71, 2821-2825.

Lamb, L.E., Knudsen, B.S., and Miranti, C.K. (2010). E-cadherin-mediated survival of androgen-receptor-expressing secretory prostate epithelial cells derived from a stratified in vitro differentiation model. J Cell Sci 123, 266-276.

Lyu, J., Yu, X., He, L., Cheng, T., Zhou, J., Cheng, C., Chen, Z., Cheng, G., Qiu, Z., and Zhou, W. (2015). The protein phosphatase activity of PTEN is essential for regulating neural stem cell differentiation. Mol Brain 8, 26.

Paulsen, M.T., Veloso, A., Prasad, J., Bedi, K., Ljungman, E.A., Magnuson, B., Wilson, T.E., and Ljungman, M. (2014). Use of Bru-Seq and BruChase-Seq for genome-wide assessment of the synthesis and stability of RNA. Methods 67, 45-54.

Yan, R., He, L., Li, Z., Han, X., Liang, J., Si, W., Chen, Z., Li, L., Xie, G., Li, W., Wang, P., Lei, L., Zhang, H., Pei, F., Cao, D., Sun, L., and Shang, Y. (2015). SCF(JFK) is a bona fide E3 ligase for ING4 and a potent promoter of the angiogenesis and metastasis of breast cancer. Genes Dev 29, 672-685.

APPENDEX:

Abstracts from oral and poster presentations

Frank SB and Miranti CK. 2014. p38-MAPK Regulation of Notch via Myc is Required for Prostate Epithelial Cell Differentiation. **Society for Basic Urologic Research**. Dallas, TX, November 13-16.

Frank SB, Berger PL and Miranti CK. 2015. Myc Governs a Prostate Epithelial Differentiation Program involving Chromatin Remodeling Protein ING4 and Notch3: Disruption of Which is Necessary for Human Prostate Cancer Development. **AACR: MYC: From Biology to Therapy**, San Diego, CA, Jan 7-10.

Berger PL, Watson M, Winn ME and Miranti CK. 2015. Key Intermediate Progenitor in Luminal Prostate Epithelial Differentiation Dictates Susceptibility to Myc Overexpression and Pten Loss in Prostate Cancer Cell of Origin. **AACR: Developmental Biology and Cancer**, Boston, MA, Nov 30-Dec 3.

Berger PL, Watson M, Winn ME and Miranti CK. 2015. Elucidating ING4 Targets Important in Prostate Epithelial Cell Differentiation and Examining CREB as a Key Regulator of ING4 Expression. **Society for Basic Urologic Research: Environment-Gene Interface in Urologic Disease**, Fort Lauderdale, FL, Nov 12-15.

Frank SB, Berger PL, Ljungman M and Miranti CK. 2016. Human Prostate Luminal Cell Differentiation requires NOTCH3 Induction by p38-MAPK and MYC. **Society for Basic Urologic Research**. Phoenix, AZ November 10-14.

Miranti, CK. 2016. PTEN and CREB Cooperativity during Prostate Luminal Epithelial Differentiation is Disrupted in Prostate Cancer. **11th Prostate Cancer Symposium at Clark Atlanta University**, Atlanta, GA, Sep 26-28.

Miranti, CK. 2017. Pten Loss Promotes Prostate Cancer Tumorigenesis through Disruption of a CREB-Dependent Differentiation Pathway. **University of Arizona Cancer Center Retreat**, Tucson, AZ, Apr 21.

Watson MJ, Burger P, Frank SB, Winn M, and Miranti CK. 2017. CREB1 and ATF1 Differentially Regulate Terminal Prostate Luminal Cell Differentiation by Controlling the Timing of ING4 Expression, while CREB1 Prevents ING4 Expression upon PTEN Loss in Prostate Cancer. **Society for Basic Urologic Research**, Tampa, FL, Nov 9-12.
Am J Clin Exp Urol 2017;5(Suppl 1):1-92 Poster P51, p60. www.ajceu.us

Watson MJ, Burger P, Frank SB, Winn M, and Miranti CK. 2017. CREB1 and ATF1 Differentially Regulate Terminal Prostate Luminal Cell Differentiation by Controlling the Timing of ING4 Expression, while CREB1 Prevents ING4 Expression upon PTEN Loss in Prostate Cancer. **AACR Special Conference on Prostate Cancer**, Orlando, FL, Dec 2-5, 2017.

Copies of published papers

Berger PL, Frank SB, Schulz VV, Nollet EA, Edick MJ, Holly B, Chang TA, Hostetter G, Kim S and Miranti CK. 2014. Transient induction of ING4 by MYC drives prostate epithelial cell differentiation and its disruption drives prostate tumorigenesis. **Cancer Res** 74:3357-68.

Berger PL, Winn ME, and Miranti CK. 2017. Miz1, a novel target of ING4, can drive prostate luminal epithelial cell differentiation. **The Prostate**, 77:49-59.

Frank SB, Schultz VV, and Miranti CK. 2017. A streamlined method for the design and cloning of shRNAs into an optimized Dox-inducible lentiviral vector. **BMC Biotechnology**, 17:24

Frank SB, Berger PL, Ljungman M and Miranti CK. 2017. Prostate luminal cell differentiation requires Notch3 induction via p38α-MAPK and Myc. **J Cell Sci**, 130:1952-1964.

p38-MAPK Regulation of Notch via Myc is Required for Prostate Epithelial Cell Differentiation

Frank SB and Miranti CK

Background: Researchers have made progress identifying major drivers of aggressive prostate cancer (e.g. AR, Myc, Erg) but mechanistic understanding of the early events of tumorigenesis remain poorly understood. The epithelium of the prostate is composed of basal and luminal cells that can be identified by distinctive protein markers which are often co-expressed in prostate tumors. Moreover, many of the signaling pathways that are misregulated in prostate tumors have also been broadly implicated in epithelial differentiation (e.g. Myc, p38-MAPK, Notch). Thus, we propose that better understanding of differentiation pathways in the prostate will provide insight into understanding tumorigenesis. Specifically, we hypothesize that p38-MAPK regulation of Notch3 via Myc is required for prostate epithelial differentiation.

Methods: To test our hypothesis we utilized an in vitro differentiation model in which primary human basal prostate epithelial cells (PrECs) are cultured and induced to differentiate into luminal cells. RNAi techniques were used to knockdown expression of various genes in the context of PrEC differentiation. Alternately, tet-inducible expression of constitutively active MKK6 was used to temporally activate p38-MAPK signaling. Differentiation was monitored by phase-contrast microscopy while changes in gene expression were measured via quantitative real-time PCR and immunoblot. Promoter sequences were cloned from BACs into luciferase reporters to test Notch regulatory regions.

Results: Pharmacological inhibition of p38 with SB202190 or shRNA knockdown demonstrated that p38□ was required for differentiation. Likewise, inhibition of Notch signaling with a □-secretase inhibitor (RO4929097) prevented proper differentiation. Notch3 was highly upregulated at the mRNA and protein level during differentiation. Constitutive p38-MAPK signaling led to increased Notch3 mRNA and protein expression which was greatly abrogated upon knockdown of Myc. Notch3 mRNA upregulation was partially explained by increased mRNA stability but likely relies primarily on transcriptional upregulation independent of the classic promoter region.

Conclusions: This work is the first to define specific roles for the p38-MAPK and Notch pathways in human prostate epithelial differentiation. Moreover, we provide evidence for Myc as a novel direct link between p38-MAPK and Notch pathways. Additionally, we provide evidence of a unique role for Notch3 in prostate differentiation. We expect that further understanding of these differentiation pathways will provide new insight into how oncogenic transformation in a transient differentiating prostate epithelial cell may give rise to cancer.

Society for Basic Urologic Research. Dallas, TX, November 13-16, 2014.

Myc Governs a Prostate Epithelial Differentiation Program involving Chromatin Remodeling Protein ING4; Disruption of Which is Necessary for Human Prostate Cancer Development

Berger PL[1], Frank SB[1,5], Schulz VV[1], Nollet EA[1,6], Chang TA[2], Hostetter G[3], Kim S[4], and Cindy K. Miranti[1]

[1]Laboratory of Integrin Signaling, [2]Laboratory of Translational Imaging, and [3]Laboratory of Analytical Pathology, Van Andel Research Institute, Grand Rapids, MI; [4]Tranlational Genomics Research Institute and University of Arizona College of Medicine, Phoenix, AZ; [5]Genetics Graduate Program, Michigan State University, Lansing, MI; and [6]Van Andel Institute Graduate School, Grand Rapids, MI

The cell of origin from which many human cancers develop remains controversial; is it a stem cell, a progenitor, or a differentiated cell? In the absence of satisfactory human models, answering this question has relied heavily on mouse models. Using a novel human *in vitro* differentiation model in which prostate basal epithelial cells are induced to differentiate into luminal cells, we tested the hypothesis that prostate cancer develops in an intermediate progenitor cell population whose full differentiation is derailed upon oncogenic transformation. In this study, we demonstrate how loss of the chromatin-binding protein ING4, whose expression during differentiation is dependent on Myc, arrests prostate epithelial differentiation and permits Myc-dependent tumorigenesis. We found that Myc is required for transient expression of ING4 and differentiation of basal epithelial cells into luminal cells. ING4-mediated differentiation requires its chromatin binding activity and is accompanied by global chromatin modifications. Sustained Myc or ING4 expression induces apoptosis of the emerging luminal cells, indicating limited Myc/ING4 expression is required for normal differentiation. Myc is overexpressed in the majority of human prostate cancers. In human tissues, ING4 expression is lost in >60% of primary prostate tumors. These data suggested loss of ING4 is necessary for Myc-induced tumorigenesis to prevent death and stall differentiation. Loss of ING4, directly by shRNA or indirectly through loss of Pen, prevented differentiation and was necessary for Myc-dependent tumorigenesis *in vivo*. ING4 re-expression in tumorigenic cells rescues differentiation and blocks tumorigenesis. ING4 loss generated tumor cells that co-express basal and luminal markers, indicating oncogenesis disrupted an intermediate step in the prostate epithelial differentiation program. Our findings demonstrate that Myc-mediated oncogenesis through loss of ING4 alters epithelial fate determination, which is integral to Myc-mediated transformation.

AACR: MYC: From Biology to Therapy, San Diego, CA, Jan 7-10, 2015.

Key Intermediate Progenitor in Luminal Prostate Epithelial Differentiation Dictates Susceptibility to Myc Overexpression and Pten Loss in Prostate Cancer Cell of Origin

Penny Berger[1], McLane Watson[1], Mary E. Winn[2], Cindy K. Miranti[1]

[1]Laboratory of Integrin Signaling, [2]Bioinformatics and Biostatistics Core, Van Andel Research Institute, Grand Rapids, MI

Overexpression of Myc and loss of Pten are very common oncogenic events in prostate cancer. However, why these specific oncogenic events, as opposed to others, are involved in prostate cancer develop remains unclear. While the impact of Myc and Pten on cell proliferation is well-characterized, their role in differentiation and the resulting impact on tumorigenesis is poorly understood. We recently developed an *in vitro* differentiation model in which basal prostate epithelial cells (PrECs) can be differentiated into secretory luminal cells. Our model offers several advantages, in that it is human-specific and readily manipulated genetically and biochemically; providing a rare opportunity to dissect the specific genetic and biochemical events associated with human PrEC differentiation and determining how it is impacted by specific oncogenic events. Using this model, we tested the **hypothesis** that overexpression of Myc and loss of Pten induce prostate cancer because their dysregulation impairs differentiation of an intermediate progenitor cell population that marks the tumor cell of origin. Transient induction of both Pten and Myc are required for normal PrEC differentiation. Constitutive Myc overexpression initially accelerates differentiation, but the differentiated cells ultimately die via a p53-independent mechanism. Overexpression of Myc in combination with loss of Pten (Myc+shPten), is required for tumorigenesis because it rescues cell survival and blocks terminal differentiation. We identified the chromatin binding protein, ING4, as a Myc target required for PrEC terminal differentiation. ING4 is lost in over 60% of human prostate tumors and in the Myc+shPten cells, ING4 expression is blocked. Loss of ING4 in Myc overexpressing cells is sufficient to replace loss of Pten; ING4 loss, like Pten loss, is required for tumorigenesis to block terminal differentiation and keep cells alive. We further identified Miz1, a component of the Myc repressor complex, as a direct target of ING4 required for terminal PrEC differentiation. Myc/Miz1 is required to suppress integrin α6 and β1 expression during terminal PrEC differentiation; in Myc+shPten cells, Miz1 fails to be induced and integrin α6β1 is aberrantly co-expressed with AR in an intermediate progenitor and tumorigenic cell population. **Conclusions:** Prostate cancer oncogenesis requires dysregulation of Myc and Pten, because they are required for the normal PrEC terminal differentiation pathway. Pten loss is required to remove the ING4/Miz1-mediated terminal differentiation program initiated by Myc overexpression, to maintain the intermediate progenitor cells in a partially differentiated, yet proliferative state, and to evade cell death.

AACR: Developmental Biology and Cancer, Boston, MA, Nov 30-Dec 3, 2015.

Elucidating ING4 Targets Important in Prostate Epithelial Cell Differentiation and Examining CREB as a Key Regulator of ING4 Expression

Penny Berger[1], McLane Watson[1], Mary E. Winn[2], Cindy K. Miranti[1]

[1]Laboratory of Integrin Signaling, [2]Bioinformatics and Biostatistics Core, Van Andel Research Institute, Grand Rapids, MI

Background: Chromatin remodeling protein ING4 is integral to prostate epithelial cell (PrEC) differentiation, and its loss, in 60% of human PCa tumors, is required for PCa development. How ING4 is lost and how its loss initiates PCa is unknown.

Methods: Using our human PrEC in vitro differentiation assay, we interrogated the gene expression profile by RNA-Seq at different time points during differentiation to identify upstream and downstream ING4 regulators. ING4 is transiently induced between 10 and 14 days of differentiation and then switched off during terminal differentiation.

Results: ING4 induction coincides with luminal cell detachment from matrix and loss of integrin α6β1 expression. Integrin α6β1 suppression requires the Myc/Miz1 repressor. In PCa, integrin α6β1 is aberrantly retained, but the mechanism is unknown. We found Miz1 expression induced coincident with ING4. Blocking ING4 prevented Miz1 induction, while ING4 overexpression induced Miz1. Using ChIP, we found Miz1 to be a direct target of ING4. GeneGo analysis of RNA-seq data identified 20% of the differentially expressed genes as CREB targets. CREB1 activity, as measured by immunoblotting (P-CREB), peaked after ING4 induction, as did CREB-induced differentiation targets, BLIMP1 and Claudin1. CREB1 was bound to the ING4 promoter at sites known to suppress ING4 expression. A second ING4 regulator and CREB target, E3 ligase JFK (FBX04), was induced when P-CREB peaked. CREB is activated by many signaling pathways, including PI3K/Akt. Pten loss prevents ING4 expression, stalls differentiation, and is required for tumorigenesis. Based on the timing of Pten, ING4, and P-CREB expression, we hypothesize Pten is required for ING4 expression, but as Pten expression decreases and PI3K/Akt activity increases, CREB is activated to turn off ING4. In support, we found constitutively elevated P-CREB and no ING4 expression in Pten null cells. RNA-Seq analysis of Pten null cells revealed an abundance of CREB targets. However, these were distinctly different from the CREB targets identified in normal differentiated cells.

Conclusions: **1)** ING4 is required to induce Miz1 to suppress integrin α6 and β1 expression during PrEC terminal differentiation, and loss of ING4 in prostate cancer prevents Miz1 induction and allows integrin α6 and β1 to be retained. **2)** CREB promotes PrEC terminal differentiation by suppressing ING4 transcription and activating its E3 ligase. **3)** Pten loss in human PrECs results in constitutive CREB activation, prevents ING4 induction, stalls differentiation, and induces a 'tumor-specific' CREB signature.

Society for Basic Urologic Research: Environment-Gene Interface in Urologic Disease, Fort Lauderdale, FL, Nov 12-15, 2015.

Human Prostate Luminal Cell Differentiation requires NOTCH3 Induction by p38-MAPK and MYC

Frank SB, Berger PL, Ljungman M and Miranti CK.

Background: Prostate tumors co-express markers normally restricted to basal or luminal epithelium (e.g. ITGα6+AR). Moreover, many pathways dysregulated in prostate cancer are also involved in epithelial differentiation. To better understand how defective differentiation may lead to tumor initiation in prostate epithelium, we sought to investigate specific genes and mechanisms required for normal basal to luminal cell differentiation. p38-MAPK, MYC, and NOTCH have all been implicated in epithelial differentiation, however there are few detailed mechanisms for their functions and downstream targets. We tested the hypothesis that p38-MAPK regulation of NOTCH3, via MYC, is required for luminal differentiation.

Methods: Immortalized primary prostate basal epithelial cells (iPrECs) were differentiated *in vitro* into luminal cells using KGF and androgen. Differentiation was monitored by immunofluorescence for basal (ITGα6) and luminal (AR) markers. Additionally, cells were harvested at various time points and analyzed for various gene expression at the mRNA (qRT-PCR) and protein (immunoblot) levels. Pathways were antagonized by siRNA, lentiviral Dox-induced shRNA, or pharmacologic inhibitors. Overexpression and constitutive activation were achieved with lentiviral Dox-inducible cDNA constructs. Transcriptional regulation of NOTCH3 was investigated by cloning candidate enhancer elements into a luciferase reporter vector and eRNA was detected via BruUV-seq. Lastly, mRNA half-life was determined by ActinomycinD mRNA decay timecourse with qRT-PCR.

Results: Inhibition (SB202190, BIRB796) or knockdown of p38α and/or p38δ prevented proper differentiation. Additionally, treatment with a γ-secretase inhibitor (RO4929097) or knockdown of NOTCH1 or NOTCH3 greatly impaired differentiation and caused luminal cell death. Acute p38-MAPK activation via Dox-induced MKK6(CA) (constitutively active MKK6 mutant) increased NOTCH3 (but not NOTCH1) mRNA/protein levels and was diminished upon MYC inhibition (10058-F4) or knockdown. Furthermore, we validated two *NOTCH3* enhancer elements by a combination of eRNA detection and luciferase reporter assay. Lastly, we found that *NOTCH3* mRNA half-life increased during differentiation or upon acute p38-MAPK activation.

Conclusions: Our results reveal a new connection between p38-MAPK and NOTCH signaling that is bridged by MYC. Moreover, this work demonstrates two mechanisms of *NOTCH3* mRNA regulation both by enhancer-driven transcription and increased mRNA stability and provides evidence for NOTCH3 playing a specialized role in the prostate. Together, these findings reveal a new mechanism to unite multiple key differentiation pathways in the prostate and may provide new insights into possible mechanisms of oncogenesis.

Society for Basic Urologic Research Phoenix, AZ November 10-14, 2016.

Pten and CREB Cooperativity during Prostate Luminal Epithelial Differentiation is Disrupted in Prostate Cancer

Watson M[1], Berger PL[1], Frank SB[1,2], and Cindy K. Miranti[1]

[1]Laboratory of Integrin Signaling and Tumorigenesis, Van Andel Research Institute, Grand Rapids, MI and [2]Genetics Graduate Program, Michigan State University, Lansing, MI

Myc is overexpressed in the majority of human prostate cancers (PCa), yet the mechanisms by Myc drives (PCa) are not fully understood. Using a novel *in vitro* differentiation model in which human basal prostate epithelial cells (PrECs) are induced to differentiate into luminal cells, we previously demonstrated that Myc is required for transient expression of the chromatin-binding protein ING4, whose transient induction and subsequent down regulation is required for normal luminal cell differentiation. ING4 expression is lost in >60% of primary prostate tumors, loss of ING4 prevented PrEC differentiation, and was necessary for Myc-dependent tumorigenesis *in vivo*. Furthermore, loss of Pten prevented ING4 induction and differentiation (Cancer Res 74:3357-68, 2014). Our objective is to identify the mechanism by which ING4 expression is controlled by Pten. Using RNA-Seq to interrogate genes induced during PrEC differentiation we determined that ~20% of the differentially regulated genes are targets of the transcription factor, CREB. Furthermore, CREB-regulated genes were highly expressed in PrECs transformed by overexpression of Erg, Myc, and shRNA to Pten (EMP cells). However, the CREB genes induced in normal PrECs were completely different from the genes induced in EMP cells, suggesting there is a major genetic switch surrounding CREB-mediated transcription in tumor cells vs normal cells. We found that during normal PrEC differentiation, Pten is elevated until around Day 8-10, then its expression drops and CREB is then activated around Day 12. Loss of Pten results in constitutive activation of CREB indicating that Pten acts to control the timing of CREB activation. ING4 is induced prior to CREB activation and decreases when CREB activity is high, and removal of CREB by shRNA results in constitutive induction of ING4. Thus, CREB is a negative regulator of ING4, downstream of Pten during normal PrEC differentiation. Thus, in the tumor cells when Pten is lost, CREB is constitutively activated and prevents ING4 induction. Furthermore, in this context CREB induces a different set of genes that promote tumorigenesis, rather than differentiation. Defining these differential targets may allow us to identify specific therapeutic targets or biomarkers.

11th Prostate Cancer Symposium at Clark Atlanta University, Atlanta, GA, September 26-28, 2016

Pten Loss Promotes Prostate Cancer Tumorigenesis through Disruption of a CREB-Dependent Differentiation Pathway

McLane J. Watson[1], Penny L. Berger[1], Sander B. Frank[2], Ashton J. Basile[2], and Cindy K. Miranti[1,2]

[1]Van Andel Research Institute, Grand Rapids, MI and [2]Dept of Cellular and Molecular Medicine, University of Arizona, Tucson, AZ.

Background: Genetic drivers of prostate cancer (PCa) development, including Myc overexpression or Pten loss, are linked to prostate epithelial differentiation. But, how these oncogenes alter the differentiation program during PCa development remains unresolved. We previously showed, in normal human prostate epithelium, that Myc induces transient expression of a chromatin-binding protein, ING4, which is required for prostate luminal cell differentiation. However, ING4 expression is lost in >60% of primary tumors and ING4 loss prevents luminal cell differentiation. In fact, ING4 loss is necessary for Myc-overexpressing cells to produce tumors. We further found that Pten loss prevents luminal cell differentiation by blocking ING4 induction and 50% of primary tumors with ING4 loss also lack Pten. We sought to determine how Pten loss suppresses ING4 expression and differentiation.

Methods: We used RNA-Seq to identify gene signatures induced during human luminal cell differentiation and compared them to those induced in tumor cells with combined Myc overexpression and Pten loss (Myc/shPten). Gene signatures were validated by qRT-PCR and immunoblotting. Functional assessment of the role of specific genes on differentiation, ING4 expression, and tumorigenesis was carried out using shRNA knock-down and chromatin immunoprecipitation (ChIP).

Results: During luminal cell differentiation, ~30% of the differentially regulated genes are targets of the transcription factor CREB. We found that late in luminal cell differentiation, ATF1 activation precedes CREB1, at a time when Pten expression drops. CREB-target genes associated with luminal cell differentiation are induced at this time, including ING4 and its E3-ligase JFK. Accordingly, CREB1/ATF1 are bound to the promoters of both ING4 and JFK. Paradoxically, knock-down of CREB1 results in overexpression of ING4 and accelerated differentiation, while knock-down of ATF1 prevents ING4 induction and differentiation. Loss of CREB1 also eventually induces luminal cell death. Surprisingly, a large set of CREB-regulated genes are highly expressed in the Myc/shPten tumor cells; however, this set of genes is distinctly different from those induced in the normal cells. Pten loss, with or without Myc overexpression, is sufficient to constitutively activate CREB1 and ATF1 in normal prostate epithelium. Several CREB targets involved in progenitor cell maintenance, including GATA2 and Twist1, are elevated in the tumor cells. Knock-down of CREB1 in tumor cells restores ING4 expression and rescues differentiation.

Conclusions: Early in prostate luminal cell differentiation, elevated Pten prevents premature activation of ATF1 and CREB1. ATF1 is required for the transcriptional induction of ING4 and initiation of luminal differentiation, while CREB1 limits ING4 expression, possibly through induction of its E3-ligase, and is required for luminal cell survival. However, in the absence of Pten, CREB1 and ATF1 are activated prematurely, preventing ING4 induction and terminal differentiation, leading to maintenance of a progenitor cell-like proliferative population.

Impact: Determining which PCa patients are at risk for lethal disease remains a major challenge. We propose there will be a specific combination of oncogenic events and differentiation alterations that produce an aggressive subtype of PCa. If this signature can be identified, then the ability to distinguish indolent from lethal disease can be achieved.

University of Arizona Cancer Center Retreat, Tucson, AZ, Apr 21, 2017

CREB1 and ATF1 differentially regulate terminal prostate luminal cell differentiation by controlling the timing of ING4 expression, while CREB1 prevents ING4 expression upon PTEN loss in prostate cancer

McLane Watson[1], Penny Burger[1], Sander Frank[2], Mary Winn[1], and Cindy K. Miranti[1,2]

[1]Van Andel Research Institute, Grand Rapids, MI and [2]University of Arizona Cancer Center, Tucson, AZ

We previously demonstrated that transient ING4 expression is required for luminal cell differentiation. Additionally, ING4 is downregulated in ~60% of primary prostate tumors and its loss is correlated with loss of PTEN. We further demonstrated in a primary prostate cancer model overexpressing ERG, MYC, and shPTEN (EMP) that loss of PTEN was responsible for ING4 downregulation, though the mechanism remained elusive. Utilizing RNA-seq and our *in vitro* differentiation model, we identified transcriptional nodes required for luminal differentiation. Of the ~600 differentially regulated genes during differentiation, the largest transcription factor signature (29% of genes) was CREB/ATF. A subset of these targets (Blimp1, Claudin1, Plk2, Chek1) were further validated by qRT-PCR and immunoblotting.

CREB/ATF bind constitutively to open chromatin CRE elements and can be activated by multiple kinases, including AKT. Both CREB1 and ATF1 are inducibly phosphorylated midway through luminal differentiation, with ATF1 preceding CREB1. Knockdown of CREB1 with shRNA increased ING4, accelerated differentiation, and induced premature luminal cell death. Conversely, knockdown of ATF1 blocked ING4 induction and prevented supra-basal layer formation. CREB1/ATF1 ChIP was enriched at the ING4 promoter at mid-differentiation, when ING4 expression peaks. Additionally, CREB1/ATF1 was constitutively bound to the promoter of JFK, an E3-ligase that targets ING4 and whose mRNA levels increase during differentiation. Thus, we propose that ATF1 is required to induce ING4 transcription while CREB1 suppresses ING4 by both transcriptional repression and induction of JFK. We compared the gene signature of differentiated cells to that of the tumorigenic EMPs. Surprisingly, 30% of the differentially expressed genes were CREB/ATF targets but there is less than 10% overlap, indicating CREB/ATF control distinct subsets of genes in differentiated luminal cells versus cancer cells. Some EMP-specific CREB/ATF targets (GATA2, TWIST1, Necdin, PPM1F) were further validated by qRT-PCR and immunoblotting. CREB1 and ATF1 were highly phosphorylated in EMP cells and knockdown of CREB1 restored ING4 expression and supra-basal formation.

Our working model is that AKT activation upon PTEN loss in transiently differentiating luminal cells results in premature and constitutive activation of CREB1/ATF1 bound to genes prior to induction of the ING4 chromatin switch. This prevents ING4 induction and the chromatin rearrangements required for terminal differentiation. In normal PrECs, CREB/ATF1 activation is tightly controlled by as of yet undetermined factors and is only permitted when the proper CRE binding sites are exposed. This model helps to explain how loss of PTEN disrupts luminal cell terminal differentiation to promote prostate cancer oncogenesis.

SBUR Annual Meeting: Multiple Genetic and Epigenetic Mechanisms of Urologic Disease, Tampa, FL, Nov 9-12, 2017. Abstract Published in **Am J Clin Exp Urol** 2017;5(Suppl 1):1-92 Poster P51, p60. www.ajceu.us

CREB1 and ATF1 differentially regulate terminal prostate luminal cell differentiation by controlling the timing of ING4 expression, while CREB1 prevents ING4 expression upon PTEN loss in prostate cancer

McLane Watson[1], Penny Burger[1], Sander Frank[2], Mary Winn[1], and Cindy K. Miranti[1,2]

[1]Van Andel Research Institute, Grand Rapids, MI and [2]University of Arizona Cancer Center, Tucson, AZ

Many genes aberrantly expressed in prostate cancer are involved in normal basal to luminal cell differentiation. We previously demonstrated that transient ING4 expression is required for luminal cell differentiation and is downregulated in ~60% of primary prostate tumors. We further demonstrated in a primary prostate cancer model overexpressing ERG, MYC, and shPTEN (EMP) that loss of PTEN was responsible for ING4 loss. Furthermore, half of the human tumor samples that lose ING4 have also lost PTEN. However, we did not know how PTEN loss inhibits ING4 expression. Utilizing our *in vitro* differentiation model, whereby prostate basal epithelial cells (iPrEC) treated with KGF and androgen induce a supra-basal layer of luminal-like cells, and RNA-seq we identified transcriptional nodes required for luminal differentiation. Differentially expressed genes were analyzed by GeneGo to identify enriched transcription-factor signatures. Of the ~600 differentially regulated genes during differentiation, the largest signature (29% of genes) was CREB/ATF targets. Induction of Blimp1, Claudin1, and Plk2 and inhibition of Chek1 were further validated by qRT-PCR and immunoblotting.

CREB/ATF bind constitutively to open chromatin CRE elements in the promoters of genes and are activated through signaling-induced phosphorylation at Ser133 by kinases, including AKT. We found that both CREB1 and ATF1 are inducibly phosphorylated midway through luminal differentiation, with ATF1 preceding CREB1. Knockdown of CREB1 with shRNA increased ING4, accelerated differentiation, and induced premature luminal cell death. Conversely, knockdown of ATF1 blocked ING4 induction and prevented supra-basal layer formation. CREB1/ATF1 ChIP was enriched at the ING4 promoter at mid-differentiation, when ING4 expression peaks. Additionally, CREB1/ATF1 was constitutively bound to the promoter of JFK, an E3-ligase that targets ING4 and whose mRNA levels increase during differentiation. Thus, we propose that ATF1 is required to induce ING4 transcription, while CREB1 suppresses ING4 and simultaneously activates its E3-ligase to tightly control the timing of ING4 expression. We compared the gene signature of luminal cells to that of the tumorigenic EMP cells and surprisingly found 30% of the differentially expressed genes were also CREB/ATF targets. However, there is less than 10% overlap in these targets, indicating CREB/ATF control distinct subsets of genes in differentiated luminal cells versus cancer cells. Some of EMP-specific CREB/ATF targets included GATA2, TWIST1, Necdin, and PPM1F, which were further validated by qRT-PCR and immunoblotting. CREB1 and ATF1 were highly phosphorylated in EMP cells and knockdown of CREB1 restored ING4 expression and supra-basal formation.

Our working model is that AKT activation upon PTEN loss in transiently differentiating luminal cells results in premature and constitutive activation of CREB1/ATF1 bound to genes prior to induction of the ING4 chromatin switch. This prevents ING4 induction and the chromatin rearrangements required for terminal differentiation. In normal PrECs, CREB/ATF1 activation is tightly controlled by as of yet undetermined factors and is only permitted when the proper CRE binding sites are exposed. This model helps to explain how loss of PTEN disrupts luminal cell terminal differentiation to promote prostate cancer oncogenesis.

AACR Special Conference on Prostate Cancer, Orlando, FL, Dec 2-5, 2017.

Published OnlineFirst April 24, 2014; DOI: 10.1158/0008-5472.CAN-13-3076

Transient Induction of ING4 by Myc Drives Prostate Epithelial Cell Differentiation and Its Disruption Drives Prostate Tumorigenesis

Penny L. Berger[1], Sander B. Frank[1,5], Veronique V. Schulz[1], Eric A. Nollet[1,4], Mathew J. Edick[1], Brittany Holly[2], Ting-Tung A. Chang[2], Galen Hostetter[3], Suwon Kim[6], and Cindy K. Miranti[1]

Abstract

The mechanisms by which Myc overexpression or Pten loss promotes prostate cancer development are poorly understood. We identified the chromatin remodeling protein, ING4, as a crucial switch downstream of Myc and Pten that is required for human prostate epithelial differentiation. Myc-induced transient expression of ING4 is required for the differentiation of basal epithelial cells into luminal cells, while sustained ING4 expression induces apoptosis. ING4 expression is lost in >60% of human primary prostate tumors. ING4 or Pten loss prevents epithelial cell differentiation, which was necessary for tumorigenesis. Pten loss prevents differentiation by blocking ING4 expression, which is rescued by ING4 re-expression. Pten or ING4 loss generates tumor cells that co-express basal and luminal markers, indicating prostate oncogenesis occurs through disruption of an intermediate step in the prostate epithelial differentiation program. Thus, we identified a new epithelial cell differentiation switch involving Myc, Pten, and ING4, which when disrupted leads to prostate tumorigenesis. Myc overexpression and Pten loss are common genetic abnormalities in prostate cancer, whereas loss of the tumor suppressor ING4 has not been reported. This is the first demonstration that transient ING4 expression is absolutely required for epithelial differentiation, its expression is dependent on Myc and Pten, and it is lost in the majority of human prostate cancers. This is the first demonstration that loss of ING4, either directly or indirectly through loss of Pten, promotes Myc-driven oncogenesis by deregulating differentiation. The clinical implication is that Pten/ING4 negative and ING4-only negative tumors may reflect two distinct subtypes of prostate cancer. *Cancer Res; 74(12); 3357–68. ©2014 AACR.*

Introduction

Normal prostate glands contain prostatic ducts composed of two distinct layers of epithelial cells: luminal cells that express androgen receptor (AR) and secrete prostate-specific antigen (PSA) and basal cells that express nuclear p63. It is thought that the stem or progenitor cells within or in proximity of the basal layer differentiate and give rise to the luminal cells (1, 2). Prostate tumors are often devoid of the cell layer distinction and express both luminal and basal cell markers, suggesting deregulated cell differentiation. That prostate cancer arises from deregulated differentiation is also supported by mouse models. The most notable example is loss of Nkx3.1, a known prostate-specific differentiation gene, which predisposes mice to develop prostate cancer in the context of additional oncogenic events (3). Two other well characterized oncogenic events linked with prostate cancer are loss of Pten or overexpression of Myc (4, 5). Both of which lead to downregulation of Nkx3.1 expression, but are also sufficient to induce prostate cancer in mice (6, 7). The prostate-specific oncogene, TMPRSS2-Erg, when overexpressed in mouse prostates leads to prostate intraepithelial neoplasia (PIN), with a corresponding change in differentiation, where progenitor cell markers Sca1 and integrin α6 are increased, whereas basal cell keratin is diminished and AR is expressed (8, 9). In addition, overexpression of Erg upregulates Myc expression and produces an expression profile consistent with a change in differentiation (10). A recent mouse study where Pten was deleted in either basal or luminal cells, demonstrated the appearance of $K5^+/K8^+$ intermediate tumor cells, further supporting the idea that deregulated differentiation is a hallmark of prostate cancer (11). However, the mechanism by which differentiation is deregulated is unknown.

We recently reported on an *in vitro* differentiation model in which AR-negative human basal prostate epithelial cells can be differentiated into AR-positive and androgen-responsive

Authors' Affiliations: [1]Laboratory of Integrin Signaling; [2]Laboratory of Translational Imaging; and [3]Laboratory of Analytical Pathology; and [4]Van Andel Institute Graduate School, Grand Rapids; [5]Genetics Graduate Program, Michigan State University, Lansing, Michigan; and [6]Tranlational Genomics Research Institute and University of Arizona College of Medicine, Phoenix, Arizona

Note: Supplementary data for this article are available at Cancer Research Online (http://cancerres.aacrjournals.org/).

Corresponding Author: Cindy K. Miranti, Laboratory of Integrin Signaling, Van Andel Research Institute, 333 Bostwick Avenue NE, Grand Rapids, MI 49503. Phone: 616-234-5358; Fax: 616-234-5359; E-mail: cindy.miranti@vai.org

doi: 10.1158/0008-5472.CAN-13-3076

Published OnlineFirst April 24, 2014; DOI: 10.1158/0008-5472.CAN-13-3076

postmitotic secretory cells (12). Based on known prostate and epithelial differentiation markers, and the demonstration that PSA can be secreted into the medium from the differentiated cells, this model recapitulates the biology and physiology of the human prostate gland *in vivo*. A major step in the differentiation process is the loss of integrin expression and cell–matrix adhesion, which is crucial to generate stable AR-expressing cells. This is accompanied by a dramatic shift in survival signaling pathways, whereby basal cells, which survive primarily through integrin-mediated activation of the Erk signaling pathway, give rise to secretory cells that depend on E-cadherin based cell–cell adhesion and activation of Akt for survival.

The separation of AR and integrin functions in the two different epithelial populations is wholly consistent with what is observed *in vivo*; that integrin expression is limited to the basal cells and AR is only in the secretory cells (13, 14). In prostate cancer this distinction is lost, whereby AR and integrin α6β1 are coexpressed in the tumors, where integrin α6β1 cooperates with AR to promote the survival of prostate cancer cells (15). Other markers typically associated with basal or intermediate cells, such as receptor tyrosine kinases EGFR and Met, bcl-2, and coexpression of basal and secretory keratins K5 and K8, are also found in tumor cells that express AR-dependent differentiation genes (14, 16, 17). Thus, the majority of the primary tumor population in prostate cancer resembles a potential differentiation intermediate. In addition, the unexplained loss of basal cells in prostate cancer points to altered differentiation as a major factor in prostate cancer (18).

Myc is overexpressed in up to 90% of primary prostate tumors, presenting itself as a major driver in prostate cancer (4). Recent studies have unraveled the function of Myc in reprogramming of somatic cells into pluripotent stem cells and the maintenance of self-renewal in stem cells (19), and is consistent with the idea that deregulated Myc prevents full differentiation of prostate epithelial cells, leading to prostate cancer when given additional molecular lesions. ING4 is a tumor suppressor whose expression is lost in several cancers; but whose role in prostate cancer is unknown (20). ING4 is a plant homeodomain–containing transcriptional regulator, which binds trimethylated histone H3 and recruits the HBO1 acetyltransferase to increase histone acetylation (21). ING4 was shown to block Myc-induced anchorage-independence and mammary hyperplasia in a mouse model of breast cancer, suggesting ING4 may function to suppress Myc (22, 23). We hypothesized there would be an interplay between Myc and ING4 in prostate epithelial cell differentiation that would be disrupted in prostate tumorigenesis. In this study, we determine how Myc, Pten, and ING4 are involved in normal prostate epithelial differentiation and demonstrate the importance of ING4 loss in promoting prostate oncogenesis through suppressing differentiation.

Materials and Methods

Cell lines

Primary basal prostate epithelial cells were isolated from clinical prostectomies as previously described (24, 25). Cultures were validated to be Mycoplasma-free and express only basal epithelial cell markers (12, 25). Cells were immortalized with retroviruses expressing HPV E6/E7 and hTert, selected in 150 μg/mL neomycin for 3 days, and the resulting population pooled. Cells retain all the basal markers of primary cells. Immortalized cells (iPrEC) were transformed by retroviruses expressing Erg and Myc (EM), and lentivirus expressing Pten shRNA (EMP) or ING4 shRNA (EMI), then selected and maintained in 0.35 μg/mL puromycin. All lines were maintained and passaged as previously described (24, 25).

Differentiation protocol

Differentiation and layer separation protocols were detailed previously (12). Briefly, iPrECs at confluency were treated in complete growth medium with 10 ng/mL keratinocyte growth factor (KGF; Cell Sciences) and 5 nmol/L R1881 (PerkinElmer) every other day for up to 21 days. For biochemical analysis, the suprabasal differentiated layer was separated from the basal layer as previously described (12).

Constructs

The wild-type retroviral pBabe-Myc construct was obtained from Dr. B. Knudsen. pLPCX-Erg was generated by subcloning the *ERG* cDNA *Not*I/*Spe*I fragment from pMax Dest ΔN-Erg (9), supplied by Dr. Vasioukhin, into *Not*I/*Xho*I of pLPCX. The wild-type (pMIG-ING4) and C-terminal deletion mutant (pMIG-ING4-ΔC1) of ING4 were described previously (23). The ING4 shRNA construct was generated by subcloning the oligo 5'-CCGGGCTAGGTGTGATCAACACTTTCTCGAGAAAGTGTT-GATCACACCTAGCTTTTTTG-3', complementary to the 3'-UTR of ING4, into a lentiviral vector to generate pLKO.1-shING4. The pLKO vector containing Pten shRNA was generated by first creating a pCR8-GW-TOPO-shLEGO shuttle vector. A 344bp PCR product containing a multicloning site, *Eco*RV/*Xba*I/*Sal*I/*Pst*I, the pLKO U6 promoter, an *Age*I site, a *Hin*dIII site, followed by a reverse multicloning site, *Pst*I/*Sal*I/*Xba*I/*Eco*RV, and an *Eco*RI site was TA cloned into pCR8-GW-TOPO. Oligo shPten2, 5′-CCGGTCCACAGCTAGAACTTAT-CAAACTCGAGTTTGATAAGTTCTAGCTGTGGTTTTTA-3′, was cloned into the *Age*I/*Hin*dIII site of the pCR8-GW-TOPO-shLEGO shuttle vector. The *Age*I/*Eco*RI fragment was subcloned into pLKO to generate pLKO-shPten2.

Virus generation and infection

Lentivirus shRNAs were generated by transfecting a packaging cell line, harvesting virus 3 days later and immediately infecting iPrECs. Cells were selected and pools maintained in 0.35 μg/mL puromycin. Retroviruses expressing ING4 or Myc were generated by transfecting Phoenix cells (National Gene Vector Biorepository), harvesting 2 days later and immediately infecting iPrECs. Myc expressing cells were selected and maintained in 0.35 μg/mL puromycin. ING4 construct has no selectable marker and cells were generated *de novo* as needed.

siRNA transfection

A pool of siRNAs against Myc and a nontargeting sequence were purchased from Origene. ON-Targetplus SMARTpool targeted to Bnip3, came from Dharmacon. Differentiated cultures were serially transfected every 2 days with Myc or

Published OnlineFirst April 24, 2014; DOI: 10.1158/0008-5472.CAN-13-3076

control siRNA using siLentFect lipid reagent (Bio-Rad) following manufacturer's directions. Cells were placed in differentiation medium 18 hours after transfection.

Antibodies

Immunofluorescence. AR (C-19), Nkx3.1 (H-50), and TMPRSS2 (H-50) were purchased from Santa Cruz. ITGα6 (GoH3) was purchased from BD Pharmingen, and PSA (18127) from R&D Systems. Keratin 8 (M20) came from Abcam and Keratin 5 (AF-138) came from Covance. ING4 monoclonal antibody was generated as previously described (26) and a polyclonal antibody was obtained from Proteintech. Cleaved caspase-3 (Asp175)(5A1E) was purchased from Cell Signaling.

Immunoblotting. Myc (o6–340) was purchased from Millipore, Erg (C-20) from Santa Cruz, Pten (138G6) and p27 (Kip1) from Cell Signaling, and ING4 (EP3804) from GeneTex. Tubulin antibody (DM1A) was purchased from Sigma and GAPDH (6CS) from Millipore. Polyclonal integrin α6 (AA6A) antibody was a gift from Dr. A. Cress (University of Arizona; ref. 27).

Immunostaining and microscopy

Differentiated cultures were fixed in 4% paraformaldehyde and permeabilized with 0.2% Triton-X 100. After washing, cells were blocked with 2% normal goat serum for 2 hours. Primary antibodies, diluted in 1% BSA/PBS, were applied to samples overnight at 4°C. After washing, secondary conjugated antibodies diluted in 1% BSA/PBS were incubated for 1 to 2 hours. Nuclei were stained with Hoechst 33258 (Sigma) for 10 minutes at room temperature. Coverslips were mounted using Fluoromount-G (SouthernBiotech). Epifluorescent images were acquired on a Nikon Eclipse TE300 fluorescence microscope using OpenLab v5.5.0 image analysis software (Improvision). Confocal images were acquired by sequential detection on an Olympus FluoView 1000 LSM using FluoView software v5.0.

Immunoblotting

Total cell lysates were prepared for immunoblotting as previously described (24). Briefly, cells were lysed in RIPA buffer, 30 to 50 μg of total cell lysates were run on SDS polyacrylamide gels and transferred to PVDF membranes. Membranes were blocked in 5% BSA in TBST overnight at 4°C then probed with primary antibody, and HRP-conjugated secondary antibodies (Bio-Rad) in TBST + 5% BSA. Signals were visualized by chemiluminescence reagent with a CCD camera in a Bio-Rad Chemi-Doc Imaging System using Quantity One software v4.5.2 (Bio-Rad).

RT-PCR

Total RNA was isolated using Qiagen's RNeasy Kit. RNA was purified with RNase-free DNase and RNeasy Mini Kits (Qiagen). For qRT-PCR, 0.5 μg RNA was reversed transcribed using a reverse transcription system (Promega). Synthesized cDNA was amplified for qRT-PCR using SYBR Green Master Mix (Roche) with gene-specific primers and an ABI 7500 RT-PCR system (Applied Biosystems). Gene expression was normalized to 18s rRNA by the 2-ΔΔCt method (28). Primers for ING4 and Myc were as follows: ING4: 5′-TCGGAAGTTGCTTTGTTTTGC-3′, Myc: 5′-TTCGGGTAGTGGAAAACCAG-3′.

Mouse tumorigenesis

Half a million iPrEC, EM, EMP, EMI, or EM-vector cells were injected orthotopically into the prostates of 8-week nude mice. Mice were monitored by ultrasound between 8 and 18 weeks for the development of tumors. Mice were sacrificed between 16 and 18 weeks and prostate glands analyzed histologically for tumors. In one cohort of EMPs, 5 mice with tumors were castrated 16 weeks postorthotopic transplantation and measured by ultrasound for regression of tumors. All animal work was carried out following Institutional Animal Care and Use Committee approval at an Association for Assessment and Accreditation of Laboratory Animal Care-accredited facility.

Histology

Prostates isolated from mice were formalin-fixed and paraffin-embedded. Sections were analyzed following hematoxylin and eosin or immunohistochemical (IHC) staining. Human-specific MHC class I was purchased from Abcam, polyclonal ING4 was purchased from ProteinTech, and AR (N-20) was purchased from Santa Cruz. IHC was performed using automated immunostaining (Ventana Discovery XT). A human prostate tumor survey tissue microarray (TMA) was constructed as previously described (29). The prostate survey TMA contained 52 de-identified unique prostate carcinomas ranging from Gleason 6 to 9 and 23 control cores, including 14 cases of benign prostatic hypertrophy (BPH). TMA sectioned at 5 μm thicknesses was stained using standard DAB. IHC was performed with ING4 antibody as previously described (26, 30). For validation, sections were also stained with a commercial ING4 antibody (ProteinTech). Negative control was nonimmune rabbit antiserum without primary antibody. TMA staining was scored manually with IHC assigned to each core as composite scores of 0, 1, 2, or 3 with 0 to 1 representing complete to major loss of protein, and 2 to 3 near normal to wild-type levels.

Results

Myc and ING4 are transiently expressed during differentiation

When grown to confluency and treated with KGF plus androgen, primary cultures of basal prostate epithelial cells (PrEC) undergo differentiation such that a second suprabasal layer forms on top of the basal layer in about 2 weeks (12). An immortalized primary prostate epithelial cell line (iPrEC) was established by expressing the E6/E7 viral oncogenes and hTert. Treatment of confluent iPrEC cultures with 10 ng/mL KGF and 5 nmol/L R1881, a synthetic AR agonist, for 18 days resulted in a distinct top layer of cells that no longer expressed integrin α6, K14, or p63 but expressed AR and AR-dependent targets, such as TMPRSS2 and Nkx3.1 (Fig. 1A and Supplementary Figs. S1 and S2). These data indicate iPrECs retain the ability to differentiate.

ING4 expression was low to undetectable in untreated iPrECs, but by as early as 8 days of differentiation, distinct nuclear staining was detected in the newly forming suprabasal layer of differentiated cells (Fig. 1B). The initial increase in

Published OnlineFirst April 24, 2014; DOI: 10.1158/0008-5472.CAN-13-3076

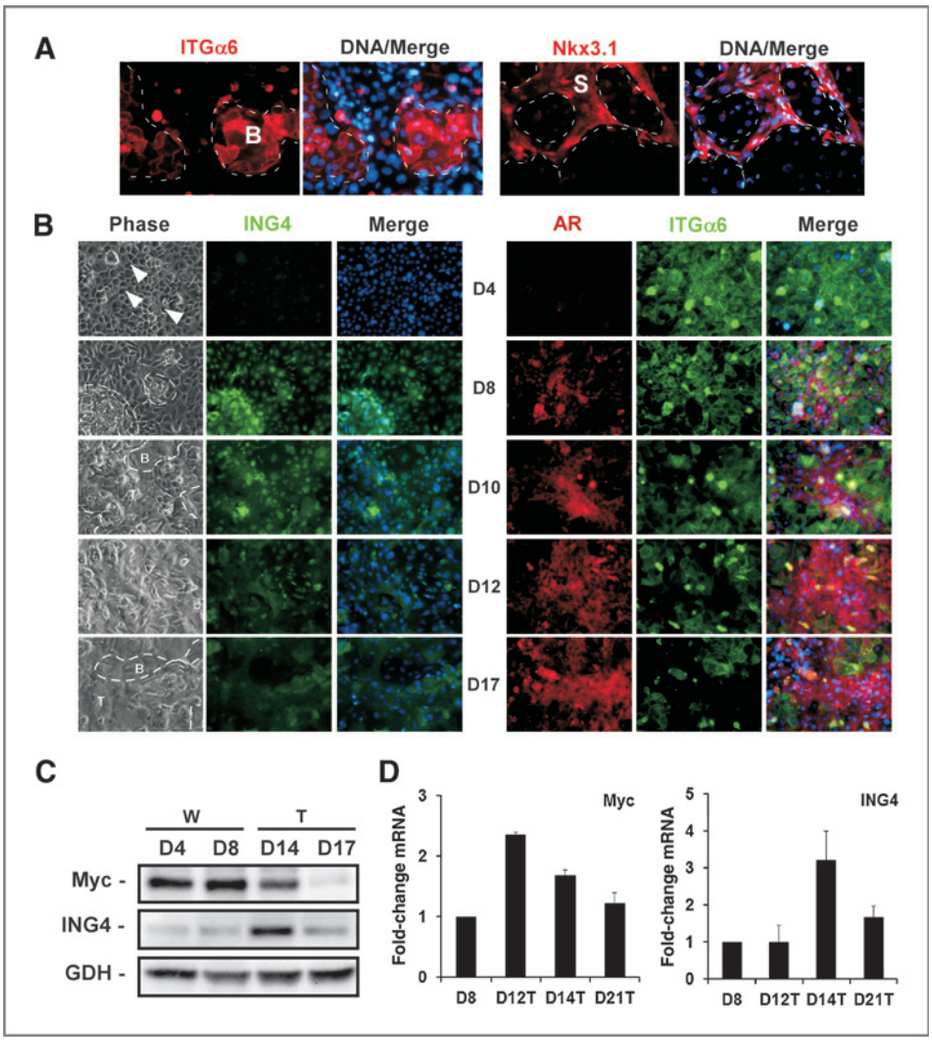

Figure 1. ING4 is transiently expressed in differentiated immortalized prostate epithelial cells. Confluent immortalized prostate epithelial cells (iPrEC) were induced to differentiate with 10 ng/mL KGF and 5 nmol/L R1881 for 4 to 21 days. A, terminally differentiated iPrECs were immunostained (red) and counterstained with Hoechst (blue), then imaged by confocal microscopy. Suprabasal cells (S) express NKX3.1, whereas only basal cells (B) express integrin α6. Dashed lines demarcate suprabasal and basal layer cells. B, iPrECs were immunostained 4 to 17 days after differentiation to detect ING4 (green), AR (red), or integrin α6 (green). C and D, protein or RNA was isolated from whole (W) differentiated cultures at days 4 to 8 or only the suprabasal (T, top) cells at days 12 to 21. C, ING4, Myc, and GAPDH (GDH) were detected by immunoblotting. D, ING4 and Myc mRNA were measured by qRT-PCR. Data are normalized to 18S rRNA and are mean ± SD.

ING4 expression was coincident with the increase in AR expression and the loss of integrin α6 expression, two hallmarks of differentiation (Fig. 1B and Supplementary Fig. S1B). At no time point were we able to dissociate ING4 expression from changes in AR or integrin α6 expression; nor were we able to separate loss of basal keratin K14 from integrin α6 loss (Supplementary Fig. S2), suggesting ING4 controls a major differentiation switch. Although AR persisted in the differentiated layer, ING4 expression was transient and no longer nuclear at later time points.

Once a sufficient number of cells have differentiated, typically between day 12 and 14, it is possible to separate the top layer of differentiated cells from the bottom layer (12). Immunoblot analysis of whole cultures from days 4 and 8, and the top layers from days 14 and 17 indicated a transient increase in ING4 protein expression at day 14, which returned to basal level expression by day 17 (Fig. 1C). ING4 mRNA expression also peaked at day 14 (Fig. 1D). The apparent lag in ING4 expression seen biochemically, compared with the immunostaining data, is most likely because of the low number of differentiated cells within the culture relative to the basal cells at early time points.

Over the same time course, Myc protein and mRNA expression were also transiently elevated (Fig. 1C and D). Myc expression preceded that of ING4 expression, suggesting a concerted temporal regulation of Myc and ING4 during iPrEC differentiation.

Myc-induced ING4 expression is required for differentiation

Cells were engineered to overexpress ING4, Myc, and/or ING4 shRNA (Fig. 2A). Although ING4 expression levels did not affect Myc expression, most notable was the increase in ING4 expression in the Myc overexpressing cells (Fig. 2A and B). These results suggest that Myc is responsible for the increase in ING4 expression during iPrEC differentiation.

Overexpression of ING4 or Myc accelerated the emergence of differentiated cells compared with the control iPrECs. The appearance of suprabasal layer cells, loss of integrin α6, and gain in Nkx3.1 expression was more robust between days 8 and

Published OnlineFirst April 24, 2014; DOI: 10.1158/0008-5472.CAN-13-3076

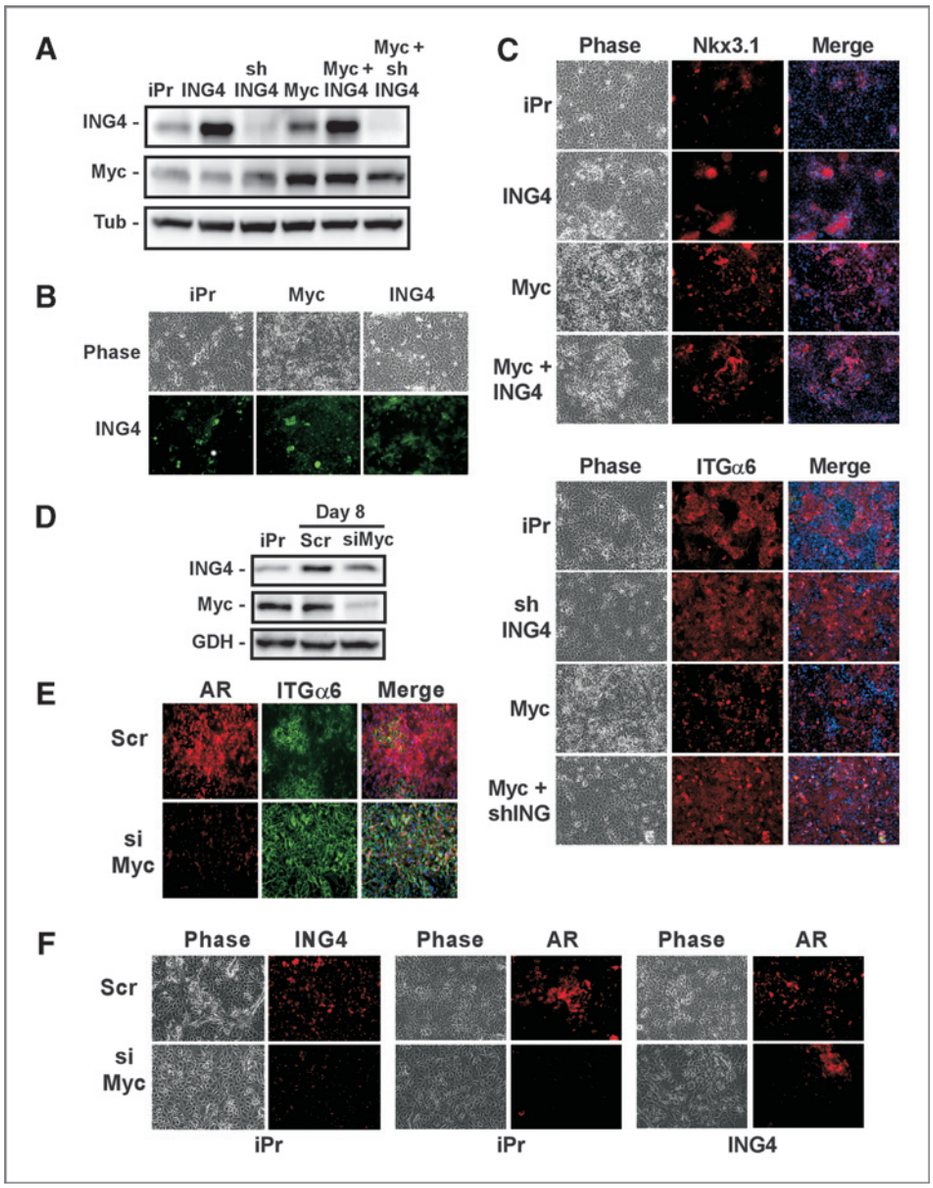

Figure 2. Myc-induced ING4 expression is required for differentiation. iPrECs were engineered to overexpress ING4, Myc, ING4 and Myc, ING4 shRNA (shING4), or Myc with shING4. A, ING4, Myc, and tubulin (Tub) expression in basal cells were measured by immunoblotting. B, cells differentiated for 8 days were immunostained for ING4 (green) and imaged by fluorescent microscopy. C, cells differentiated for 12 days were immunostained (red) to detect NKX3.1 or ITGα6, counterstained with Hoechst (blue), and imaged by fluorescent microscopy. D–F, one day after inducing differentiation, iPrECs (iPr) or iPrECs overexpressing ING4 (ING4) were serially transfected with Myc siRNA (siMyc) or a scrambled sequence (Scr) on days 2, 4, and 6. D, ING4 and Myc expression were detected in undifferentiated (iPr) or in siRNA-treated differentiated cells on day 8 by immunoblotting. E and F, differentiated iPrECs (iPr) or ING4-overexpressing cells were immunostained for ING4 (red), AR (red), or ITGα6 (green) on day 9.

12 in the ING4 or Myc overexpressing cells, whereas the control iPrECs do not robustly express the same set of differentiation markers until days 14 to 16 (day 12 shown in Fig. 2C). Combined overexpression of Myc and ING4 did not exert an additive effect on accelerating differentiation compared with cells overexpressing either Myc or ING4 alone (Fig. 2C). However, it should be noted that the higher levels of ING4 expression in the Myc+ING4 cell line (Fig. 2A) was not always observed; most likely it is not tolerated because of enhanced cell death (see Fig. 3). Thus, it is possible we did not achieve levels of ING4 overexpression required for an additive effect. Downregulation of ING4 expression by shRNA (shING4) severely retarded the emergence of differentiated cells (Fig. 2C). Reduced ING4 expression prevented cells from appearing in the suprabasal layer, and the concomitant loss of integrin α6 (Fig. 2C) and gain of AR, indicating an absolute necessity for ING4 to suppress integrin α6 and permit AR expression.

The ability of Myc to accelerate differentiation was blocked by shING4 (Fig. 2C), indicating ING4 functions downstream of Myc during differentiation. This epistatic relationship is further supported by the fact that transient inhibition of Myc expression between days 2 to 6 failed to induce ING4 expression (Fig. 2D and F) and completely blocked differentiation (Fig. 2E and F). Furthermore, ING4 overexpression rescued the differentiation blocked by siMyc (Fig. 2F). Taken together, our results indicate that a temporal peak in Myc expression is required for the subsequent induction and transient expression of ING4 during iPrEC differentiation.

Published OnlineFirst April 24, 2014; DOI: 10.1158/0008-5472.CAN-13-3076

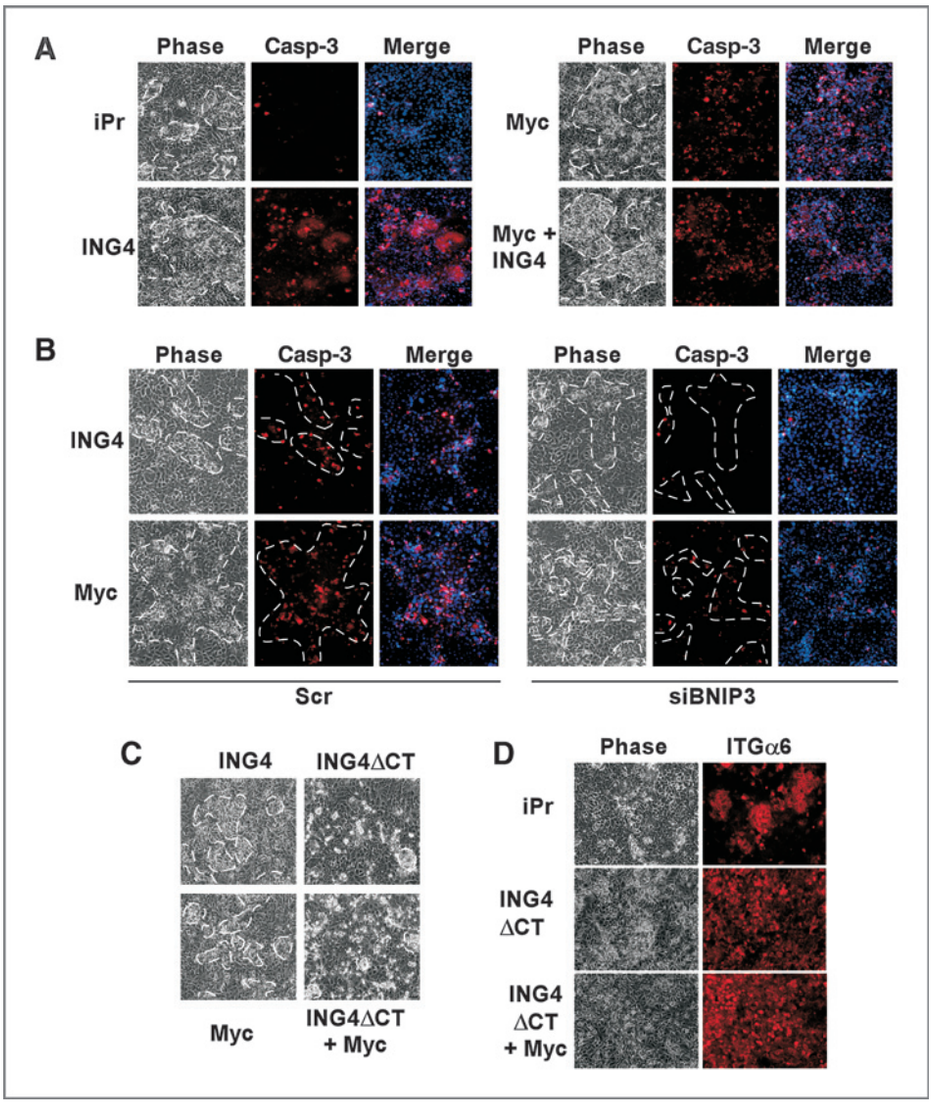

Figure 3. Constitutive Myc and ING4 expression leads to cell death. A, cell death was measured in cells differentiated for 12 days by immunostaining for caspase-3 activity (red). Nuclei were counterstained with Hoechst (blue). B, after 6 days of differentiation, Myc or ING4 overexpressing cells were transfected with Bnip3 siRNA (siBnip3) or a scrambled sequence (Scr) and immunostained 72 hours later for caspase-3 activity (red) and counterstained with Hoechst (blue). White dashes demarcate top layer. C, the C-terminal truncation mutant of ING4 was overexpressed in iPrECs (ING4ΔCT) or in Myc overexpressing cells and compared 8 days after differentiation by phase contrast to cells overexpressing wild-type ING4. D, after 12 days of differentiation, iPrECs (iPr), ING4ΔCT, and Myc plus ING4ΔCT expressing cells were immunostained for integrin α6 (red) and imaged by fluorescent microscopy.

Constitutive Myc and ING4 expression leads to cell death of the differentiated cells via Bnip3

Although Myc or ING4 overexpression initially accelerated iPrEC differentiation, the differentiated cells eventually became disorganized and dissociated from the basal cells, resulting in the loss of the differentiated cell layer (not shown). Differentiated cells from the control iPrEC cultures remained healthy and viable. At day 12, many more apoptotic cells were detected in the differentiating Myc or ING overexpressing cultures as evidenced by increased cleaved caspase-3 (Fig. 3A) and TUNEL staining (not shown) specifically in the suprabasal layer. The basal cell layer remained intact and displayed no evidence of cell death. Thus, sustained overexpression of Myc or ING4, specifically in the differentiated cells, ultimately causes their death.

A qRT-PCR screen for cell death effectors identified elevated expression of Bnip3 (not shown), which encodes a BH3-only proapoptotic protein. Inhibiting Bnip3 expression with siRNA blocked the death induced by ING4 or Myc overexpression, as measured by a reduction in caspase-3–positive cells (Fig. 3B). Blocking Bnip3 expression did not inhibit differentiation (Supplementary Fig. S3), indicating death occurs after differentiation. Thus, the death induced by Myc and ING4 overexpression in differentiated cells is mediated by elevated Bnip3 expression, leading to apoptosis.

The C-terminal domain of ING4 is required for iPrEC differentiation

Myc promotes the trimethylation of H3 at K4 (H3K4me3; ref. 31). ING4 functions in chromatin remodeling complexes by binding to histone H3K4me3 sites via its C-terminal PHD motif and recruiting the HBO1 acetyltransferase via the N-terminal domain (21, 32). Deletion of the PHD motif generates a dominant inhibitory mutant (23). The ability of ING4 to accelerate differentiation was abrogated when the C-terminal domain of ING4 (ING4ΔCT) was deleted (Fig. 3C). This is

Published OnlineFirst April 24, 2014; DOI: 10.1158/0008-5472.CAN-13-3076

further evidenced by the failure to suppress integrin α6 expression (Fig. 3D) in the cells expressing ING4ΔCT. Furthermore, ING4ΔCT blocked the ability of Myc to induce differentiation. Cells that did appear in the suprabasal layer were dying as determined by caspase-3 immunostaining (not shown). Thus, the C-terminus of ING4 containing the PHD domain is required for iPrEC differentiation and survival of the emerging cells, suggesting that the Myc-ING4 differentiation program depends on ING4-dependent chromatin remodeling.

ING4 expression is lost in patient with prostate cancer tumors

To determine whether ING4 expression is altered in prostate cancer, a tissue microarray containing 50 malignant prostate tumors and 12 noncancerous prostates was surveyed for ING4 and AR expression (Fig. 4A). ING4 expression was detected in the nuclei of the luminal cell population of noncancerous samples (Fig. 4B). ING4 expression levels were scored on a scale ranging from 0 to 3; 0 for no detectable expression and 3 for distinct nuclear expression in accordance with a previous study (30). Although 100% of control (BPH or TURP) samples were positive for ING4, only 36% of tumor samples (18/50) were positive for nuclear ING4 expression (Fig. 4A). In contrast, 83% benign lesion sample (10/12) and 90% of the tumors were positive for AR (Fig. 4A). These results demonstrate that more than 60% of prostate tumors downregulate ING4 expression and this loss occurs in AR-positive cancer, indicating that ING4 loss may be a main event in prostate tumorigenesis.

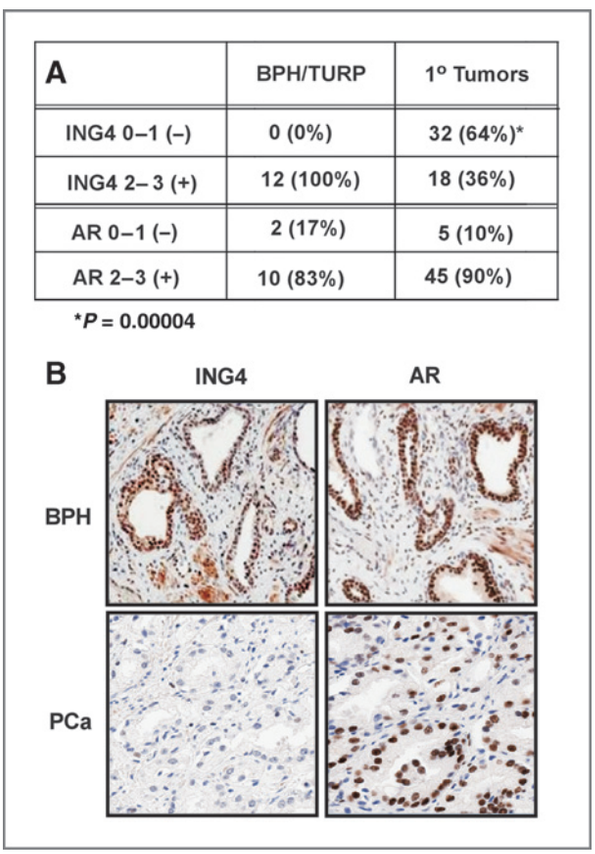

A	BPH/TURP	1° Tumors
ING4 0–1 (–)	0 (0%)	32 (64%)*
ING4 2–3 (+)	12 (100%)	18 (36%)
AR 0–1 (–)	2 (17%)	5 (10%)
AR 2–3 (+)	10 (83%)	45 (90%)

*$P = 0.00004$

Figure 4. ING4 expression is lost in patients with prostate cancer. A tissue microarray of 50 cancerous and 12 noncancerous human prostate samples was immunostained for ING4 or AR. A, table of ING4 and AR histologic grading (scale 0–3; 3 being highest expression) comparing benign prostate hyperplasia/transurethral resection (BPH/TURP) and primary tumors (1°). *, $P = 0.0004$; $n = 50$. B, IHC staining of ING4 and AR in benign hyperplastic prostate tissue (BPH) and prostate cancer (PCa) tissue.

Loss of ING4 expression cooperates with Myc/Erg in prostate tumorigenesis

As reported previously, Myc overexpression alone in human iPrECs was not sufficient to generate a cell line that is tumorigenic in mice (33). Combined overexpression of Myc and the prostate-specific oncogene, Erg (10), was also not sufficient to generate human tumors. To test whether loss of ING4 is also required, we orthotopically injected iPrECs overexpressing Erg and Myc (EM) with or without shING4 (EMI), or a nontargeting shRNA (EMshCV) into prostates of nude mice. Cells overexpressing the two oncogenes Myc and Erg (EM) or in conjunction with a nontargeting shRNA (EMshCV) did not produce tumors in the mice 18 weeks following orthotopic injection. However, EMI cells produced tumors in 60% of the mice (Fig. 5A). Ultrasound imaging of tumors in mice 18 weeks following orthotopic injection is shown in Fig. 5B. Tumors were positive for AR, but negative for ING4 expression when compared with adjacent normal tissue (Fig. 5C and D). Thus, loss of ING4 is required in human cells to cooperate with Myc and Erg to produce prostate tumors.

Pten loss prevents ING4 expression

To further develop prostate cancer models, Pten expression was silenced by overexpressing Pten shRNA in the EM cells (EMP). Overexpression of Myc and Erg and knockdown of Pten was verified in EMP cells by immunoblotting (Fig. 6A). In EMP cells, the expression of integrin α6 was increased whereas the expression of the p27 cell-cycle inhibitor was reduced (Fig. 6A), consistent with changes observed in prostate cancer (13, 34).

Orthotopic injection of EMP, but not iPrECs, into the prostates of nude mice produced tumors that were detectable by ultrasound imaging as early as 8 weeks after injection. At 16 weeks, the tumors averaged 2.85 mm in diameter, ranging from 2.11 to 3.68 mm (Fig. 6B). The tumor penetrance was 60%, as 17 of 30 injections resulted in prostate tumor formation (Fig. 6C). IHC with human-specific MHC class I antibody revealed the presence of human cells demarcating the tumorigenic foci. The EMP tumors stained positive for AR (Fig. 6D) and castrating the mice 16 weeks after the tumors were established resulted in complete tumor regression, indicating a dependence on androgen for tumor maintenance (Fig. 6C).

When subjected to the differentiation protocol, EM cells were completely competent at differentiating as evidenced by the formation of distinct layers, loss of integrin α6, and gain of AR in the suprabasal layer (Fig. 7A). In contrast, the EMI cells failed to differentiate as evidenced by reduced numbers of suprabasal cells, poor AR expression, and retention of integrin α6 in all the cells. EMP cells also failed to differentiate, as evidenced by the lack of a suprabasal layer, and failure to lose

Published OnlineFirst April 24, 2014; DOI: 10.1158/0008-5472.CAN-13-3076

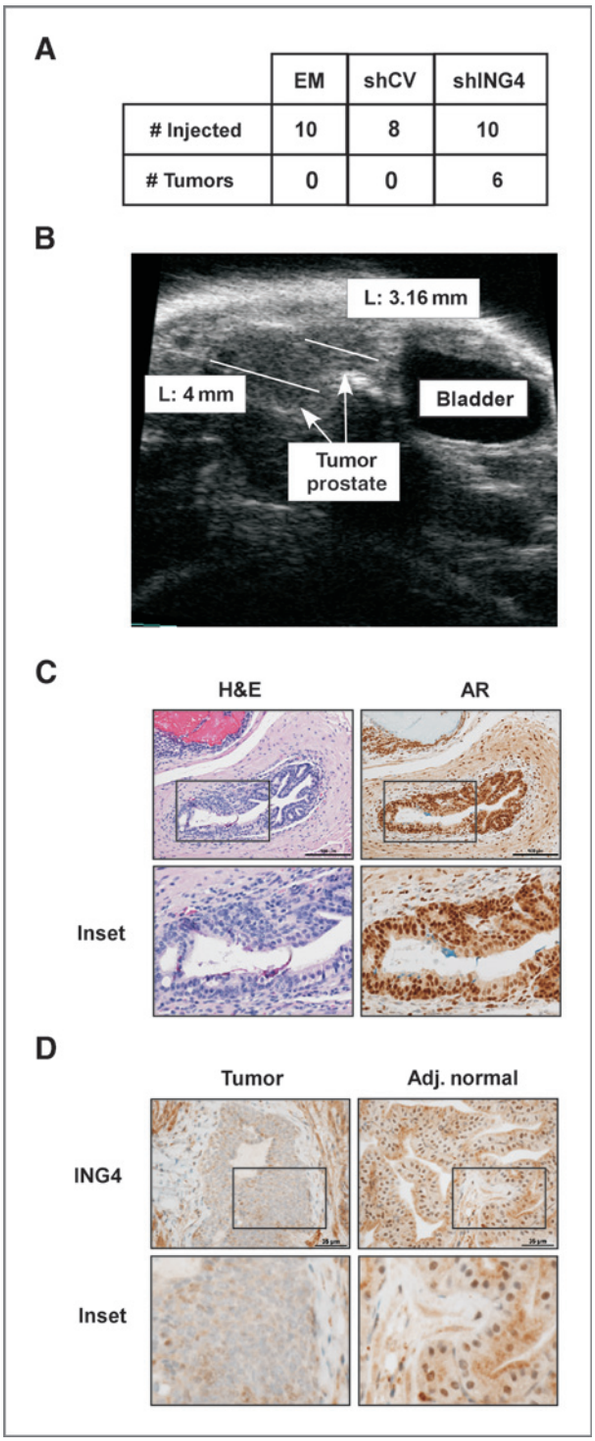

Figure 5. Loss of ING4 expression is required for tumorigenesis. A, iPrECs were engineered to stably overexpress Myc and Erg (EM) with or without shING4 (EMshING4) or a nontargeting shRNA (shCV). Number of mice in which tumors formed following orthotopic injection of EMshING4 compared with control EM and EMshCV cells 18 weeks postinjection. B, tumor measured by ultrasound imaging 18 weeks after orthotopic injection of EMshING4 into the prostates of nude mice. C, hematoxylin and eosin (H&E) and IHC staining of a tumor sample with AR. D, IHC staining of ING4 in normal mouse prostate and tumor sample.

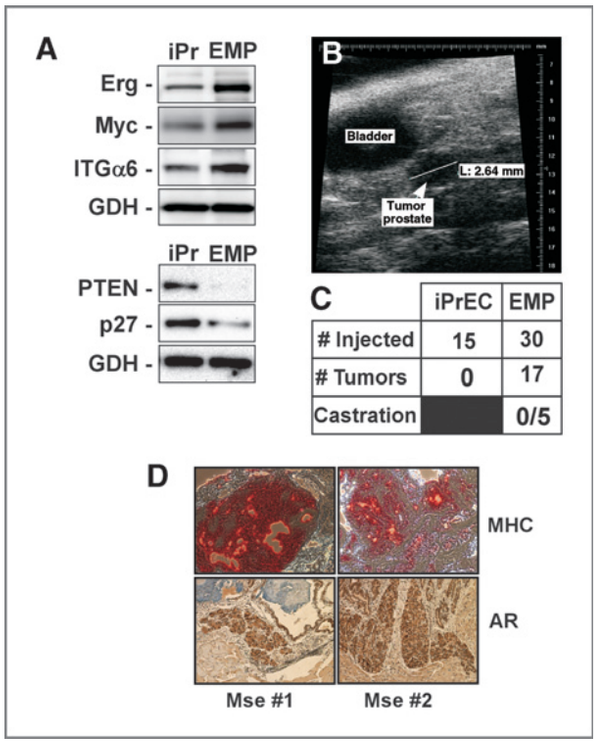

Figure 6. Pten loss promotes tumorigenesis. A, iPrECs (iPr) were engineered to stably overexpress Myc and Erg, along with Pten shRNA (EMP). Immunoblotting confirmed overexpression of Myc, Erg, integrin α6 (ITGα6), and loss of Pten and p27Kip. B, tumor measured by ultrasound imaging 16 weeks after orthotopic injection of EMP cells into the prostates of nude mice. C, number of mice in which tumors formed following orthotopic injection of EMP cells compared with control iPrECs 16 weeks postinjection. Sixteen weeks postinjection, 5 mice harboring EMP tumors were castrated and 11 weeks later the number of tumors that regressed was recorded. D, IHC staining of different tumor samples with human-specific MHC class I or AR.

integrin expression (Fig. 7A). However, in contrast to EMI cells, the EMP cells induced high AR and integrin α6 expression in the basal layer (Fig. 7A). Elevated integrin α6 expression in EMP cells was also observed by immunoblotting (Fig. 6A). This resulted in a population of cells coexpressing AR and integrin α6; reproducing the histopathology observed in clinical samples (13). The inability of EMI and EMP cells to differentiate, correlated with a failure of Myc to induce ING4 expression (Fig. 7A and B). The small clusters of AR-positive cells in the EMI culture are cells in which shING4 was poorly expressed, as evidenced by ING4 positivity in those clusters. Analysis of the keratin subtypes further revealed that EMP cells coexpress both basal keratin K5 and secretory keratin K8 (16) compared with normal iPrECs, where each keratin was distinctively expressed in their respective cell types (Fig. 7C). Thus, EMP cells have a dysfunctional differentiation program that prevents ING4 expression in the presence of Myc, resulting in tumorigenic cells with an intermediate differentiation phenotype. Re-expression of ING4 in EMP cells completely rescued the differentiation defect, restoring the suprabasal layer, AR expression, loss of integrin (Fig. 7B), and separation of the K5

Published OnlineFirst April 24, 2014; DOI: 10.1158/0008-5472.CAN-13-3076

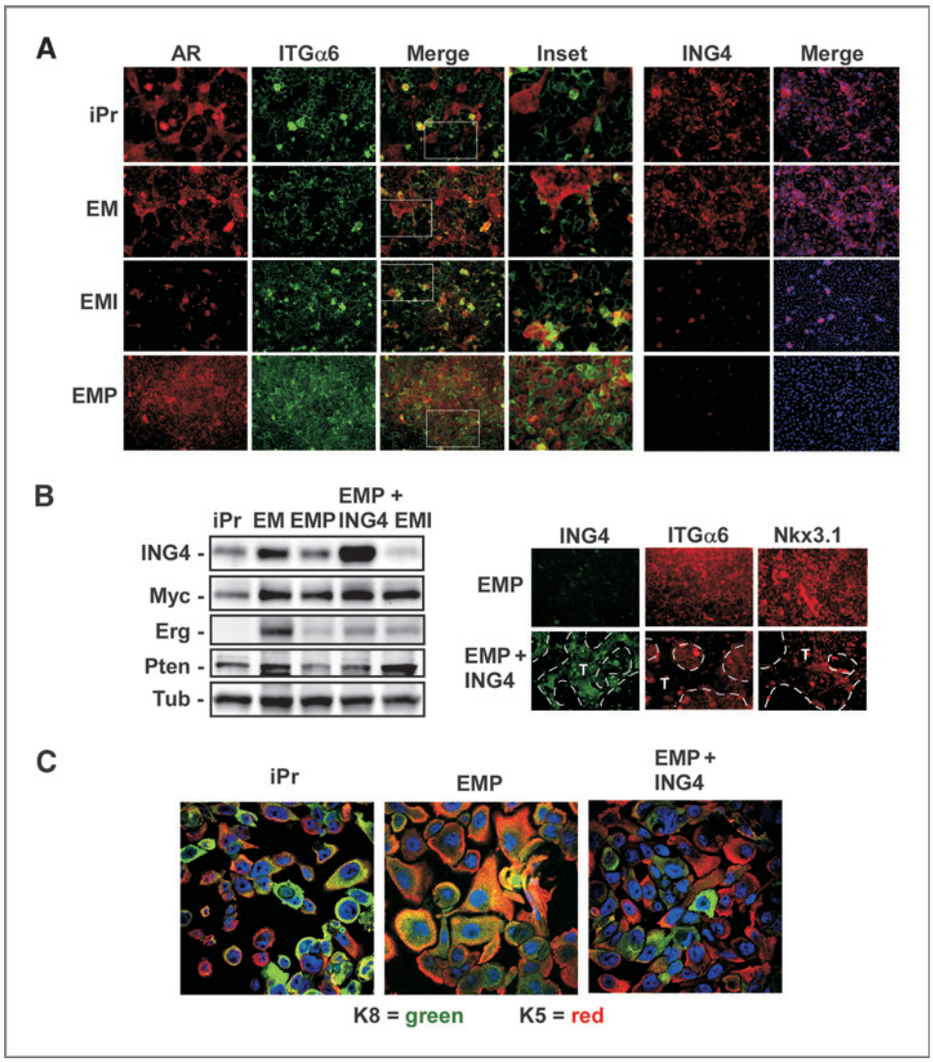

Figure 7. Pten-mediated loss of ING4 and altered differentiation in tumorigenic cells. A, iPrECs (iPr), EM, EMI, or EMP cells differentiated for 12 to 14 days were immunostained for AR (red), ITGα6 (green), or ING4 (red), counterstained with Hoechst (blue), and imaged by fluorescent microscopy. B, ING4, Myc, Erg, and Pten expression in undifferentiated iPrECs (iPr), EM, EMP, EMP+ING4, or EMI cells detected by immunoblotting. EMP or EMP-ING4 cells differentiated for 12 to 14 days were immunostained for ING4 (green), ITGα6 (red), or Nkx3.1 (red). Dashed lines demarcate supra (T) and basal cell layers. C, cultures of iPrECs, EMP, or EMP-ING4 cells were differentiated for 17 days, immunostained for keratins K8 (green) and K5 (red), counterstained with Hoechst (blue), and imaged by confocal microscopy.

and K8 populations (Fig. 7C). Expression of the ING4ΔCT mutant in EMP cells did not rescue the differentiation defect (not shown). Thus, the Myc-ING4 differentiation relay is no longer functional in the oncogenic EMP cells and Pten loss is responsible. Together our results support the conclusion that ING4 is required for differentiation of iPrECs and suggest that one of the major oncogenic events in prostate cancer is the uncoupling of the Myc-ING4 differentiation program.

Discussion

In immortalized human prostate epithelial cells with the capacity to differentiate *in vitro*, transient ING4 expression, dependent on Myc, is required for prostate epithelial differentiation. ING4 expression coincides with loss of matrix-based adhesion, downregulation of integrin, and acquisition of AR; blocking ING4 prevents the initiation of these processes. In normal differentiating iPrECs, the acquisition of AR expression and androgen responsiveness is observed only in cells in which integrin expression is lost (12). We found that neither AR nor androgen is required for ING4 expression (not shown), nor were we able to demonstrate any influence of ING4 on AR expression or its ability to activate its transcriptional targets in cells expressing AR. Thus, the role of ING4 in prostate epithelial differentiation lies at least in part within its capacity to target integrins. This is consistent with the observations in the Myc breast cancer mouse model, where overexpression of the C-terminal deletion mutant of ING4 (ING4ΔCT) restored integrin expression in the tumors (unpublished results; ref. 23). This is also consistent with the established role for Myc in directly suppressing integrin α6 and β1 transcription during differentiation (35). Our data indicate that ING4 is an essential component of the Myc-dependent effect on integrin expression, because removal of ING4 prevents Myc from suppressing integrin expression.

Myc or ING4 overexpression in basal cells is sufficient to accelerate differentiation toward luminal cells; however, improper prolonged expression of Myc or ING4 leads to cell death. Thus, the temporal, that is, Myc expression preceding ING4, and transient nature of Myc and ING4 expression is

Published OnlineFirst April 24, 2014; DOI: 10.1158/0008-5472.CAN-13-3076

crucial for normal epithelial cell differentiation. The molecular mechanism of this concerted transcriptional relay is currently unclear. Previous ChIP analysis identified Myc bound to the ING4 promoter, suggesting ING4 is a direct target of Myc (36). However, we failed to detect an increase in ING4 mRNA in undifferentiated basal cells overexpressing Myc (not shown). Similarly, Myc overexpression in breast epithelial cells also did not increase ING4 expression (unpublished results). Thus, our results point to an indirect action of Myc in ING4 induction, or requiring additional factor(s) during the course of differentiation.

Differentiation is dependent on the ING4 C-terminal domain containing the PHD motif required for H3K4me3 binding (21). ING4 overexpression alters chromatin modifications (not shown), suggesting ING4 association with chromatin is required for differentiation. To our knowledge, this is the first time that the chromatin remodeling properties of ING4 have been linked to differentiation. Once bound, ING4 recruits the HBO1 acetyltransferase (21, 37), facilitates histone H3/H4 acetylation, and activates gene transcription (21, 38). Like ING4, Myc is extensively involved in chromatin remodeling (39, 40). In addition, recent studies have brought to light the chromatin remodeling activity of Myc in the maintenance of pluripotent stem cells (19, 41). Taken together, the relay from Myc to ING4 is likely to install epigenetic changes that govern differential transcription and ultimately prostate epithelial cell differentiation.

Myc overexpression alone often fails to transform normal human cells because of induction of cell death (33, 42). Myc or ING4 overexpression specifically induces death of the differentiated cells, but not the underlying basal cells. This supports the current paradigm that Myc activity manifests in a context-dependent manner such that Myc induces cell death in more differentiated cells, but maintains the proliferative and self-renewal capacity of less differentiated stem or progenitor cells. The death phenotypes induced by Myc overexpression are mediated in part by p53 and ING4 enhances p53 function (43). However, the death induced by Myc or ING4 overexpression in iPrECs is likely p53-independent, because the iPrECs express E6 that blocks p53 function. In iPrECs, Bnip3 is responsible for the observed cell death. Although p53 is reported to regulate Bnip3 (44, 45), our results describe an alternate mechanism of Bnip3 activation that is p53 independent. Nonetheless, ING4 may be part of the mechanism by which p53 regulates Bnip3. In prostate cancer, p53 loss is rare and associated with a small subset of late stage disease (46). Thus, loss of ING4 may be a mechanism by which prostate cancer cells escape the tumor suppressive effects of p53 when Myc is overexpressed. This idea is further supported when contrasting the prostate cancer tissue data, which demonstrate a 60% loss of ING4, with that of breast cancer where p53 loss is more highly prevalent and only 34% of the samples lack ING4.

ING4 expression is lost in more than 60% of prostate tumors, suggesting for the first time a significant contribution of ING4 loss to prostate tumorigenesis. The high prevalence of Myc overexpression in prostate cancer and its tendency to induce cell death suggests loss of ING4 is necessary for Myc-dependent prostate oncogenesis. Indeed, only Myc-overexpressing cells without ING4 are capable of generating tumors in mice. Moreover, loss of ING4 blocked tumor cell differentiation generating cells coexpressing both basal and luminal markers, a phenotype often seen in prostate cancer. The mechanism by which ING4 is lost in prostate cancer needs more investigation, but LOH at 12p13, the genomic region that contains the ING4 gene, has been reported in 10% to 20% of primary and up to 45% of metastatic prostate tumors (47, 48). Our data demonstrate loss of Pten is another mechanism that leads to ING4 loss. The molecular mechanism of Pten in the regulation of ING4 expression is presently unknown and likely to be indirect.

We have established a genetic link between Myc and ING4 in prostate epithelial differentiation and prostate cancer. Our data demonstrate that a Myc-ING4 temporal relay is required for normal prostate cell differentiation and when this relay is missing, it leads to prostate cancer. Whether the Myc-ING4 relay also governs cell differentiation in other cell types, including breast epithelia, needs to be addressed. We propose that ING4 dictates the downstream program driven by Myc toward differentiation, and in its absence Myc is directed toward targets that promote tumorigenesis. Pten loss resulting in the loss of ING4 expression, disruption of the Myc-ING4 relay, a block in differentiation, and susceptibility to tumorigenesis, reinforces the idea that ING4 plays a pivotal role in determining prostate epithelial cell fate.

Disclosure of Potential Conflicts of Interest

No potential conflicts of interest were disclosed.

Authors' Contributions

Conception and design: P.L. Berger, E.A. Nollet, G. Hostetter, S. Kim, C.K. Miranti

Development of methodology: P.L. Berger, S.B. Frank, T.-T.A. Chang, G. Hostetter, C.K. Miranti

Acquisition of data (provided animals, acquired and managed patients, provided facilities, etc.): S.B. Frank, B. Holly, T.-T.A. Chang, G. Hostetter, S. Kim, C.K. Miranti

Analysis and interpretation of data (e.g., statistical analysis, biostatistics, computational analysis): P.L. Berger, B. Holly, T.-T.A. Chang, C.K. Miranti

Writing, review, and/or revision of the manuscript: P.L. Berger, B. Holly, T.-T.A. Chang, G. Hostetter, S. Kim, C.K. Miranti

Administrative, technical, or material support (i.e., reporting or organizing data, constructing databases): P.L. Berger, V.V. Schulz, C.K. Miranti

Study supervision: T.-T.A. Chang, C.K. Miranti

Acknowledgments

The authors thank J. Trahey for technical assistance, B. Knudsen at Cedars Sinai for help with PrEC immortalization, D. Janssens for generating the Pten shRNA construct, V. Vasioukhin at FHCRC and E. Graf for the ΔN-Erg constructs, A. Cress at University of Arizona for integrin α6 immunoblotting antibody, and L. Frame and E. Park for assistance with confocal imaging.

Grant Support

This work was supported by the Association for International Cancer Research (P.L. Berger and S.B. Frank), NIH/NCI CA154835 (P.L. Berger, V.V. Schulz, and C.K. Miranti), the Van Andel Research Institute (M.J. Edick, B. Holly, T.-T.A. Chang, G. Hostetter, and C.K. Miranti), Van Andel Institute Graduate School (E.A. Nollet), and TGEN (S. Kim).

The costs of publication of this article were defrayed in part by the payment of page charges. This article must therefore be hereby marked *advertisement* in accordance with 18 U.S.C. Section 1734 solely to indicate this fact.

Received October 28, 2013; revised March 5, 2014; accepted March 21, 2014; published OnlineFirst April 24, 2014.

Published OnlineFirst April 24, 2014; DOI: 10.1158/0008-5472.CAN-13-3076

References

1. Burger PE, Xiong X, Coetzee S, Salm SN, Moscatelli D, Goto K, et al. Sca-1 expression identifies stem cells in the proximal region of prostatic ducts with high capacity to reconstitute prostatic tissue. Proc Natl Acad Sci U S A 2005;102:7180–5.
2. Lawson DA, Xin L, Lukacs RU, Cheng D, Witte ON. Isolation and functional characterization of murine prostate stem cells. Proc Natl Acad Sci U S A 2007;104:181–6.
3. Gao H, Ouyang X, Banach-Petrosky W, Borowsky AD, Lin Y, Kim M, et al. A critical role for p27kip1 gene dosage in a mouse model of prostate carcinogenesis. Proc Natl Acad Sci U S A 2004;101:17204–9.
4. Koh CM, Bieberich CJ, Dang CV, Nelson WG, Yegnasubramanian S, De Marzo AM. MYC and prostate cancer. Genes Cancer 2010;1:617–28.
5. Schmitz M, Grignard G, Margue C, Dippel W, Capesius C, Mossong J, et al. Complete loss of PTEN expression as a possible early prognostic marker for prostate cancer metastasis. Int J Cancer 2007;120:1284–92.
6. Ellwood-Yen K, Graeber TG, Wongvipat J, Iruela-Arispe ML, Zhang J, Matusik R, et al. Myc-driven murine prostate cancer shares molecular features with human prostate tumors. Cancer Cell 2003;4:223–38.
7. Wang S, Gao J, Lei Q, Rozengurt N, Pritchard C, Jiao J, et al. Prostate-specific deletion of the murine Pten tumor suppressor gene leads to metastatic prostate cancer. Cancer Cell 2003;4:209–21.
8. Zong Y, Xin L, Goldstein AS, Lawson DA, Teitell MA, Witte ON. ETS family transcription factors collaborate with alternative signaling pathways to induce carcinoma from adult murine prostate cells. Proc Natl Acad Sci U S A 2009;106:12465–70.
9. Klezovitch O, Risk M, Coleman I, Lucas JM, Null M, True LD, et al. A causal role for ERG in neoplastic transformation of prostate epithelium. Proc Natl Acad Sci U S A 2008;105:2105–10.
10. Sun C, Dobi A, Mohamed A, Li H, Thangapazham RL, Furusato B, et al. TMPRSS2-ERG fusion, a common genomic alteration in prostate cancer activates C-MYC and abrogates prostate epithelial differentiation. Oncogene 2008;27:5348–53.
11. Choi N, Zhang B, Zhang L, Ittmann M, Xin L. Adult murine prostate basal and luminal cells are self-sustained lineages that can both serve as targets for prostate cancer initiation. Cancer Cell 2012;21:253–65.
12. Lamb LE, Knudsen BS, Miranti CK. E-cadherin-mediated survival of androgen-receptor-expressing secretory prostate epithelial cells derived from a stratified *in vitro* differentiation model. J Cell Sci 2010;123:266–76.
13. Cress AE, Rabinovitz I, Zhu W, Nagle RB. The $\alpha 6\beta 1$ and $\alpha 6\beta 4$ integrins in human prostate cancer progression. Cancer Metastasis Rev 1995;14:219–28.
14. Litvinov IV, De Marzo AM, Isaacs JT. Is the Achilles' heel for prostate cancer therapy a gain of function in androgen receptor signaling? J Clin Endocrinol Metab 2003;88:2972–82.
15. Lamb LE, Zarif JC, Miranti CK. The androgen receptor induces integrin $\alpha 6\beta 1$ to promote prostate tumor cell survival via NF-κB and Bcl-xL independently of PI3K signaling. Cancer Res 2011;71:2739–49.
16. Myers RB, Grizzle WE. Changes in biomarker expression in the development of prostatic adenocarcinoma. Biotech Histochem 1997;72:86–95.
17. Verhagen AP, Aalders TW, Ramaekers FC, Debruyne FM, Schalken JA. Differential expression of keratins in the basal and luminal compartments of rat prostatic epithelium during degeneration and regeneration. Prostate 1988;13:25–38.
18. Nagle RB, Ahmann FR, McDaniel KM, Paquin ML, Clark VA, Celniker A. Cytokeratin characterization of human prostatic carcinoma and its derived cell lines. Cancer Res 1987;47:281–6.
19. Buganim Y, Faddah DA, Jaenisch R. Mechanisms and models of somatic cell reprogramming. Nat Rev Genet 2013;14:427–39.
20. Coles AH, Jones SN. The ING gene family in the regulation of cell growth and tumorigenesis. J Cell Physiol 2009;218:45–57.
21. Hung T, Binda O, Champagne KS, Kuo AJ, Johnson K, Chang HY, et al. ING4 mediates crosstalk between histone H3 K4 trimethylation and H3 acetylation to attenuate cellular transformation. Mol Cell 2009;33:248–56.
22. Kim S, Chin K, Gray JW, Bishop JM. A screen for genes that suppress loss of contact inhibition: identification of ING4 as a candidate tumor suppressor gene in human cancer. Proc Natl Acad Sci U S A 2004;101:16251–6.
23. Kim S, Welm AL, Bishop JM. A dominant mutant allele of the ING4 tumor suppressor found in human cancer cells exacerbates MYC-initiated mouse mammary tumorigenesis. Cancer Res 2010;70:5155–62.
24. Edick MJ, Tesfay L, Lamb LE, Knudsen BS, Miranti CK. Inhibition of integrin-mediated crosstalk with epidermal growth factor receptor/Erk or Src signaling pathways in autophagic prostate epithelial cells induces caspase-independent death. Mol Biol Cell 2007;18:2481–90.
25. Gmyrek GA, Walburg M, Webb CP, Yu HM, You X, Vaughan ED, et al. Normal and malignant prostate epithelial cells differ in their response to hepatocyte growth factor/scatter factor. Am J Pathol 2001;159:579–90.
26. Tapia C, Zlobec I, Schneider S, Kilic E, Güth U, Bubendorf L, et al. Deletion of the inhibitor of growth 4 (ING4) tumor suppressor gene is prevalent in human epidermal growth factor 2 (HER2)-positive breast cancer. Hum Pathol 2011;42:983–90.
27. Pawar SC, Demetriou MC, Nagle RB, Bowden GT, Cress AE. Integrin $\alpha 6$ cleavage: a novel modification to modulate cell migration. Exp Cell Res 2007;313:1080–9.
28. Livak KJ, Schmittgen TD. Analysis of relative gene expression data using real-time quantitative PCR and the $2(-\Delta\Delta C)$T Method. Methods 2001;25:402–8.
29. Watanabe A, Hostetter G. Tissue microarray applications in drug discovery for pancreatic cancer. In: Han H, Grippo P., editors. Drug discovery in pancreatic cancer, models and techniques. New York: Springer; 2010. pg. 205–222.
30. Byron SA, Min E, Thal TS, Hostetter G, Watanabe AT, Azorsa DO, et al. Negative regulation of NF-κB by the ING4 tumor suppressor in breast cancer. PLoS One 2012;7:e46823.
31. Lin CH, Lin C, Tanaka H, Fero ML, Eisenman RN. Gene regulation and epigenetic remodeling in murine embryonic stem cells by c-Myc. PLoS One 2009;4:e7839.
32. Palacios A, Munoz IG, Pantoja-Uceda D, Marcaida MJ, Torres D, Martin-Garcia JM, et al. Molecular basis of histone H3K4me3 recognition by ING4. J Biol Chem 2008;283:15956–64.
33. Berger R, Febbo PG, Majumder PK, Zhao JJ, Mukherjee S, Signoretti S, et al. Androgen-induced differentiation and tumorigenicity of human prostate epithelial cells. Cancer Res 2004;64:8867–75.
34. De Marzo AM, Meeker AK, Zha S, Luo J, Nakayama M, Platz EA, et al. Human prostate cancer precursors and pathobiology. Urology 2003;62:55–62.
35. Gebhardt A, Frye M, Herold S, Benitah SA, Braun K, Samans B, et al. Myc regulates keratinocyte adhesion and differentiation via complex formation with Miz1. J Cell Biol 2006;172:139–49.
36. Zhou L, Picard D, Ra Y-S, Li M, Northcott PA, Hu Y, et al. Silencing of thrombospondin-1 is critical for Myc-induced metastatic phenotypes in medulloblastoma. Cancer Res 2010;70:8199–210.
37. Doyon Y, Cayrou C, Ullah M, Landry AJ, Cote V, Selleck W, et al. ING tumor suppressor proteins are critical regulators of chromatin acetylation required for genome expression and perpetuation. Mol Cell 2006;21:51–64.
38. Coles AH, Gannon H, Cerny A, Kurt-Jones E, Jones SN. Inhibitor of growth-4 promotes IκB promoter activation to suppress NF-κB signaling and innate immunity. Proc Natl Acad Sci U S A 2010;107:11423–8.
39. Pellakuru LG, Iwata T, Gurel B, Schultz D, Hicks J, Bethel C, et al. Global levels of H3K27me3 track with differentiation *in vivo* and are deregulated by MYC in prostate cancer. Am J Pathol 2012;181:560–9.
40. Secombe J, Eisenman RN. The function and regulation of the JARID1 family of histone H3 lysine 4 demethylases: the Myc connection. Cell Cycle 2007;6:1324–8.
41. Soufi A, Donahue G, Zaret KS. Facilitators and impediments of the pluripotency reprogramming factors' initial engagement with the genome. Cell 2012;151:994–1004.
42. Larsson LG, Henriksson MA. The Yin and Yang functions of the Myc oncoprotein in cancer development and as targets for therapy. Exp Cell Res 2010;316:1429–37.

Published OnlineFirst April 24, 2014; DOI: 10.1158/0008-5472.CAN-13-3076

43. Shiseki M, Nagashima M, Pedeux RM, Kitahama-Shiseki M, Miura K, Okamura S, et al. p29ING4 and p28ING5 bind to p53 and p300, and enhance p53 activity. Cancer Res 2003;63:2373–8.
44. Jafarnejad S, Li G. Regulation of p53 by ING family members in suppression of tumor initiation and progression. Cancer Metastasis Rev 2011;31:1–19.
45. Feng X, Liu X, Zhang W, Xiao W. p53 directly suppresses BNIP3 expression to protect against hypoxia-induced cell death. EMBO J 2011;30:3397–415.
46. Markert EK, Mizuno H, Vazquez A, Levine AJ. Molecular classification of prostate cancer using curated expression signatures. Proc Natl Acad Sci U S A 2011;108:21276–81.
47. Kawana Y IT, Suzuki H, Ueda T, Komiya A, Ichikawa Y, Furuya Y, et al. Loss of heterozygosity at 7q31.1 and 12p13-12 in advanced prostate cancer. Prostate 2002;53:60–4.
48. Kibel AS, Faith DA, Bova GS, Isaacs WB. Loss of heterozygosity at 12P12-13 in primary and metastatic prostate adenocarcinoma. J Urol 2000;164:192–6.

Miz1, a Novel Target of ING4, Can Drive Prostate Luminal Epithelial Cell Differentiation

Penny L. Berger,[1] Mary E. Winn,[2] and Cindy K. Miranti[1]*

[1]*Laboratory of Integrin Signaling, Van Andel Research Institute, Grand Rapids, Michigan*
[2]*Bioinformatics and Biostatistics Core, Van Andel Research Institute, Grand Rapids, Michigan*

BACKGROUND. How prostate epithelial cells differentiate and how dysregulation of this process contributes to prostate tumorigenesis remain unclear. We recently identified a Myc target and chromatin reader protein, ING4, as a necessary component of human prostate luminal epithelial cell differentiation, which is often lost in primary prostate tumors. Furthermore, loss of ING4 in the context of oncogenic mutations is required for prostate tumorigenesis. Identifying the gene targets of ING4 can provide insight into how its loss disrupts differentiation and leads to prostate cancer.

METHODS. Using a combination of RNA-Seq, a best candidate approach, and chromatin immunoprecipitation (ChIP), we identified Miz1 as a new ING4 target. ING4 or Miz1 overexpression, shRNA knock-down, and a Myc-binding mutant were used in a human in vitro differentiation assay to assess the role of Miz1 in luminal cell differentiation.

RESULTS. ING4 directly binds the Miz1 promoter and is required to induce Miz1 mRNA and protein expression during luminal cell differentiation. Miz1 mRNA was not induced in shING4 expressing cells or tumorigenic cells in which ING4 is not expressed. Miz1 dependency on ING4 was unique to differentiating luminal cells; Miz1 mRNA expression was not induced in basal cells. Although Miz1 is a direct target of ING4, and its overexpression can drive luminal cell differentiation, Miz1 was not required for differentiation.

CONCLUSIONS. Miz1 is a newly identified ING4-induced target gene which can drive prostate luminal epithelial cell differentiation although it is not absolutely required. *Prostate 77:49–59, 2017.* © 2016 Wiley Periodicals, Inc.

KEY WORDS: **chromatin; integrins; RNA-Seq; Myc; human**

INTRODUCTION

The manner in which prostate epithelial cells differentiate, that is, how cells in the prostate epithelium transition from basal to sejcretory luminal cells, still remains to be fully elucidated. The process is one that demands attention since dysregulated differentiation is implicated in prostate oncogenesis [1]. Several different models have been used to investigate prostate epithelial differentiation, the most common being in vivo mouse models [2–4]. We developed an in vitro differentiation model using human basal prostate epithelial cells to better assess both differentiation and oncogenesis in a human model [5]. Stimulation of human basal cells with KGF and DHT for 14–18 days results in a bilayer culture with fully differentiated AR-positive secretory luminal cells sitting atop basal cells that mimics human prostate histology. Utilizing this model, we identified the chromatin binding protein and Myc target, ING4 [6–8], as a major luminal cell determinant [1]. ING4 is induced downstream of Myc and required for luminal differentia-

Grant sponsor: Department of Defense Prostate Cancer Research Program; Grant number: W81XWH-14-1-0479; Grant sponsor: NIH/NCI; Grant number: CA154835; Grant sponsor: Van Andel Research Institute.

Conflicts of interest: The authors have no conflicts to disclose.

*Correspondence to: Cindy K. Miranti, Laboratory of Integrin Signaling, Van Andel Research Institute, 333 Bostwick Ave NE, Grand Rapids, MI 49503. E-mail: cindy.miranti@vai.org

Received 13 July 2016; Accepted 3 August 2016
DOI 10.1002/pros.23249
Published online 16 August 2016 in Wiley Online Library (wileyonlinelibrary.com).

tion, and its induction is coincident with integrin loss within the luminal cell population.

Introduction of oncogenes, that is, overexpression of Erg and Myc and knock-down of Pten, into differentiating basal cells generated AR-positive luminal-like tumorigenic cells that retained some basal markers including integrin α6β1 analogous to what is seen in human tumors [1,9]. These same tumorigenic cells lost their ability to fully differentiate and this was shown to be due to loss of ING4. To better understand how ING4 drives integrin loss during normal differentiation, we sought to identify the gene targets of ING4.

The loss of integrin expression during epithelial cell differentiation has been studied in other contexts including mammary and skin [10,11]. In addition to Notch being a strong suppressor of both integrins and matrix [11], a Myc/Miz1 (*ZBTB17*) repressive complex, which binds integrin α6 and β1 promoters, was shown to be necessary for Myc-induced differentiation of keratinocytes [10]. Miz1 is also necessary in the mammary gland for proper transitioning from late stage pregnancy to early lactation [12]. ING4 expression is also lost in some breast cancers [13] where it may suppress NF-κB signaling [14], and elevated expression of an ING4 E3-ligase, SCF(JFK), promotes breast cancer metastasis [15]. Interestingly, expression of an ING4 mutant unable to bind chromatin induced integrin expression in a mouse breast cancer model [8]. Thus, we hypothesized that Miz1 might be the link between ING4 and α6β1 integrin that could explain its loss during normal differentiation and its retention in tumor cells.

MATERIALS AND METHODS

Cell Lines

Immortalized human basal prostate epithelial cells (iPrEC) were generated from primary clinical prostectomies as previously described [1,5]. Cultures were validated to be Mycoplasma-free and express only basal epithelial cell markers [5]. Tumorigenic iPrEC-EMP (Erg/Myc/shPten overexpression) and ING4 or shING4 overexpressing (iPrEC-ING4; iPrEC-shING4) cells were generated as previously described [1,8]. All lines were maintained and passaged in keratinocyte serum-free media (Invitrogen) [1,5].

Differentiation Protocol

Differentiation and layer separation protocols were detailed previously [5]. Briefly, iPrECs at confluency were treated in complete growth medium with 2 ng/ml keratinocyte growth factor (KGF) (Cell Sciences) and 5 nM R1881 (PerkinElmer) every other day for up to 18 days. For biochemical analysis, the differentiated luminal layer was separated from the basal layer using disassociation buffer (Invitrogen) as previously described [5].

Constructs

The pLKO vector containing Pten shRNA was generated by subcloning the oligo 5′- CCGGTGGGCT TTAACTGTAGTATTTGTACTAGTCAAATACTACA GTTAAAGCCCTTTTTG-3′, complementary to the 3′-UTR of Pten, into a lentiviral vector to generate pLKO.1-shPten. The shPten in the iPrEC-EMP cells reported here contain the above targeting sequence, which is more stable and generated subsequent to the initial report on iPrEC-EMP [1]. The pLKO vector containing ING4 shRNA was purchased from Sigma–Aldrich (Clone ID:NM_016162.3-522s21c1) and used to generate the iPrEC-shING4 cells. ING4 shRNA targeting sequence: 5′-CCGGTTAAAG CTCGTGCGCACAAGTCTCGAGACTTGTGCGCAC-GAGCTTTAATTTTTTG-3′. The pLKO-TetON-shMiz1 constructs were generated by subcloning each of two oligos into the pLKO-TetON vector purchased from Addgene [16]. The Tet-pLKO-Puro vector was first modified, EZ-Tet-pLKO-Puro, to contain a shortened stuffer region by inserting an EcoRI site at base 222 of the stuffer (primer 5′-GCTACTCCACCACTT-GAATTCCTAAGCGGTCAGC-3′). The vector was then digested with EcoRI and re-ligated. Mutagenesis was then used to mutate the AgeI site to NheI (primer 5′-TATCAGTGATAGAGACGCTAGCGTGTTGTAAA TGAGCA-3′). shMiz1 oligo sequences were as follows: 5′-CTAGTGTCCAAGCACATCATCATT-CAACTAGTGAGAATGATGATGTGCTTGGACATTT TT-3′ (5730), 5′-CTAGGTTCACTTTAAGGCTCA-TAAAAACTAGTGATTTATGAGCCTTAAAGTGAAC TTTTT-3′ (5729). Wild-type Miz1 (pLenti-Myc-DDK-ZBTB17)(PS100064) was purchased from OriGene Technologies (Rockville, MD). Wild-type c-Myc (pMSCV-c-Myc-GFP) and Myc-Miz1 binding mutant (pMSCV-c-Myc-V394D-RFP) were generous gifts from Dr. Martine Roussel [10,17].

Virus Generation and Infection

Lentiviruses expressing shRNAs or Miz1 cDNA were generated by co-transfecting the 293FT packaging cell line with 6 μg each of the lentiviral packaging plasmids, pVSVG, pLP1, and pLP2 with Lipofectamine 2000 (ThermoFisher) following manufacturers recommended protocol. Virus was harvested 3 days later and immediately used to infect iPrECs. Pooled cells were selected and maintained in 0.75 μg/ml puromycin.

Retroviruses expressing Myc or MycV394D were generated by transfecting Phoenix cells (National Gene Vector Biorepository) using Lipofectamine 2000 following manufacturers recommended protocol, harvesting 2 days later and immediately infecting iPrECs. Pools of Myc expressing cells were selected and maintained in 0.75 μg/ml puromycin.

Antibodies

Immunofluorescence: AR (C-19) and Miz1 (H-190) were purchased from Santa Cruz. ITGα6 (GoH3) antibody was purchased from BD Pharmingen. Immunoblotting: Myc (N-term) and ING4 (EP3804) antibodies were purchased from Abcam. Polyclonal Miz1 antibody was purchased from GeneTex. Tubulin antibody (DM1A) was purchased from Sigma and GAPDH (6CS) from Millipore.

Immunostaining and Microscopy

Differentiated cultures were fixed in 4% paraformaldehyde and permeabilized with 0.2% Triton-X 100 for 5 min. After washing with PBS, cells were blocked with 4% normal goat serum for 2 hr. Primary antibodies, diluted in 1% BSA/PBS, were applied to samples overnight at 4°C. After washing, secondary conjugated antibodies diluted in 1% BSA/PBS were incubated for 1–2 hr. Nuclei were stained with Hoechst 33258 (Sigma) for 10 min at room temperature. Coverslips were mounted using Fluoromount-G (SouthernBiotech). Epifluorescent images were acquired on a Nikon Eclipse TE300 fluorescence microscope using OpenLab v5.5.0 image analysis software (Improvision).

Immunoblotting

Total cell lysates were prepared for immunoblotting as previously described [18]. Briefly, cells were lysed in RIPA buffer and 30–50 μg total protein was separated on SDS polyacrylamide gels and transferred to PVDF membranes. Membranes were blocked in 5% BSA in TBST overnight at 4°C then probed with primary antibody, and HRP-conjugated secondary antibodies (Bio-Rad) in TBST + 5% BSA. Signals were visualized by chemiluminescence reagent with a CCD camera in a Bio-Rad Chemi-Doc Imaging System using Quantity One software v4.5.2 (Bio-Rad).

qRT-PCR

Total RNA was isolated and purified using RNase-free DNase and Life Technology's RNeasy PureLink Kits. For qRT-PCR, 0.5 μg RNA was reversed transcribed using a reverse transcription system (Promega). Synthesized cDNA was amplified for qRT-PCR using SYBR green master mix (Roche) with gene-specific primers and an ABI 7500 RT-PCR system (Applied Biosystems). Gene expression was normalized to 18 sec rRNA by the 2-ΔΔCt method (Livak, 2001). qRT-PCR primers for Miz1 were as follows: Miz1 Fwd: 5′-CTACTCTTTTCTGACAGTTTGCC-3′, Miz1 Rev: 5′-CCTTTGTCTGCTCTGGAGT-3′.

Chromatin Immunoprecipitations

Cells (3.0×10^6) were fixed in 1% formaldehyde (Thermo Scientific) for 1–5 min and washed 3× with ice cold calcium-magnesium free PBS (CMF-PBS) supplemented with protease inhibitors: pepstatin, aprotinin, leupeptin, and phenylmethylsulfonyl (PMSF). Cells were scraped and pelleted at 2,000 rpm for 8 min at 4°C. Pellet was resuspended in swelling buffer (5 mM PIPES pH 8.0, 85 mM KCl, 0.5% IGEPAL, and incubated on ice for 30 min). Nuclei were dounce homogenized and then pelleted at 4,000 rpm for 10 min, 4°C. Nuclei were resuspended in sonication buffer (0.1% SDS, 10 mM EDTA, 50 mM Tris–HCl pH 8.1) and incubated on ice for 10 min prior to sonication. Chromatin was sheared at 4°C using the Covaris E220 Ultra Sonicator following manufacturer's suggested settings of 2% Duty Cycle, 105 Watt Peak Intensity, 200 Cycles/Burst. Chromatin was sonicated for 10 min to achieve 300–500 bp fragments.

Chromatin immunoprecipitations (ChIPs) were performed with 1 million cells/IP using magnetic beads (NEB). The following antibodies were used: ING4 (EP3804) and anti-HBO1 (ab70183) from Abcam. Chromatin was incubated with 6 μg of appropriate antibody overnight at 4°C with rotation. Following incubation, magnetic beads blocked with 1% BSA supplemented with 10 μg/ml salmon sperm, were added to samples and incubated at 4°C with rotation for 6 hr. Following immunoprecipitations, beads were washed in the following buffers at 4°C for 10 min with rotation: Triton Wash Buffer (50 mM Tris–HCl pH 7.4, 150 mM NaCl, 1% Triton X-100), followed by Lysis Buffer 500 (0.1% NaDOC, 1 mM EDTA, 50 mM HEPES pH 7.5, 500 mM NaCl, 1% Triton X-100), LiCl Detergent buffer (0.5% NaDOC, 1 mM EDTA, 250 mM LiCl, 0.5% IGEPAL, 10 mM Tris–HCl pH 8.1), and Tris–EDTA pH 8.1. Chromatin was eluted from beads in Elution Buffer (10 mM EDTA, 1% SDS, Tris–HCl pH 8.0) for 30 min at 65°C. Samples were then treated with 20 μg proteinase K, and 10 μg RNase A, and NaCl (200 mM) was added and incubated at 65°-C overnight to reverse cross-links. DNA was purified using phenol/chloroform extraction followed by ethanol precipitation.

ChIP Primer Sequences

Primers were designed referencing the UCSC Genome Browser to determine transcriptional start sites of promoters, and in the case of ING4-ChIP, regions within the promoter region with high H3K4me3 were used to design targeting primers. Primer sequences are as follows: Miz1: Fwd: 5′-AACAGTCTCCCC ACTGCATA-3′, Rev: 5′-GTAGCTCTAGGCCACTG ACT-3′; Histone 3: Fwd: 5′-TTTTGTTTTCCA AAGCGCCC-3′, Rev: 5′-TCAGATTGTTCCCTTTC CGC-3′; SAT2: Fwd: 5′-ATCGAATGGAAATGAAAG-GAGTCA-3′, Rev: 5′-GACCATTGGATGATTGCAG TCA-3′.

RNA-Sequencing

The iPrEC and EMP lines were grown and differentiated as described above and harvested at days 0 (basal), 4, 8, 11, 14, and 17. At day 14 and 17, iPrEC differentiated cultures were treated with CFM-PBS supplemented with 1 mM EDTA and dissociation buffer for 40–45 min to isolate the luminal cells. Total RNA was isolated and purified using Life Technologies RNeasy and Purelink RNA mini kits. TruSeq mRNA libraries were prepared for sequencing using standard Illumina protocols from PolyA-enriched RNA. Illumina RNAseq—single read, 50 bp, approximately 30 million reads per sample. Sequenced reads were mapped to the hg19 whole genome using the Subread aligner (v1.4.3). Reads were assigned to genes using featureCounts. Raw read counts were voom transformed and differential expression performed using limma.

NCBI GEO Database Access to RNA-Sequencing

http://www.ncbi.nlm.nih.gov/geo/query/acc.cgi?token=utahcoigpdubpcj&acc=GSE77460

RESULTS

Miz1 Expression Is Increased During Prostate Luminal Cell Differentiation

When grown to confluency and treated with KGF plus androgen, basal prostate epithelial cells (iPrEC) undergo differentiation such that a second suprabasal luminal layer forms on top of the basal layer in 14–18 days [1,5]. To identify genes associated with luminal cell differentiation, iPrECs differentiated for 0–17 days were subjected to RNA sequencing. Miz1 (*ZBTB17*) transcript levels first dropped and then increased over the course of differentiation, peaking at day 14 in the luminal cells (Fig. 1A top panel). ING4 expression (Fig. 1A bottom panel) followed a similar trend, except that it peaked earlier at day 11. This trend of increased Miz1 mRNA expression over time was further validated by qRT-PCR (Fig. 1B), with a 1.8-fold peak in expression occurring after 14 days of differentiation in the luminal cells; paralleling the RNA-Seq data. There was a similar steady and significant increase in Miz1 protein expression over time, subsequent to the induction of ING4 expression (Fig. 1C). Highest expression of Miz1 was at day 14, mirroring the mRNA. Immunofluorescence imaging at day 3 versus day 12 revealed Miz1 was dramatically induced in the luminal cells (Fig. 1D). It should be noted that Miz1 expression is not restricted to the luminal cells; Miz1 staining is also seen in the basal cells of differentiated cultures, where its expression also increased but less dramatically.

ING4 Induces Miz1 Expression in Prostate Luminal Cells and Binds Directly to its Promoter

Because Miz1 was induced subsequent to ING4, we tested the effect of constitutive ING4 expression on Miz1. ING4 overexpression (iPrEC-ING4), resulted in an earlier and more robust induction of Miz1 expression around day 8 of differentiation, compared to a modest increase at day 12 in normal iPrECs (Fig. 2A). Constitutive ING4 expression also resulted in a sustained ~1.8-fold induction in Miz1 mRNA over the course of differentiation (Fig. 2B), which peaked at 2.5-fold in the luminal cells. Despite ING4 overexpression in the basal cells, Miz1 mRNA was not constitutively expressed in basal cells. Thus, the effect of ING4 on Miz1 is limited to luminal cells. We previously demonstrated that ING4 overexpression accelerates luminal cell differentiation [1] and as seen before there is significantly more luminal cells at day 8 in the ING4 overexpressing cells compared to normal iPrECs (Fig. 2C). There is also a concomitant increase in Miz1 expression in this luminal population as seen by immunostaining (Fig. 2C). These data indicate that ING4 overexpression in the luminal population enhances induced Miz1 expression.

Since constitutive ING4 expression was able to enhance the induction of Miz1 expression in luminal cells, we tested whether Miz1 is a direct target of ING4 using chromatin immunoprecipitation (ChIP). For these experiments, we compared iPrEC, iPrEC-ING4, and iPrEC-shING4 cells. Cell lines were differentiated for 3 days (low ING4) or 10 days (high ING4). ChIP of ING4 in normal iPrECs revealed that after 10 days of differentiation, ING4 was inducibly bound to the Miz1 promoter (Fig. 2D). ING4 overexpression resulted in its constitutive association at the Miz1 promoter at day 3. Cells lacking ING4

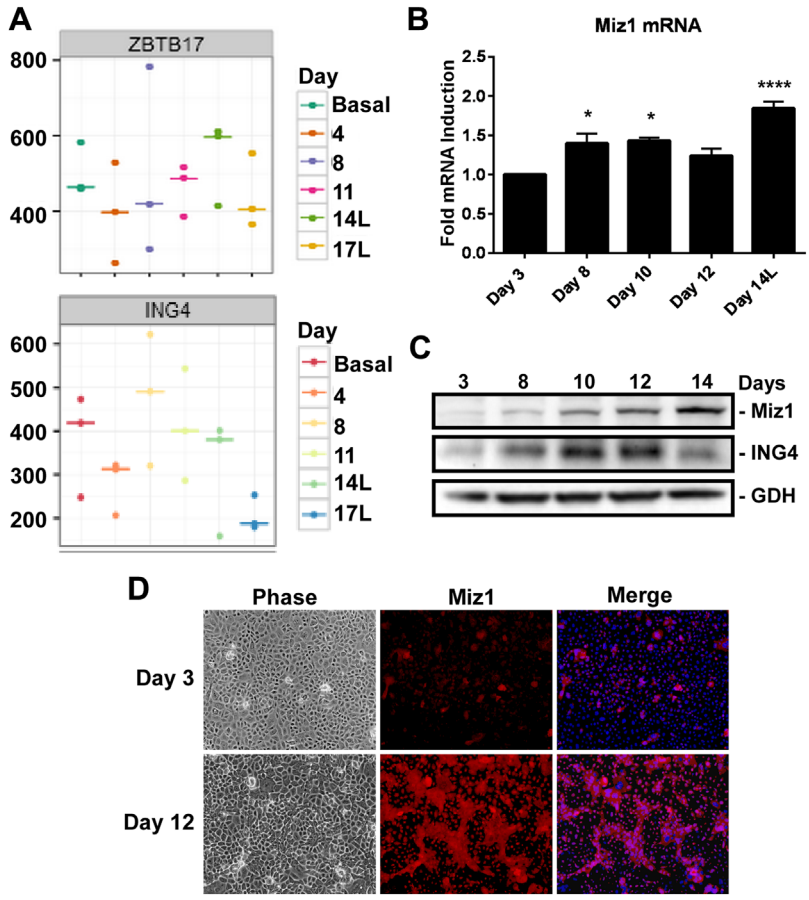

Fig. 1. Miz1 expression increasing during prostate luminal cell differentiation. Confluent immortalized prostate basal epithelial cells (iPrECs) were induced to differentiate with 2 ng/ml KGF and 5 nM R1881 for 0–17 days. ``L'' denotes isolated luminal-specific cells. (**A**) RNA sequencing was performed on samples isolated at the specified time points during iPrEC differentiation. Raw transcript counts are shown for Miz1 (*ZBTB17*) and ING4. (**B**) qRT-PCR was used to validate Miz1 mRNA expression. Data is normalized to 18 sec rRNA and expressed as fold induction relative to day 3 of differentiation. Error bars denote S.D. One-way ANOVA multiple comparisons *t*-test was used to calculate significance relative to day 3; $^{*}P < 0.05$; $^{****}P < 0.0001$. (**C**) Miz1 and ING4 protein levels were measured by immunoblotting. GAPDH (GDH) served as a loading control. (**D**) iPrECs differentiated for 3 or 12 days were immunostained for Miz1 (red), nuclei stained with Dapi (blue), and imaged by phase and epifluorescence microscopy.

ablated its ChIP at the Miz1 promoter (Fig. 2D) and ING4 did not bind the Histone 3 promoter. ING4 is thought to recruit the histone acetyltransferase HBO1 to chromatin [7]; however, we found HBO1 to be constitutively bound to the Miz1 promoter independent of ING4 (Fig. 2E). On the other hand, a gene known to be repressed during differentiation, SAT2 [19], lost HBO1 association at day 10 of normal differentiation and at day 3 in ING4 overexpressing cells (Fig. 2E).

ING4 is Necessary for Miz1 mRNA Induction in Luminal Cells

To determine if ING4 is necessary for Miz1 induction, we utilized two cell lines that do not express ING4 and do not differentiate; iPrEC-shING4 and tumorigenic iPrEC-EMP [1]. RNA-Seq data from iPrEC-EMP cells indicated Miz1 mRNA was not induced during the differentiation time course (not shown), and this was similarly observed by qRT-PCR (Fig. 3A). Miz1 mRNA also was not significantly induced in the iPrEC-shING4 cells (Fig. 3B). Thus, ING4 expression is necessary for Miz1 mRNA induction during luminal cell differentiation.

Miz1 Protein is Stabilized in Basal Cells

Despite the lack of significant Miz1 mRNA induction, Miz1 protein was still induced by the differentiation conditions in the undifferentiated "basal-like" EMP and shING4 cells in absence of ING4 (Fig. 3C). We attempted to measure Miz1 protein stability in iPrEC-shING4 cells by treating

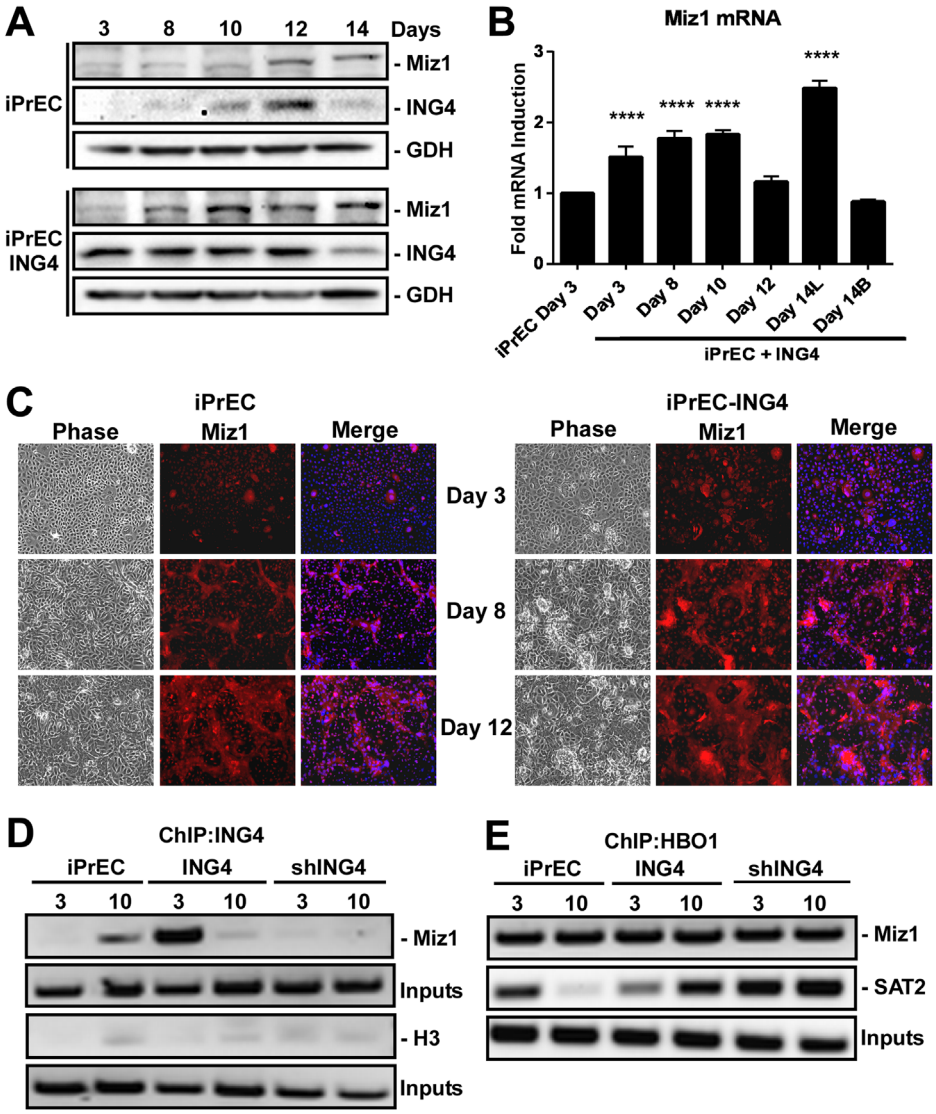

Fig. 2. ING4 is sufficient to induce Miz1 expression in prostate luminal cells and binds directly to its promoter. Confluent iPrEC, iPrEC-ING4, and shING4-iPrEC cell lines were induced to differentiate with 2 ng/ml KGF and 5 nM R1881 for 3–14 days. (**A**) Miz1 and ING4 protein levels were measured by immunoblotting. GAPDH (GDH) served as a loading control. (**B**) qRT-PCR analysis of Miz1 mRNA isolated from iPrECs + ING4 over the indicated time course of differentiation. Data normalized to 18 sec rRNA and expressed as fold induction relative to day 3 of iPrEC differentiation. (L and B) denotes isolated luminal and basal cell populations. Error bars denote S.D. One-way ANOVA multiple comparisons *t*-test was used to calculate significance relative to day 3 of iPrEC differentiation; $^{****}P < 0.0001$. (**C**) Cells differentiated for indicated times were immunostained for Miz1 (red), nuclei stained with Dapi (blue), and imaged by phase and epifluorescence microscopy. (**D**) Chromatin immunoprecipitation (ChIP) of ING4 on the Miz1 promoter at day 3 or 10 of differentiation. Histone 3 served as a negative control and shING4 controlled for antibody specificity. (**E**) ChIP of HBO1 on the Miz1 and SAT2 promoters at day 3 or 10 of differentiation.

with cycloheximide for different times. Regardless of the length of time of CHX treatment (up to 6 hr), we were unable to detect a change in Miz1 protein expression (Fig. 3E), suggesting Miz1 protein in basal cells is very stable. Under the same conditions, Myc protein was rapidly lost. Thus, ING4 expression is necessary for Miz1 mRNA induction in luminal cells, but Miz1 protein stability may be enhanced independent of ING4 in basal cells.

Constitutive Miz1 Expression Is Sufficient to Drive Luminal Cell Differentiation

If Miz1 is a primary target of ING4 required for differentiation, then overexpression of Miz1 could be

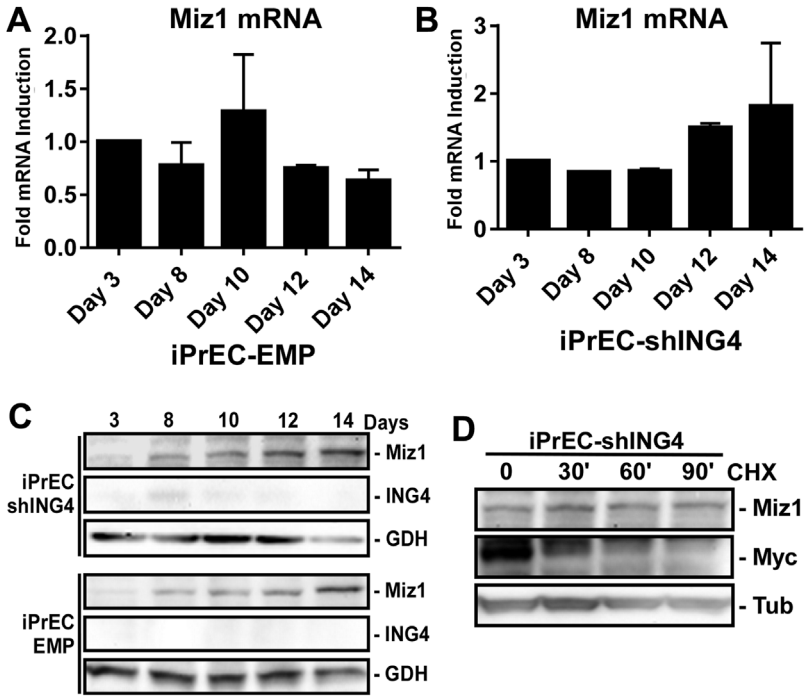

Fig. 3. ING4 is necessary for Miz1 induction in luminal cells, while Miz1 protein is stabilized in basal cells. iPrECs, iPrEC-shING4, and EMP-iPrECs were induced to differentiate with 2 ng/ml KGF and 5 nM R1881 for 3–17 days. (**A** and **B**) qRT-PCR analysis of Miz1 mRNA isolated from iPrEC-shING4 and EMP cells. Error bars denote S.D. No statistical difference between time points. (**C**) Miz1 and ING4 protein levels were measured by immunoblotting. GAPDH (GDH) served as a loading control. (**D**) iPrEC-shING4 cells were differentiated for 12 days and then treated with 50 μg/ml cycloheximide (CHX) for 0–90 min and levels of Miz1 and Myc protein measured by immunoblotting. Tubulin (Tub) served as a loading control.

sufficient to drive iPrEC differentiation. To address Miz1 sufficiency, we generated iPrECs that constitutively overexpress Miz1 (iPrEC-Miz1) as assessed by immunoblotting and immunostaining (Fig. 4A and B). Compared to normal iPrECs differentiated for 10 days, when a few AR-positive, integrin α6-negative luminal cells appear, there was considerably more of these luminal cells in the iPrEC-Miz1 cultures (Fig. 4C). This is the same phenotype that is observed in ING4 overexpressing cells (see Fig. 2C). Thus, overexpression of Miz1 is sufficient to induce luminal cell differentiation equivalent to that observed when ING4 is overexpressed.

Miz1 Is Not Required for Luminal Cell Differentiation

To determine if Miz1 is necessary for luminal cell differentiation, we generated cells that express a Tet-inducible shRNA targeting Miz1. This allowed us to selectively inhibit Miz1 expression late in differentiation, when it is maximally induced in the luminal cells. To test Miz1 knock-down, iPrEC-TetON-shMiz1 cells were differentiated for 10 days, and Miz1 expression suppressed by Dox induction of Miz1 shRNA during the last 5 or 3 days of differentiation. Miz1 expression was significantly reduced in as little as 3 days (Fig. 5A). To test the dependency on Miz1, iPrEC-TetON-shMiz1 cells were differentiated for 8 days, then treated with doxycycline for an additional 6 days of differentiation (14 days total). Miz1 expression was effectively inhibited under these conditions (Fig. 5B). The same amount of AR-positive, integrin α6-negative luminal cells were induced in the presence or absence of Miz1 (Fig. 5B), indicating that the cells were fully able to differentiate without Miz1. This was observed with two different shRNAs (not shown).

This lack of necessity was surprising given previous findings indicating Miz1 is required for differentiation in other models [10,12,20]. Furthermore, one of these studies indicated Miz1 interaction with Myc was required for differentiation and a Myc mutant which cannot bind Miz1, MycV394D, blocked differentiation [10]. We previously showed that Myc is required for ING4 induction and luminal cell differentiation [1]. Therefore, we generated iPrECs that overexpress Myc-GFP or Myc-V394D-RFP (Fig. 5D). Expression of MycV394D had no impact on the ability of these cells to differentiate; inducing comparable

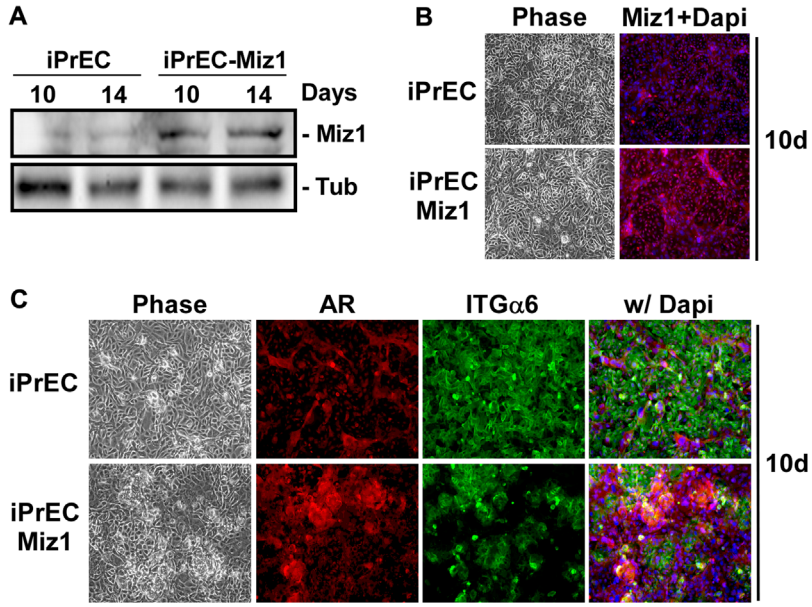

Fig. 4. Constitutive Miz1 expression is sufficient to drive luminal cell differentiation. iPrECs overexpressing Miz1 (iPrEC-Miz1) were induced to differentiate with 2 ng/ml KGF and 5 nM R1881 for 10–14 days. (**A**) Level of Miz1 expression was measured by immunoblotting. Tubulin (Tub) served as a loading control. (**B**) Cells differentiated for 10 days were immunostained for Miz1 (red) and nuclei were stained with Dapi (blue). (**C**) Differentiation was measured after 10 days by immunostaining of basal cells for integrin α6 (ITGα6; green) and luminal cells for AR (red), and nuclei were stained with Dapi (blue). All cells were visualized by phase and epifluorescence microscopy.

levels of AR-positive and integrin α6-negative luminal cells (Fig. 5E).

DISCUSSION

We set out to determine how ING4 induction during prostate luminal cell differentiation leads to the suppression of integrin expression by defining ING4 target genes that might control integrin expression. Our studies successfully identified Miz1 as a direct downstream target of ING4 in luminal cells, and demonstrated that Miz1 overexpression is sufficient to mimic the differentiation phenotype induced by ING4 including loss of integrin α6 expression. However, Miz1 is not necessary for luminal cell differentiation as determined by shRNA knock-down or expression of a dominant Myc-Miz1 binding mutant and therefore is not absolutely necessary for integrin loss during luminal cell differentiation.

ING4 is a chromatin binding protein that specifically recognizes and binds the H3K4me3 chromatin mark [21]. It has been shown to recruit HBO1, an acetyltransferase that can acetylate histone H4 or H3 to promote transcription of target genes [7,22]. However, the exact targets that ING4 actually binds have largely not been identified, and are limited to Smc4, Egln1, Ext1 in HT1080 cells [22], and a few NF-κB targets such as Cox2 and MMP9 [23]. Using RNA-Seq, a best candidate approach, and ChIP, we identified the Miz1 promoter as a binding target of ING4 during prostate luminal epithelial differentiation. We further demonstrate that genetically increasing or decreasing ING4 expression results in a concomitant increase or decrease in Miz1 mRNA expression, respectively. However, this coordinated expression is not present in basal cells, even when ING4 is constitutively overexpressed, being restricted to the luminal cells. Thus, there are likely to be other "competency" factors required, that is, a signal that defines a pre-luminal state induced by the differentiation conditions of KGF and androgen. Similarly, we demonstrate that overexpression of Miz1 is sufficient to robustly accelerate luminal cell differentiation to the same degree seen with ING4 overexpression. However, this effect is still dependent on the differentiation factors; constitutive Miz1 overexpression in the absence of KGF and androgen is not sufficient to induce differentiation on its own.

Given the reported ability of ING4 to specifically recruit HBO1 to H3K4me3-marked promoters [7,21,22], we were surprised to find that HBO1 was constitutively bound to the Miz1 promoter. This was not true for all genes, as we saw HBO1 loss at SAT2, a gene that is down regulated upon luminal cell differentiation in our model. We noted that Miz1 is also expressed in basal cells, where it is not subject to ING4 regulation. These data are consistent with Miz1 being an already active gene in prostate epithelial cells. Thus, ING4 may be acting to enhance transcription via recruitment of

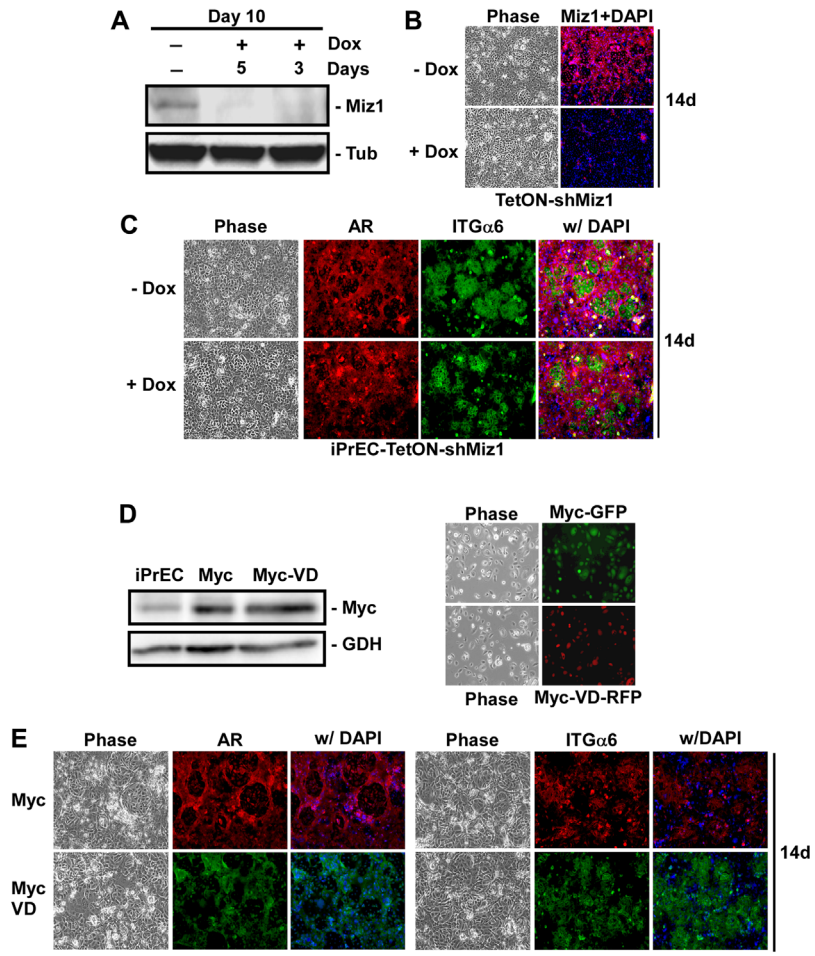

Fig. 5. Miz1 is not required for luminal cell differentiation. iPrECs overexpressing Miz1 Tet-inducible shRNA (iPrEC-TetON-shMiz1), Myc (Myc-GFP), or MycV394D mutant (Myc-V394D-RFP) were induced to differentiate with 2 ng/ml KGF and 5 nM R1881 for 10–14 days. (**A**) Cells were differentiated for 10 days and treated with 100 ng/ml doxycycline (Dox) during the last 5 or 3 days of differentiation. Miz1 and tubulin (Tub) expression were measured by immunoblotting. (**B** and **C**) Cells were differentiated for 14 days and treated with Dox during the last 6 days of differentiation. (**B**) Control cultures were immunostained for Miz1 (red) and nuclei stained with Dapi (blue). (**C**) Differentiation was measured by immunostaining of basal cells for integrin α6 (ITGα6; green) and luminal cells for AR (red), and nuclei were stained with Dapi (blue). All cells were imaged by phase and epifluorescence microscopy. (**D**) Myc-GFP or Myc-VD-RFP expression was assessed in undifferentiated cells by western blot (left panel), with GAPDH (GDH) as a loading control, and epifluorescence microscopy (right panel). (**E**) Differentiation was measured after 14 days by immunostaining of luminal cells for AR (red-Myc; green-MycVD) and basal cells for integrin α6 (ITGα6; red-Myc; green-MycVD), and nuclei were stained with Dapi (blue). All cells were visualized by phase and epifluorescence microscopy.

other factors specifically during luminal cell differentiation. ChIP-Seq experiments are underway to define other ING4 targets and associated chromatin modifiers.

We previously showed that oncogenic conversion of human iPrECs by Erg, Myc, and shPten overexpression (EMP cells), generates tumorigenic cells that are arrested in differentiation and fail to induce ING4 expression [1]. We also demonstrated Erg/Myc overexpressing cells are not tumorigenic, but loss of ING4 is sufficient to transform them and that ING4 is lost in over 60% of human primary prostate tumors [1]. Consistent with Miz1 dependency on ING4 expression, the EMP cells also did not induce Miz1 expression in response to the differentiation conditions. Correspondingly, these cells do not properly differentiate as defined by a lack of a distinct AR-positive and integrin α6-negative population.

Loss of Miz1 expression per se is not likely to be a good distinguishing marker for prostate cancer as basal cells and EMP cells still express Miz1; it is just not induced or regulated by ING4. Nonetheless, this allowed us to identify at least two mechanisms by which Miz1 expression is regulated. However, the most striking finding was the apparent lack of dependency on Miz1 for luminal cell differentiation. Despite the presence of distinct mechanisms for

regulating Miz1 mRNA and protein expression, cells were still capable of differentiating without Miz1. This indicates there are other, potentially compensatory, factors that control differentiation, and integrin expression in particular. It also indicates there are other ING4 targets required for luminal cell differentiation. One potential target could be Notch signaling [24]. Studies are currently underway to determine the relationship between ING4, Notch, and luminal cell differentiation.

CONCLUSIONS

The Myc repressor, Miz1, is a direct target of the chromatin binding protein ING4, whose induction during luminal cell differentiation is dependent on ING4. Miz1 is capable of accelerating luminal cell differentiation when overexpressed, but is not absolutely required for differentiation.

ACKNOWLEDGMENTS

We thank the Michigan State University Research Technology Support Core for the RNA sequencing. Dr. Sander Frank generated the modified pLKO-TetON-Puro shRNA vector, which was originally purchased from Addgene and Dr. Martine Roussel provided the wild-type Myc and MycV394D mutant constructs. This project was supported by funding from the Department of Defense Prostate Cancer Research Program W81XWH-14-1-0479 (PLB), NIH/NCI CA154835 (CKM; PLB), and the Van Andel Research Institute (CKM, MEW).

REFERENCES

1. Berger PL, Frank SB, Schulz VV, Nollet EA, Edick MJ, Holly B, Chang TT, Hostetter G, Kim S, Miranti CK. Transient induction of ING4 by Myc drives prostate epithelial cell differentiation and its disruption drives prostate tumorigenesis. Cancer Res 2014;74(12):3357–3368.
2. Li X, Wang Y, Sharif-Afshar AR, Uwamariya C, Yi A, Ishii K, Hayward SW, Matusik RJ, Bhowmick NA. Urothelial transdifferentiation to prostate epithelia is mediated by paracrine TGF-beta signaling. Differentiation 2009;77(1):95–102.
3. Wu CT, Altuwaijri S, Ricke WA, Huang SP, Yeh S, Zhang C, Niu Y, Tsai MY, Chang C. Increased prostate cell proliferation and loss of cell differentiation in mice lacking prostate epithelial androgen receptor. Proc Natl Acad Sci USA 2007;104(31):12679–12684.
4. Luo W, Rodriguez M, Valdez JM, Zhu X, Tan K, Li D, Siwko S, Xin L, Liu M. Lgr4 is a key regulator of prostate development and prostate stem cell differentiation. Stem cells 2013;31(11):2492–2505.
5. Lamb LE, Knudsen BS, Miranti CK. E-cadherin-mediated survival of androgen-receptor-expressing secretory prostate epithelial cells derived from a stratified in vitro differentiation model. J Cell Sci 2010;123(2):266–276.
6. Coles AH, Jones SN. The ING gene family in the regulation of cell growth and tumorigenesis. J Cell Physiol 2009;218(1):45–57.
7. Doyon Y, Cayrou C, Ullah M, Landry A-J, Côté V, Selleck W, Lane WS, Tan S, Yang X-J, Côté J. ING tumor suppressor proteins are critical regulators of chromatin acetylation required for genome expression and perpetuation. Mol Cell 2006;21(1):51–64.
8. Kim S, Welm AL, Bishop JM. A dominant mutant allele of the ING4 tumor suppressor found in human cancer cells exacerbates MYC-initiated mouse mammary tumorigenesis. Cancer Res 2010;70(12):5155–5162.
9. Cress AE, Rabinovitz I, Zhu W, Nagle RB. The α6β1 and α6β4 integrins in human prostate cancer progression. Cancer Metastasis Rev 1995;14(3):219–228.
10. Gebhardt A, Frye M, Herold S, Benitah SA, Braun K, Samans B, Watt FM, Elsässer H-P, Eilers M. Myc regulates keratinocyte adhesion and differentiation via complex formation with Miz1. J Cell Biol 2006;172(1):139–149.
11. Mazzone M, Selfors LM, Albeck J, Overholtzer M, Sale S, Carroll DL, Pandya D, Lu Y, Mills GB, Aster JC, Artavanis-Tsakonas S, Brugge JS. Dose-dependent induction of distinct phenotypic responses to Notch pathway activation in mammary epithelial cells. Proc Natl Acad Sci USA 2010;107(11):5012–5017.
12. Sanz-Moreno A, Fuhrmann D, Wolf E, von Eyss B, Eilers M, Elsässer H-P. Miz1 deficiency in the mammary gland causes a lactation defect by attenuated stat5 expression and phosphorylation. PloS ONE 2014;9(2):e89187.
13. Tapia C, Zlobec I, Schneider S, Kilic E, Guth U, Bubendorf L, Kim S. Deletion of the inhibitor of growth 4 (ING4) tumor suppressor gene is prevalent in human epidermal growth factor 2 (HER2)-positive breast cancer. Hum Pathol 2011;42(7):983–990.
14. Byron SA, Min E, Thal TS, Hostetter G, Watanabe AT, Azorsa DO, Little TH, Tapia C, Kim S. Negative regulation of NF-kappaB by the ING4 tumor suppressor in breast cancer. PloS ONE 2012;7(10):46823.
15. Yan R, He L, Li Z, Han X, Liang J, Si W, Chen Z, Li L, Xie G, Li W, Wang P, Lei L, Zhang H, Pei F, Cao D, Sun L, Shang Y. SCF(JFK) is a bona fide E3 ligase for ING4 and a potent promoter of the angiogenesis and metastasis of breast cancer. Genes Dev 2015;29(6):672–685.
16. Wiederschain D, Susan W, Chen L, Loo A, Yang G, Huang A, Chen Y, Caponigro G, Yao Y-m, Lengauer C, Sellers WR, Benson JD. Single-vector inducible lentiviral RNAi system for oncology target validation. Cell Cycle 2009;8(3):498–504.
17. Herold S, Wanzel M, Beuger V, Frohme C, Beul D, Hillukkala T, Syvaoja J, Saluz HP, Haenel F, Eilers M. Negative regulation of the mammalian UV response by Myc through association with Miz-1. Mol Cell 2002;10(3):509–521.
18. Edick MJ, Tesfay L, Lamb LE, Knudsen BS, Miranti CK. Inhibition of integrin-mediated crosstalk with epidermal growth factor Receptor/Erk or src signaling pathways in autophagic prostate epithelial cells induces caspase-independent death. Mol Biol Cell 2007;18(7):2481–2490.
19. Chen Y, Vujcic S, Liang P, Diegelman P, Kramer DL, Porter CW. Genomic identification and biochemical characterization of a second spermidine/spermine N1-acetyltransferase. Biochem J 2003;373(Pt 3):661–667.

20. Kerosuo L, Bronner ME. Biphasic influence of Miz1 on neural crest development by regulating cell survival and apical adhesion complex formation in the developing neural tube. Mol Biol Cell 2014;25(3):347–355.

21. Culurgioni S, Munoz IG, Moreno A, Palacios A, Villate M, Palmero I, Montoya G, Blanco FJ. Crystal structure of inhibitor of growth 4 (ING4) dimerization domain reveals functional organization of ING family of chromatin-binding proteins. J Biol Chem 2012;287(14):10876–10884.

22. Hung T, Binda O, Champagne KS, Kuo AJ, Johnson K, Chang HY, Simon MD, Kutateladze TG, Gozani O. ING4 mediates crosstalk between histone H3 K4 trimethylation and H3 acetylation to attenuate cellular transformation. Mol Cell 2009;33(2): 248–256.

23. Nozell S, Laver T, Moseley D, Nowoslawski L, De Vos M, Atkinson GP, Harrison K, Nabors LB, Benveniste EN. The ING4 tumor suppressor attenuates NF-kappaB activity at the promoters of target genes. Mol Cell Biol 2008;28(21):6632–6645.

24. Chakrabarti R, Wei Y, Romano RA, DeCoste C, Kang Y, Sinha S. Elf5 regulates mammary gland stem/progenitor cell fate by influencing notch signaling. Stem Cells 2012;30(7): 1496–1508.

Frank et al. BMC Biotechnology (2017) 17:24
DOI 10.1186/s12896-017-0341-x

BMC Biotechnology

METHODOLOGY ARTICLE Open Access

A streamlined method for the design and cloning of shRNAs into an optimized Dox-inducible lentiviral vector

Sander B. Frank[1,2,3], Veronique V. Schulz[1] and Cindy K. Miranti[1,3*]

Abstract

Background: Short hairpin RNA (shRNA) is an established and effective tool for stable knock down of gene expression. Lentiviral vectors can be used to deliver shRNAs, thereby providing the ability to infect most mammalian cell types with high efficiency, regardless of proliferation state. Furthermore, the use of inducible promoters to drive shRNA expression allows for more thorough investigations into the specific timing of gene function in a variety of cellular processes. Moreover, inducible knockdown allows the investigation of genes that would be lethal or otherwise poorly tolerated if constitutively knocked down. Lentiviral inducible shRNA vectors are readily available, but unfortunately the process of cloning, screening, and testing shRNAs can be time-consuming and expensive. Therefore, we sought to refine a popular vector (Tet-pLKO-Puro) and streamline the cloning process with efficient protocols so that researchers can more efficiently utilize this powerful tool.

Methods: First, we modified the Tet-pLKO-Puro vector to make it easy ("EZ") for molecular cloning (EZ-Tet-pLKO-Puro). Our primary modification was to shrink the stuffer region, which allows vector purification via polyethylene glycol precipitation thereby avoiding the need to purify DNA through agarose. In addition, we generated EZ-Tet-pLKO vectors with hygromycin or blasticidin resistance to provide greater flexibility in cell line engineering. Furthermore, we provide a detailed guide for utilizing these vectors, including shRNA design strategy and simplified screening methods.

Results: Notably, we emphasize the importance of loop sequence design and demonstrate that the addition of a single mismatch in the loop stem can greatly improve shRNA efficiency. Lastly, we display the robustness of the system with a doxycycline titration and recovery time course and provide a cost/benefit analysis comparing our system with purchasing pre-designed shRNA vectors.

Conclusions: Our aim was twofold: first, to take a very useful shRNA vector and make it more amenable for molecular cloning and, secondly, to provide a streamlined protocol and rationale for cost-effective design, cloning, and screening of shRNAs. With this knowledge, anyone can take advantage of this powerful tool to inducibly knockdown any gene of their choosing.

Keywords: pLKO, shRNA, Lentivirus, Inducible

* Correspondence: cmiranti@email.arizona.edu
[1]Laboratory of Integrin Signaling and Tumorigenesis, Van Andel Research Institute, Grand Rapids, MI, USA
[3]Department of Cellular and Molecular Medicine, University of Arizona Cancer Center, 1515 N. Campbell Ave, Tucson, AZ 85724, USA
Full list of author information is available at the end of the article

Background

Knockdown of gene expression at the mRNA level via RNA interference (RNAi) is a common method for investigating gene function. For transient knockdown in mammalian cell culture, small interfering RNA (siRNA) is often favored. The benefits of siRNA include commercially available RNA oligos which can be transfected into cells for quick and efficient knockdown. However, siRNA becomes less useful when working with cell types with low transfection efficiency or in experiments that require prolonged gene knockdown [1]. Another common method for utilizing RNAi is short-hairpin RNA (shRNA), synthetic non-coding RNA that utilizes the endogenous microRNA machinery to process functional RNAi. Though not as simple to use as siRNA, shRNA can avoid concerns of low transfection efficiency and temporary knockdown by using retroviral delivery and selection for stable genomic integration [2–4].

Lentiviral shRNA vectors are popular due to their ability to infect nearly any cell type and integrate into the genome of both dividing and non-dividing cells. In 2006, the BROAD institute established the RNAi Consortium to identify and clone multiple shRNA candidate sequences for every gene in the mouse and human genomes [5]. The consortium cloned the shRNA sequences into the pLKO lentiviral vector backbone and has made them available for distribution from GE Healthcare Dharmacon and Sigma-Aldrich. The shRNAs were not all functionally validated but were given a computationally calculated score for predicated efficiency and specificity.

In 2009, Dmitri Wiederschain and colleagues built upon the pLKO vector and made multiple changes, the two most significant of which were the inclusion of the Tet-Repressor gene (TetR) and an H1 promoter containing the TetOperator (TetO) sequence to drive shRNA expression. Together, these modifications allow transcription of shRNA upon the addition of tetracycline, or its analogue doxycycline (Dox), to sequester TetR and relieve repression at the TetO [5, 6]. This vector combines the benefits of lentiviral delivery and inducible gene knockdown, providing many advantages over siRNA or constitutive shRNA. One key advantage is the ability to use the same pool of cells for the controls (no induction) and the test sample (plus inducer), thereby eliminating concerns of transfection/infection efficiency or unintentional clonal selection between 'empty/non-targeting' and 'shRNA' stable pools. By combining inducible vectors with the list of candidate shRNA sequences from the RNAi consortium it is now possible to induce knockdown of nearly any gene in virtually any cell type.

The Tet-pLKO-Puro vector is a potentially powerful tool, but the process of designing and cloning shRNAs into the vector is not without challenge. In an effort to improve this tool even further we made some modifications to make it more amenable for cloning. Furthermore, we establish clear and efficient protocols for designing and cloning shRNAs into the vector. In addition, we demonstrate the importance of loop design including using a single mismatch to improve shRNA efficiency. With our modified vector (EZ-Tet-pLKO) and a detailed description for designing and cloning shRNAs, we aim to make it easy for anyone to quickly adopt and utilize this tool.

Results

Modifications to the Tet-pLKO-Puro vector

We started with the Tet-pLKO-Puro vector and modified it to make it more amenable for molecular cloning, terming our version EZ-Tet-pLKO-Puro. First, we used mutagenesis to delete the large non-functional stuffer region (~1.9 kb), leaving a smaller stuffer of ~200 bp (Fig. 1a). Second, we mutated the 5′ AgeI cloning site to an NheI sequence to ameliorate occasional difficulties with inefficient AgeI + EcoRI co-digestion. Additionally, we generated matching vectors with mammalian selection markers for hygromycin (Hygro) or blasticidin (Blast) resistance (Fig. 1a). The smaller stuffer makes it possible to purify cut vector by size-selective DNA precipitation with polyethylene glycol (PEG). To compare precipitation methods, cut DNA was precipitated by isopropanol, 8% PEG, or 6% PEG. The 6% PEG precipitation removed nearly all of the 200 bp stuffer (Fig. 1b). Together, the combination of vector modifications and utilization of PEG precipitation provides a simplified method for preparing cut vector.

shRNA oligo design

Developing functional shRNA constructs often requires testing many targeting sequences; therefore, a process for designing shRNAs quickly and efficiently is quite valuable. Targeting sequences were selected as described in the methods section and used to generate sense and antisense shRNA oligos. shRNA oligos contain the following elements: 5′ overhang, targeting sequence, loop, reverse-complement targeting sequence, transcriptional terminator sequence, and 3′ overhang (Fig. 2a). The antisense oligo (bottom strand) is a reverse complement of the sense oligo with complementary overhangs. Without a mismatch, a 6 nt palindrome loop is predicted to collapse to a 4 nt loop and shift the targeting sequence by one base (Fig. 2b). Immortalized prostate epithelial cells (iPrECs) were infected with shRNA lentivirus (sh.p38δ or sh.Creb1) and pools were selected containing the same targeting sequence with or without a single mismatch. Immunoblot showed very efficient knockdown of p38δ with the 7 nt loop and no knockdown with the 6 nt loop (Fig. 2c). Probing for TetR showed that both pools were infected with the lentivirus and had similar expression levels of the lentiviral construct. A similar test was performed using cells containing the sh.Creb1 construct and produced similar results (Fig. 2d). Thus, when designing shRNA sequences it is crucial to

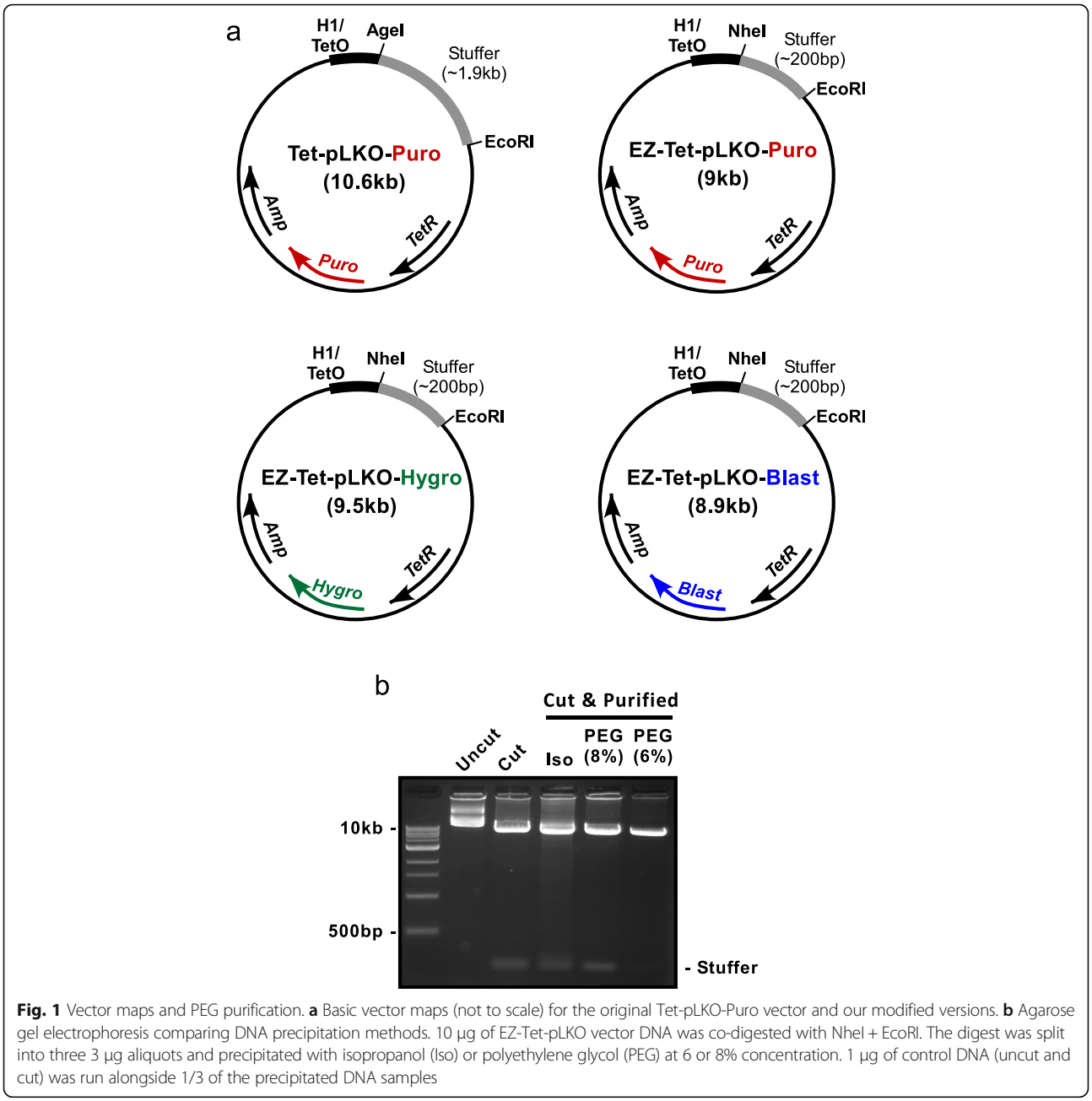

Fig. 1 Vector maps and PEG purification. **a** Basic vector maps (not to scale) for the original Tet-pLKO-Puro vector and our modified versions. **b** Agarose gel electrophoresis comparing DNA precipitation methods. 10 μg of EZ-Tet-pLKO vector DNA was co-digested with NheI + EcoRI. The digest was split into three 3 μg aliquots and precipitated with isopropanol (Iso) or polyethylene glycol (PEG) at 6 or 8% concentration. 1 μg of control DNA (uncut and cut) was run alongside 1/3 of the precipitated DNA samples

consider not only the targeting sequence, but also a mismatch in the loop stem.

Streamlined colony screening

After ligation of vector and shRNA oligos the DNA must be transformed into competent bacteria and colonies must be screened. Colony-PCR is a quick way to use small amounts of bacteria directly as template in a PCR reaction. We designed primers to span the stuffer/shRNA insert region, producing a ~450 bp band for positive clones and a ~620 bp band for background vector with retained stuffer (Fig. 3a). PCR product was visualized by agarose gel electrophoresis, which produced clearly identifiable bands for true clones and background colonies (Fig. 3b).

Additionally, clones can be further validated by restriction enzyme (RE) digest screening, which requires a miniprep step to isolate plasmid DNA. The original Tet-pLKO-Puro protocol recommended using an XhoI loop in the hairpin [6, 7]. Because there are already 3 XhoI sites in the parental EZ- Tet-pLKO vector (Fig. 3c-i), introducing a fourth XhoI site in the loop creates four fragments upon digestion (Fig. 3c-ii, d). Furthermore, in the EZ-Tet-pLKO vector two of these bands are so small, 138 bp (***) and 43 bp (****), representing less than 2% of the total DNA (Fig. 3c-ii, d)

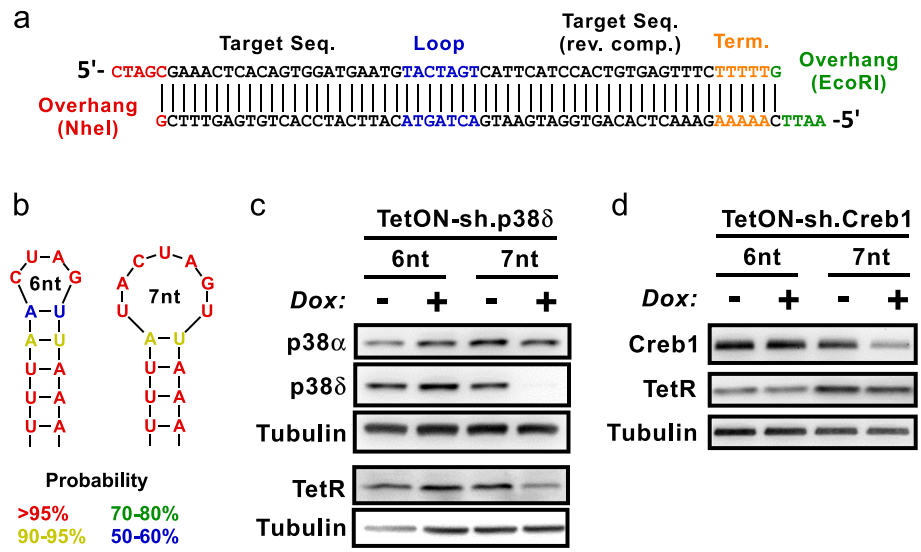

Fig. 2 shRNA oligo design and loop comparison. **a** Format for shRNA oligo design. Upper strand is sense oligo, lower strand is anti-sense oligo. **b** Diagram of predicted shRNA loop structure with a basic SpeI sequence (6 nt: ACUAGU) or including a single stem mismatch (7 nt: UACUAGU). Colors correlate to calculated likelihood of the depicted pairing. See methods for details on prediction tool. **c** Immunoblot showing two different pools of iPrEC cells with shRNA against p38δ, with the only difference being a single mismatch in the loop sequence of the shRNA. Cells were treated −/+ Dox for 72 h. TetR was probed on a separate gel. p38α and Tubulin serve as loading controls. **d** Same experiment as **c** using a different pair of shRNAs targeting Creb1. Cells were treated −/+ Dox for 5 days

making it very difficult to visualize on an agarose gel even with a long exposure (Fig. 3e). As a way to simplify and improve the RE screening process, we recommend a SpeI site for loop design (Fig. 3c-iii). When visualized on agarose, a positive SpeI screen produces a clear band at ~500 bp, which is ~5% of total DNA and easily detectable (Fig. 3d, e). We further validated the EZ-Tet-pLKO-shRNA positive clones by Sanger sequencing using the same pLKO-fwd primer as used in the PCR screen. Thus, the combination of colony-PCR as a cheap and quick primary screen and SpeI-based digest as a secondary screen creates a streamlined process for identifying positive shRNA clones.

Dox Titration and recovery time courses

Next, we validated the efficacy of the EZ-Tet-pLKO-Puro vector in cell culture. Cells were infected with lentivirus and pools were selected with puromycin. We performed a titration with Dox (0.5 to 50 ng/mL) and found that as little as 10 ng/mL was sufficient to induce target (p38α) knockdown (Fig. 4a). Furthermore, the target protein can be recovered after removal of Dox. Cells with sh.p38α were treated with Dox for 72 h and then split. Dox was removed and samples were harvested over a recovery time course (Fig. 4b). Recovery of protein began four days after removal of Dox. Thus, the EZ-Tet-pLKO system is both inducible and reversible.

Cost analysis and comparison

Our method for designing, cloning, screening, and validating lentiviral shRNAs is not only efficient but also cost effective. Most reagents can be found in a standard molecular biology lab (e.g., restriction enzymes, PCR reagents, agarose gel electrophoresis equipment). The EZ-Tet-pLKO plasmids can be acquired from the Addgene repository. The only reagent that is single-use are the shRNA oligos, which are unique for each clone and also the largest single cost. However, once the required reagents are assembled, it only costs ~ $50 in supplies and materials for each new shRNA cloned (Table 1).

Estimated costs for the various reagents needed in the cloning protocol. Note: Does not include plastic consumables or common lab reagents (e.g., LB media, alcohol, agarose, competent cells) or lentiviral packaging components. Estimated total cost is based on screening 10 colonies per shRNA ligation. The primary cost for subsequent shRNAs are the sense and anti-sense oligos ($44), with the remaining cost coming from consumable enzymes. PNK: Polynucleotide Kinase. AP: Antarctic Phosphatase. IDT: Integrated DNA Technologies. NEB: New England BioLabs.

In addition to the method described here, it is also possible to purchase shRNAs already cloned in lentiviral plasmids from an RNAi Consortium library, such as Sigma Aldrich or Dharmacon. The costs and benefits to using our custom design method vs purchasing vectors (Table 2) outweigh the others. The primary benefits of our method are the low costs and customizability, the ability to use the improved 7 nt loop, and use of any of three different selection vectors (Puro, Hygro, or Blast). The alternative options are to purchase shRNAs already cloned into a vector at a cost of $50–$100 (non-inducible) or $400–$450 (Dox inducible),

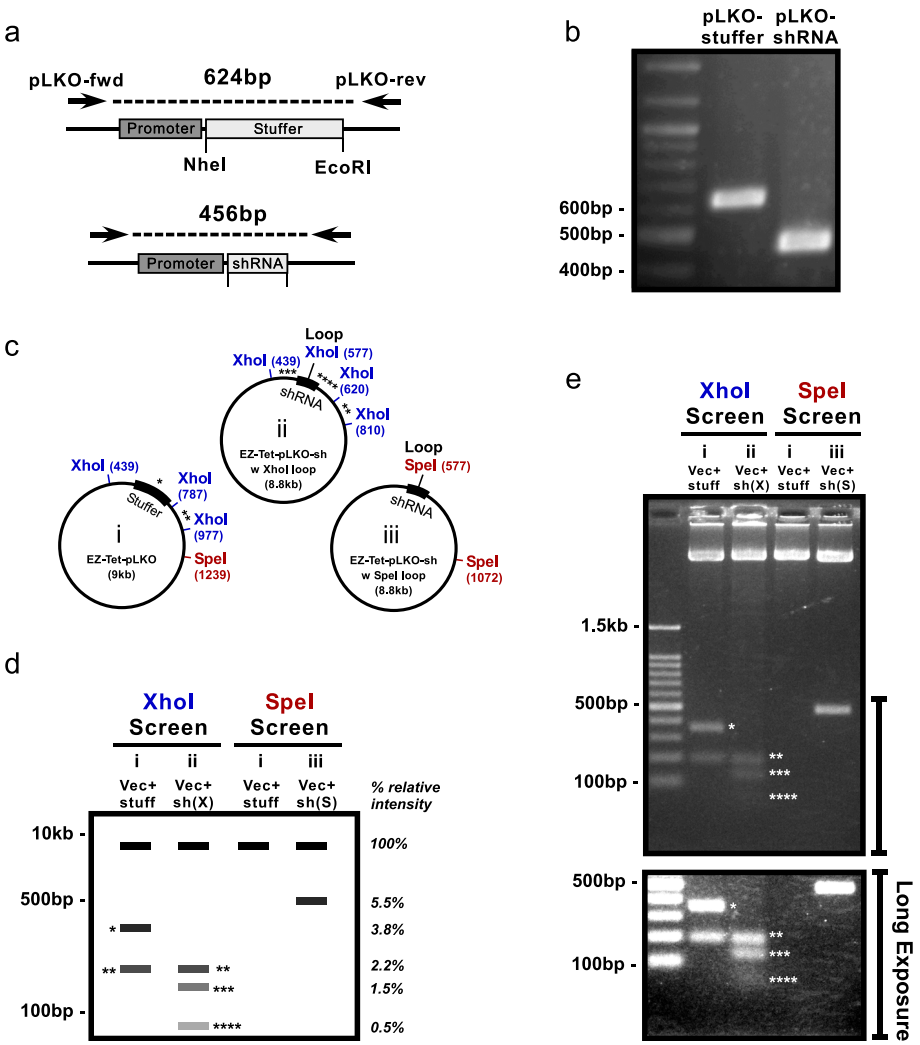

Fig. 3 Screening techniques. **a** Diagram showing expected products from PCR screening pLKO ligation-transformed colonies. **b** Agarose gel (2%) with a positive and negative PCR product. **c** Vector maps (not to scale) with XhoI and SpeI restriction digest sites labeled in bp. *Asterisks* indicate corresponding bands in Fig. 3d and e. **d** Diagram showing expected DNA fragments and relative intensity on gel from an XhoI (*blue*) vs SpeI (*red*) shRNA loop restriction digest screen of the plasmids shown in 3c (i - parental EZ- Tet-pLKO vector with stuffer (Vec + stuff), ii - EZ-Tet-pLKO with shRNA XhoI loop (Vec + sh(X)), iii - EZ-Tet-pLKO with shRNA SpeI loop (Vec + sh(S)). (*) is the predicted 348 bp XhoI fragment spanning the stuffer region in the original Tet-pLKO vector (i). In the EZ-Tet-pLKO vector harboring an shRNA with an XhoI site in the loop (ii), XhoI digestion will generate three small fragments, 190 bp (**), 138 bp (***), and 43 bp (****). In the EZ-Tet-pLKO vector harboring an shRNA with an SpeI site in the loop (iii), SpeI digestion will generate a clearly visible diagnostic 500 bp fragment. **e** Agarose gel (2%) with XhoI or SpeI shRNA screens of constructs indicated in 3c (i, ii, iii). Each lane was loaded with 4 μg of digested DNA. Bottom image shows lower part of the same gel with a longer exposure to show the barely detectable 43 bp (****) fragment

and they are limited to the 6 nt loop. In addition, lentiviral particles can also be purchased which allows for immediate infection but come at a high cost (> $1,000). Though the commercial options may be quicker, the cost, customizability, versatility, inducibility, and more efficient 7 nt loop of the EZ-Tet-pLKO method makes it a better option overall.

Comparison of cost/benefits of our cloning method versus other sources of TRC (The RNAi Consortium) library shRNAs. Note: Costs here are based on Dharmacon prices (http://dharmacon.gelifesciences.com/applications/rna-interference/shrna/, last accessed Dec. 6th, 2016).

Efficiency

The large stuffer (1.9 kb) region between the cloning sites in the original Tet-pLKO-Puro vector necessitated the tedious process of gel purifying the vector fragment. By reducing the stuffer to 200 bp we were able to more efficiently and quickly isolate the purified cut vector with PEG. Use of the original vector with the long stuffer resulted in the same number of colonies in the vector-only ligated plate as on the insert ligation plate, necessitating excessive screening of >50 colonies to find 1 transformant with the insert (i.e., 2%). With the shorter stuffer, there were typically ~0–20

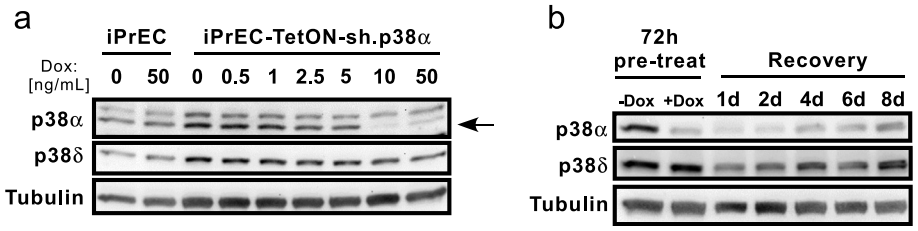

Fig. 4 Dox titration and recovery. **a** Immunoblot showing Dox titration with iPrECs containing EZ-Tet-pLKO-sh.p38α. Cells were treated with Dox for 72 h and lysed. Note: the lower band (*arrow pointing*) is p38α. **b** Cells were treated −/+ Dox (50 ng/mL) for 72 h. At that time, two samples were lysed (72 h pre-treated) while another plate of treated cells was split and allowed to recover without Dox for 1–8 days. Note: due to changes in confluency, the 'pre-treated' cells have higher basal level of p38 (α and δ) than at day 8

colonies on the vector-only ligation plate and >20–100 colonies on the insert ligation plate, equating to an efficiency of ~10–50 colonies per ng of cut vector (# colonies × 1000/100 (LB dilution) × 20/4 (ligation reaction dilution) × 1/100 (ng vector DNA per μL ligation reaction). Furthermore, ~80% of these colonies had the desired insert. In addition, the shorter stuffer allows for improved PCR screening and saves at least a day by not having to wait to grow up the colonies before standard restriction enzyme screening.

Discussion

The EZ-Tet-pLKO vector together with our detailed methods provides a descriptive guide to efficiently utilize inducible shRNAs. Though we have focused on a modified pLKO vector, the principles of shRNA design and screening could be applied to many other cloning scenarios. Our primary modification to the vector was to shrink the stuffer region. The stuffer is non-functional DNA, and we chose to keep a small 200 bp region so that double-cut vector could clearly be visualized separately from linearized single-cut vector on agarose. Moreover, retaining a small stuffer allows for size-selective precipitation of cut vector via PEG [8]. Compared to alcohol precipitation and gel extraction, PEG precipitation is faster, provides cleaner DNA, and avoids concerns of potential DNA damage from UV exposure [9, 10]. We also sought to emphasize the importance of using a proper loop design for shRNAs including adding a stem mismatch [11]. The inclusion of a mismatch in the loop region can aid hairpin formation by preventing loop collapse and thus shifting the targeting sequence, which can disrupt proper DICER binding and target mRNA cleavage [12, 13]. The mismatch was not always necessary for proper shRNA function (not shown), but in at least the two cases reported here it was crucial and should always be included to maximize the chances of developing a successful shRNA construct.

Table 1 Reagent cost analysis

Reagent	Cost	Source
EZ-Tet-pLKO plasmid	$65	Addgene
PEG-8000	$38 *(per 250 g)*	Sigma
shRNA oligo (sense/antisense)	$22 *(ea.)*	IDT
Screening primer (Fwd/Rev)	$8 *(ea.)*	IDT
Cloning enzymes (PNK, AP, ligase)	$2.50 *(per ligation)*	NEB, Affymetrix
Restriction enzymes	$0.25 *(per digest)*	NEB
PCR reagents	$0.25 *(per reaction)*	Empirical Bioscience
Total cost to clone first shRNA	~$170	
Cost per subsequent shRNA	~$50	

Though we sought to make our protocol as easy as possible, there are some potential areas of difficulty that may be avoided by taking extra precautions. One critical detail is that the DNA pellet precipitated by PEG can often be invisible, so extra caution should be taken when decanting the supernatant after centrifugation. If recovery is consistency low, consider trying 7 and 8% PEG precipitations to increase precipitation efficiency at the tradeoff for slightly more stuffer retention. When transforming the ligation into bacteria, it is important to use recombination-deficient *E.coli* strains (such as NEB-Stable) in order to minimize unwanted recombinations due to lentiviral LTR sequences. When sequencing clones, be aware that shRNA hairpin sequences can sometimes cause early termination when read by Sanger sequencing and may (but not always) require the use of specialized sequencing protocols for dealing with RNAi constructs [14, 15]. Lastly, freshly prepared lentivirus is preferred when infecting cells, though frozen virus can be used with ~50% decrease in infectivity for each freeze-thaw cycle.

One important caveat with the Dox-inducible system is that at high doses (>1 μg/mL), Dox can have detrimental effects on cell viability via disruption of mitochondrial function [16]. In our experience, we observed viability effects from prolonged treatment (>4 days) at 500 ng/mL but saw no effects from a 2-week treatment at 50 ng/mL (not shown). As an extra control, the parent cell line (without lentiviral infection) can be treated with Dox to check specifically for effects on cell viability. In most cases a 10–50 ng/mL dose of Dox should be

Table 2 Cost/benefit comparison of lentiviral shRNA methods

Method	Cost	Unit	Benefits	Drawbacks
EZ-Tet-pLKO	$50	per shRNA	Low cost, Customizable, Puro/Hygro/Blast Efficient 7 nt loop	2–3 day process
TRC library (non-inducible)	$208/$330 *(glycerol stock)*	per shRNA/Set of 3–6	No cloning required	Non-inducible, 6 nt loop
TRC library (Dox-inducible)	$450/$1100 *(glycerol stock)*	per shRNA/ Set of 3	No cloning required	High cost, 6 nt loop
	$1195 *(viral particles)*	1 unique or 3 mixed	Ready to use	

well tolerated but that should be tested by the end user in their particular cell line as a precaution.

The timing of gene knockdown and recovery is not universal. For most genes 72 h is sufficient to see knockdown at the protein level. However, this is highly dependent on protein stability. Longer-lived proteins (e.g., membrane-bound receptors, housekeeping proteins) may take up to a week for proper knockdown. We observed p38α knockdown at 72 h, but Creb1 knockdown was not observed until at least day five of Dox induction. Likewise, protein recovery will be highly dependent on the transcription rate of the gene so that lower expressed genes will take longer to recover. Furthermore, cell confluency and proliferation rate will also affect the rate of protein synthesis and turnover, thus affecting Dox knockdown and recovery timing. All these factors need to be considered when designing temporally-sensitive experiments and will be cell and context specific.

When testing new shRNA constructs, transduced cells lines need to be validated. Knockdown at the mRNA level can usually be seen by qRT-PCR at 24–48 h. However, as previously mentioned, protein knockdown can take up to five days or longer potentially. A good control to include when testing new pools is to probe an immunoblot for the TetR protein to confirm that the selected pool of cells has robust expression of the lentiviral vector. Likewise, if comparing pools or clones, those with highest TetR expression often show the greatest knockdown (not shown). When targeting a new gene, we recommend starting with at least three different targeting sequences with the expectation that one or two will work efficiently.

Lastly, we also sought to aid researchers by designing Hygro and Blast resistant variants of the EZ-Tet-pLKO vector, thus providing more flexibility in creating multiple genetic engineered cell lines. By combining all three vectors in one cell line it would be possible to knockdown two or three targets simultaneously upon Dox treatment. In addition to the Tet inducible system, there are other inducible shRNA vectors that can prove useful and are commercially available, such as cumate or IPTG-inducible vectors [17, 18]. With some creativity and strategy it would also be possible to create cells with multiple shRNAs, each activated by different inducers. Moreover, inducible shRNAs could be combined with inducible cDNA expression systems to test overexpression and knockdown simultaneously or sequentially [19]. Use of inducible vectors with various selection markers opens the door for greater quantity and variety of questions that can be addressed with molecular biology.

Conclusions

Inducible shRNAs are a very powerful tool when used properly. We sought to provide a guide to allow more people to more easily use this system with our EZ-Tet-pLKO vector. There are lots of ways to manipulate gene expression, including the recent advent of CRISPR/Cas9 technologies. Though the potential of CRISPR is great, it is not without serious limitations, including inability to study genes with lethal knockdown phenotypes and the reliance on selecting clonal populations for cell culture studies [20]. In addition to the cell culture uses shown here, the pLKO system is also useful in vivo, for example with tumor xenografts which can be induced to knockdown a gene upon addition of Dox to the animal food or water [21]. Our goal with this report was to take the already proven Tet-pLKO-Puro system and refine it further. With these new EZ-Tet-pLKO vectors and protocols, researchers will find this tool to be more versatile and user-friendly than ever.

Methods

pLKO vector modifications

The Tet-pLKO-Puro plasmid was ordered from Addgene (Plasmid 21915) [6, 7]. Mutagenesis was performed using the QuikChange II Site Directed Mutagenesis kit (Aligent). Bases 222–1869 of the stuffer region between the AgeI and EcoRI cloning sites were deleted. The deletion was performed by inserting an EcoRI site at base 222 of the stuffer (primer 5′- GCTACTCCACCACTT GAATTCCTAAGCGGTCAGC). The vector was then digested with EcoRI, re-ligated, and clones were screened for those that ligated the new EcoRI site directly to

the 3′ cloning site, thus excising the bulk of the stuffer region and preserving the 3′ cloning site. Mutagenesis was then used to mutate the AgeI restriction site to an NheI sequence (primer 5′- TATCAGTGATAGAGACGCTAG CGTGTTGTAAATGAGCA). The EZ-Tet-pLKO-Hygro vector was made by PCR subcloning the Hygro resistance gene from the pGL4.15 vector (Promega) using the following primers: 5′-ATTATGGATCCATGAAGAAGCCCG AACTC and 5′- ATTATGACGTCTTAAACTCGACC TACCTC. The EZ-Tet-pLKO-Blast construct was made by PCR subcloning the Blast resistance gene from pLenti-CMV-rtTA3-Blast (Addgene 26429). For PCR cloning, inserts were amplified with Q5 high fidelity polymerase (NEB) and ligated into Tet-pLKO-Puro between the BamHI and AatII RE sites. All experiments were carried out with the Puro variant.

Vector digest and PEG precipitation

Vector can be prepared by co-digesting EZ-Tet-pLKO-Puro DNA with NheI and EcoRI (NEB). A typical digest consisted of 5 μg of vector DNA with 20 u of each enzyme in a 50 μL digest volume for at least 3 h at 37 °C. Cut vector was then dephosphorylated with Antarctic Phosphatase (NEB) using the manufacturer's protocol and supplementing the 50 μL digest reaction with AP buffer, enzyme, and water to make a 60 μL reaction volume. Cut vector was then diluted with water to a 200 μL volume in a 1.5 mL Eppendorf tube. PEG was used to precipitate the DNA and exclude the 200 bp excised stuffer. We first prepared 2× stock of 12% (w/v) PEG-8000 and 20 mM Magnesium Chloride. The 2× stock was then added 1:1 to the cut and dephosphorylated DNA sample. The DNA/PEG mixture was gently mixed by inverting the tube a few times and left to sit at room temperature for at least 1 h. After the incubation, the DNA was centrifuged at 15,000 RCF in a bench top centrifuge (Eppendorf 5415D) for 40 min. The length of the incubation and spin are critical; any less time can greatly decrease recovery. Next, 500 μL of 70% ethanol was added to wash the DNA pellet, which was then spun again for 5–10 min. The ethanol was then aspirated and the wash was repeated once more. After the second wash the DNA pellet was allowed to air dry and then suspended in water (typically ~50 μL). DNA was then quantified by Qubit (Q32850, ThermoFisher). Accurate quantification is important for successful cloning. Typically DNA recovery following 6% PEG precipitation is ~50%.

shRNA oligo design and loop prediction

shRNA targeting sequences were chosen from the BROAD RNAi Consortium database (http://www.broadinstitute.org/rnai/trc). shRNA targeting sequences (with RNAi consortium ID) are as follows: p38α (TRCN0000196472), p38δ (TRCN0000197043), Creb1 (TRCN0000226466). Oligos were designed as described in Fig. 2 and ordered from Integrated DNA Technologies. The RNA folding probability values in Fig. 2 were calculated using RNAstructure software (v5.7) by Reuter et al. [22] (http://rna.urmc.rochester.edu/RNAstructure.html).

shRNA oligo preparation

Sense and antisense shRNA oligos were suspended at 100 μM in duplex buffer (100 mM Potassium Acetate, 30 mM HEPES, pH 7.5). Next, 20 μL (2 μ-mol) of each oligo were combined and annealed using a thermalcycler (Labnet TC9600-G) with a program set to start at 95 °C and drop ~5°/min down to room temperature. Alternately, DNA can be annealed by placing in a beaker of boiling water and moved off the heater to cool slowly to room temperature. The annealed oligos were then diluted with water to 360 μL total and precipitated with ethanol (added 40 μL of 3 M sodium acetate and 1 mL ethanol). DNA was centrifuged for 30 min at 15,000 RCF in a bench top centrifuge, washed twice with 70% ethanol, and suspended in 500 μL water. Annealed oligo DNA was then quantified by Qubit (Q32850, ThermoFisher). Synthesized oligos do not contain phosphorylated overhangs, so annealed oligo was treated with T4 poly-nucleotide kinase (M0201, NEB) and heat inactivated, according to the manufacturer's protocol.

Ligation and transformation

Prepared vector (cut, dephosphorylated, and PEG purified) was diluted to a working concentration of ~20–100 ng/μL if needed. Phosphorylated oligos were diluted (from the heat-inactivated PNK reaction) to a 1 ng/μL working concentration. Ligations were performed using the LigateIT rapid ligase kit (78400, Affymetrix) with 100 ng vector DNA and an 8:1 insert:vector molar ratio. A vector-only ligation was also prepared to control for incompletely digested and/or re-ligated vector derived colonies. Next, 2 μL of the ligation reactions were transformed into Stbl3 (Life Technologies) or NEB-Stable (NEB) chemically competent *E. coli*. Competent cells were incubated on ice for 30 min with 4 μL of ligation DNA, then heat shocked at 42 °C for 40 s and returned to ice for 1 min. Then, 1 mL of LB media was then added to the cells and they were allowed to recover at 37 °C for 30 min, after which time 100–200 μL was plated on LB-agar plates containing 100 μg/mL ampicillin and incubated 12–16 h at 37 °C.

PCR screen

Colony-PCR was used to screen bacteria for successfully ligated clones. Primers used were as follows: pLKO-Fwd 5′- ATTAGTGAACGGATCTCGACGG; pLKO-rev 5′-AACCCAGGGCTGCCTTGG. To set up the PCR

reactions, first 15 μL of water was added to PCR tubes. Colony inoculation was performed by touching a p10 pipette tip to a colony, then mixing it in the desired PCR tube with the water, and then dotting ~1 uL on a labeled fresh LB agar (+amp) plate to keep track of the colony. A positive control is always included by adding ~1–10 ng of EZ-Tet-pLKO-Puro plasmid to 15 μL water. PCR was performed using Emprical Bioscience Taq and buffer (TP-MG-500). A master mix was made containing (per reaction): 2.5 μL of 10× Taq Buffer, 0.2 μL of Taq enzyme, 2 μL of 25 mM magnesium chloride, 0.2 μL of each primer (fwd and rev, 100 μM stocks), and 3.9 μL water. Then, 10 μL of the master mix was then added to the 15 μL of inoculated water which served as the template. Thermalcycler settings used were as follows: 1× [95 °C for 2 min], 35× [95° for 30 s, 68 °C for 45 s], 1× [72 °C for 1 min]. DNA was then run on 2% agarose for visualization with a DNA ladder (N3231 or N3232, NEB). Positive clones can then be further validated by RE screening or sent directly for Sanger sequencing using the pLKO-Fwd primer.

Restriction enzyme digest screen

Clones were minipreped by alkaline lysis. DNA was digested using the SpeI restriction enzyme (NEB). A standard reaction condition was ~3 μg of DNA digested with 10 u of enzyme in a 50 μL reaction for at least 1 h at 37 °C. Digest reaction (10–20 μL) was then run out on a 2% agarose gel.

Cell culture

iPrEC cells were grown in KSFM with included supplements (17005042, Gibco) and 30 u/mL Pen/Strep (Gibco). For shRNA induction 50–100 ng/mL Dox (Sigma) was used. HEK293FT cells were used for lentivirus production and maintained in DMEM (11995, Gibco) with 2 mM L-glutamine, 10% fetal bovine serum (FBS), and 30 u/mL Pen/Strep. During transfection and infection, cells were grown without antibiotics and for infection were grown with heat inactivated serum (30 min at 56 °C) to avoid immune complement interference. Cells were maintained at 37 °C with 5% CO_2.

Virus production/infection

pLKO constructs were used to make lentivirus in HEK293FT cells using the ViraPower system (K497500, Invitrogen). One T75 flask was needed per viral construct, which were first coated with 2 μg/mL PolyD lysine in PBS for 1 h at 37 °C and then seeded with 5 million cells and left overnight at 37 °C. The next day, cells were switched to antibiotic-free media with heat-inactivated serum and transfected (Lipofectamine2000, ThermoFisher) with packaging plasmids (5 μg each: pLP1, pLP2, pVSV-G) and the desired pLKO construct or a GFP lentiviral vector as control. At 24 h post-transfection, media was changed to the target cell media (without antibiotics). HEK293FT cells were then returned to 37 °C for 48 h to produce viral particles. Viral media was collected in 15 mL conical tubes and centrifuged for 10 min at 1500 RPM in a swinging bucket centrifuge (Megafuge 1.0R) to pellet cell debris. Next, the viral media was filtered by syringe through a 0.45 μM, low protein binding filter (28145–505, VWR). Cells were typically infected by first adding half the volume with normal growth media (no antibiotics, heat inactivated serum) and half volume with the filtered viral media plus polybrene to a 5 μg/mL final concentration to improve infection rate. Infected cells were incubated 48–72 h and then given fresh growth media for 24–48 h before beginning selection. A lentivirus containing GFP was used as a positive control for viral production/infection and to estimate the percentage of infected cells. GFP was detected by fluorescence microscopy 48–72 h after infection.

Immunoblot

Cells were lysed in MAPK lysis buffer (50 mM Tris, pH 7.5, 0.5 mM EDTA, 50 mM NaF, 100 mM NaCl, 50 mM β-glycerol phosphate, 5 mM Sodium Pyrophosphate, 1% TritonX100) or RIPA lysis buffer (10 mM Tris, pH 7.5, 1 mM EDTA, 158 mM NaCl, 0.1% SDS, 1% Sodium Deoxycholate, 1% TritonX100). Cells were chilled, washed, and then lysis buffer was added and plates sat for 30 min on ice. Cells were then scrapped, centrifuged, and protein was quantified by BCA assay (Pierce). Equivalent amounts of 30–50 μg of denatured protein per sample was run on Novex SDS polyacrylamide tris-glycine gels (Life Technologies). Protein was then transferred onto PVDF membrane and blocked in 5% BSA/TBST for 1 h at room temp. Primary and secondary antibodies were diluted in blocking buffer. Primary antibodies were probed either 2–3 h at room temp or overnight at 4 °C while all secondary antibodies were probed 1 h at room temp. Luminol chemiluminescence was used with a Bio-Rad Chemi-Doc imaging system with CCD camera to image blots and analyzed on Quantity One software v4.5.2. The following antibodies were used: p38α at 1:2000 (CST 9218), p38δ at 1:1000 (Santa Cruz sc-136063), Tubulin at 1:10,000 (Sigma T9026), Creb1 at 1:1000 (CST 4820), and TetR at 1:2000 (Clone Tech 631131).

Abbreviations

Dox: Doxycycline; FBS: Fetal bovine serum; iPrEC: Immortalized prostate epithelial cell; PEG: Polyethylene glycol; RE: Restriction enzyme; Tet: Tetracycline; TetO: Tet operator; TetR: Tet Repressor; TRC: The RNAi Consortium

Acknowledgements
The Tet-pLKO-Puro plasmid was a gift from Dmitri Wiederschain. McLane Watson helped with the design of the EZ-Tet-pLKO-Hygro vector.

Funding
These studies were supported by funds from the National Cancer Institute of the National Institutes of Health under award numbers R01CA154835 (VVS, CKM) and P30CA023074 (CKM), Department of Defense award number W81XWH-14-1-0479 (SBF, CKM), Worldwide Cancer Fund # 11–0082, Van Andel Research Institute, and University of Arizona. The content is solely the responsibility of the authors and does not necessarily represent the official views of the National Institutes of Health or the Department of Defense.

Availability of data and materials
The EZ-Tet-pLKO vectors and full sequence information are available in the Addgene repository (www.addgene.org): EZ-Tet-pLKO-Puro (Addgene plasmid 85966), EZ-Tet-pLKO-Hygro (Addgene plasmid 85972), EZ-Tet-pLKO-Blast (Addgene plasmid 85973).

Authors' contributions
SBF was responsible for experimental design, analysis, execution, and writing of the manuscript. VVS was responsible for generation and validation of the iPrEC-sh.Creb1 cell lines. CKM was responsible for analysis, writing, communication, and supervising the project. All authors read and approved the final manuscript.

Competing interests
The authors declare that they have no competing interests.

Consent for publication
Not applicable.

Ethics approval and consent to participate
Not applicable.

Author details
[1]Laboratory of Integrin Signaling and Tumorigenesis, Van Andel Research Institute, Grand Rapids, MI, USA. [2]Genetics Program, Michigan State University, East Lansing, MI, USA. [3]Department of Cellular and Molecular Medicine, University of Arizona Cancer Center, 1515 N. Campbell Ave, Tucson, AZ 85724, USA.

Received: 8 June 2016 Accepted: 21 February 2017
Published online: 28 February 2017

References

1. Davidson BL, McCray Jr PB. Current prospects for RNA interference-based therapies. Nat Rev Genet. 2011;12(5):329–40.
2. Hannon GJ. RNA interference. Nature. 2002;418(6894):244–51.
3. Fellmann C, Lowe SW. Stable RNA interference rules for silencing. Nat Cell Biol. 2014;16(1):10–8.
4. Singer O, Verma IM. Applications of lentiviral vectors for shRNA delivery and transgenesis. Curr Gene Ther. 2008;8(6):483–8.
5. Moffat J, Grueneberg DA, Yang X, Kim SY, Kloepfer AM, Hinkle G, Piqani B, Eisenhaure TM, Luo B, Grenier JK, et al. A lentiviral RNAi library for human and mouse genes applied to an arrayed viral high-content screen. Cell. 2006;124(6):1283–98.
6. Wiederschain D, Wee S, Chen L, Loo A, Yang G, Huang A, Chen Y, Caponigro G, Yao YM, Lengauer C, et al. Single-vector inducible lentiviral RNAi system for oncology target validation. Cell Cycle. 2009;8(3):498–504.
7. Wee S, Wiederschain D, Maira SM, Loo A, Miller C, DeBeaumont R, Stegmeier F, Yao YM, Lengauer C. PTEN-deficient cancers depend on PIK3CB. Proc Natl Acad Sci U S A. 2008;105(35):13057–62.
8. Lis JT, Schleif R. Size fractionation of double-stranded DNA by precipitation with polyethylene glycol. Nucleic Acids Res. 1975;2(3):383–9.
9. Cariello NF, Keohavong P, Sanderson BJ, Thilly WG. DNA damage produced by ethidium bromide staining and exposure to ultraviolet light. Nucleic Acids Res. 1988;16(9):4157.
10. Grundemann D, Schomig E. Protection of DNA during preparative agarose gel electrophoresis against damage induced by ultraviolet light. BioTechniques. 1996;21(5):898–903.
11. Li L, Lin X, Khvorova A, Fesik SW, Shen Y. Defining the optimal parameters for hairpin-based knockdown constructs. RNA. 2007;13(10):1765–74.
12. McIntyre GJ, Fanning GC. Design and cloning strategies for constructing shRNA expression vectors. BMC Biotechnol. 2006;6:1.
13. Gu S, Jin L, Zhang Y, Huang Y, Zhang F, Valdmanis PN, Kay MA. The loop position of shRNAs and pre-miRNAs is critical for the accuracy of dicer processing in vivo. Cell. 2012;151(4):900–11.
14. Guo Y, Liu J, Li YH, Song TB, Wu J, Zheng CX, Xue CF. Effect of vector-expressed shRNAs on hTERT expression. World J Gastroenterol. 2005;11(19):2912–5.
15. Devroe E, Silver PA. Retrovirus-delivered siRNA. BMC Biotechnol. 2002;2:15.
16. Moullan N, Mouchiroud L, Wang X, Ryu D, Williams EG, Mottis A, Jovaisaite V, Frochaux MV, Quiros PM, Deplancke B, et al. tetracyclines disturb mitochondrial function across eukaryotic models: a call for caution in biomedical research. Cell Rep. 2015;10(10):1681–91.
17. Mullick A, Xu Y, Warren R, Koutroumanis M, Guilbault C, Broussau S, Malenfant F, Bourget L, Lamoureux L, Lo R, et al. The cumate gene-switch: a system for regulated expression in mammalian cells. BMC Biotechnol. 2006;6:43.
18. Chen Q, Gao S, He W, Kou X, Zhao Y, Wang H, Gao S. Xist repression shows time-dependent effects on the reprogramming of female somatic cells to induced pluripotent stem cells. Stem Cells. 2014;32(10):2642–56.
19. Hodkinson PS, Elliott PA, Lad Y, McHugh BJ, MacKinnon AC, Haslett C, Sethi T. Mammalian NOTCH-1 activates beta1 integrins via the small GTPase R-Ras. J Biol Chem. 2007;282(39):28991–9001.
20. Zhang F, Wen Y, Guo X. CRISPR/Cas9 for genome editing: progress, implications and challenges. Hum Mol Genet. 2014;23(R1):R40–6.
21. Chin YR, Yoshida T, Marusyk A, Beck AH, Polyak K, Toker A. Targeting Akt3 signaling in triple-negative breast cancer. Cancer Res. 2014;74(3):964–73.
22. Reuter JS, Mathews DH. RNAstructure: software for RNA secondary structure prediction and analysis. BMC Bioinf. 2010;11:129.

© 2017. Published by The Company of Biologists Ltd | Journal of Cell Science (2017) 130, 1952-1964 doi:10.1242/jcs.197152

RESEARCH ARTICLE

Human prostate luminal cell differentiation requires NOTCH3 induction by p38-MAPK and MYC

Sander B. Frank[1,2,3], Penny L. Berger[1], Mats Ljungman[4] and Cindy K. Miranti[1,3,*]

ABSTRACT

Many pathways dysregulated in prostate cancer are also involved in epithelial differentiation. To better understand prostate tumor initiation, we sought to investigate specific genes and mechanisms required for normal basal to luminal cell differentiation. Utilizing human prostate basal epithelial cells and an *in vitro* differentiation model, we tested the hypothesis that regulation of NOTCH3 by the p38 MAPK family (hereafter p38-MAPK), via MYC, is required for luminal differentiation. Inhibition (SB202190 and BIRB796) or knockdown of p38α (also known as MAPK14) and/or p38δ (also known as MAPK13) prevented proper differentiation. Additionally, treatment with a γ-secretase inhibitor (RO4929097) or knockdown of NOTCH1 and/or NOTCH3 greatly impaired differentiation and caused luminal cell death. Constitutive p38-MAPK activation through MKK6(CA) increased NOTCH3 (but not NOTCH1) mRNA and protein levels, which was diminished upon MYC inhibition (10058-F4 and JQ1) or knockdown. Furthermore, we validated two *NOTCH3* enhancer elements through a combination of enhancer (e)RNA detection (BruUV-seq) and luciferase reporter assays. Finally, we found that the *NOTCH3* mRNA half-life increased during differentiation or upon acute p38-MAPK activation. These results reveal a new connection between p38-MAPK, MYC and NOTCH signaling, demonstrate two mechanisms of *NOTCH3* regulation and provide evidence for NOTCH3 involvement in prostate luminal cell differentiation.

KEY WORDS: Prostate, Luminal cell differentiation, NOTCH, MYC, p38-MAPK, Development

INTRODUCTION

The human prostate gland contains an epithelial bilayer of basal and luminal cells. Within these layers resides a combination of uni- and bi-potent progenitors important for normal gland homeostasis (Kwon et al., 2016; Ousset et al., 2012; Uzgare et al., 2004). Basal and luminal cells display distinct markers, such as androgen receptor (AR) and keratin 8 (K8; also known as KRT8) in the luminal layer, and laminin-binding integrins and keratin 5 (K5; also known as KRT5) in the basal layer (Lamb et al., 2010). Human prostate tumors co-express some of the basal and luminal markers, suggesting a defect in differentiation (Tokar et al., 2005). Moreover, many of the commonly altered genes in prostate cancer (e.g. *MYC*, *AR*, *ERG* and *PTEN*) are also implicated in differentiation (Frank and Miranti, 2013). We previously demonstrated that manipulation of differentiation regulators (MYC, PTEN and ING4) in normal human prostate epithelial cells results in tumor formation when grafted into a mouse prostate (Berger et al., 2014). To better understand tumor initiation in prostate epithelium, we sought to investigate specific genes and mechanisms required for normal basal to luminal cell differentiation.

The p38 MAPK family (hereafter p38-MAPK) is a known driver of epithelial differentiation in various tissues including skin and lung (Cuadrado and Nebreda, 2010). p38-MAPK regulates a wide range of targets, including other kinases/phosphatases, transcription factors and RNA-binding proteins (Cuadrado and Nebreda, 2010). Moreover, p38-MAPK is a downstream target of FGFR2b, a crucial receptor for epithelial differentiation in the skin and prostate (Belleudi et al., 2011; Heer et al., 2006; Lamb et al., 2010). Despite these findings, how p38-MAPK expression in prostate epithelial cells drives differentiation, including its relevant targets, remains poorly defined.

MYC positively regulates normal skin and prostate differentiation, and is a major prostate cancer oncogene (Berger et al., 2014; Gebhardt et al., 2006; Koh et al., 2010). MYC potentially targets thousands of genes via its activity as a transcription factor, and many of its targets are tissue and context specific (Conacci-Sorrell et al., 2014; Lüscher and Vervoorts, 2012). In normal prostate, transient upregulation of MYC is required for loss of cell adhesion and stimulation of chromatin remodeling (Berger et al., 2014). Moreover, regulation of *MYC* itself is complex, occurring at many different levels including pre- and post-transcription and through post-translational modification (McKeown and Bradner, 2014). Overexpression of AR in human primary basal prostate epithelial cells is sufficient to cause growth arrest via transcriptional downregulation of MYC (Antony et al., 2014; Vander Griend et al., 2014). Thus, MYC plays a crucial role in multiple aspects of both normal prostate differentiation and cancer.

NOTCH controls cell fate, including stemness, survival and differentiation (Deng et al., 2015). Mammals express four NOTCH transmembrane receptors (NOTCH1– NOTCH4), five canonical transmembrane ligands (JAG1 and JAG2, and DLL1, DLL3 and DLL4) and ten classic downstream targets (HES1–HES7, HEY1, HEY2 and HEYL). Cell–cell contact joins ligand and receptor, triggering proteolytic cleavage of NOTCH by the γ-secretase complex which releases the active intracellular domain (ICD) of the receptor into the nucleus to activate transcription (Kopan and Ilagan, 2009). NOTCH can promote cell cycle arrest and de-adhesion from the matrix, both of which are essential for luminal differentiation (Hodkinson et al., 2007; Mazzone et al., 2010; Rangarajan et al., 2001). Furthermore, NOTCH1 signaling can promote survival of human basal cells (Dalrymple et al., 2005; Litvinov et al., 2006). In a mouse model, constitutively active NOTCH1 driven by a luminal promoter causes prostatic intraepithelial neoplasia (PIN) and increases survival of a subset of luminal cells in 3D culture (Kwon et al., 2014; Valdez et al., 2012). However, there are conflicting reports as to

[1]Laboratory of Integrin Signaling and Tumorigenesis, Van Andel Research Institute, Grand Rapids, MI 49503, USA. [2]Genetics Program, Michigan State University, East Lansing, MI 48824, USA. [3]Department of Cellular and Molecular Medicine, University of Arizona Cancer Center, Tucson, AZ 85724, USA. [4]Translational Oncology Program, University of Michigan Medical School, Ann Arbor, MI 48109, USA.

*Author for correspondence (cmiranti@email.arizona.edu)

C.K.M., 0000-0003-0668-6106

Received 2 September 2016; Accepted 17 April 2017

Journal of Cell Science

Journal of Cell Science (2017) 130, 1952-1964 doi:10.1242/jcs.197152

whether the NOTCH pathway is oncogenic or tumor suppressive, and the specific role for the other NOTCH receptors remains undefined (Carvalho et al., 2014; Kwon et al., 2016).

We sought to understand how p38-MAPK, MYC and NOTCH work together in normal prostate differentiation. We utilized an established model of *in vitro* differentiation of human basal prostate epithelial cells (PrECs) (Berger et al., 2014, 2017; Lamb et al., 2010). By using pharmacologic and genetic manipulation, we tested the hypothesis that p38-MAPK upregulation of NOTCH3, via MYC, is required for efficient induction and maintenance of the suprabasal layer during prostate differentiation. We identify two mechanisms of *NOTCH3* regulation by p38-MAPK, both at the transcriptional and post-transcriptional level. This knowledge improves our understanding of prostate epithelial differentiation by tying together multiple pathways and elucidating new mechanisms for key differentiation regulators.

RESULTS

p38-MAPK isoforms p38α and p38δ are required for prostate epithelial differentiation

PrECs were induced to differentiate by treating with keratinocyte growth factor (KGF; also known as FGF7) and synthetic androgen (R1881) for 2 weeks (Lamb et al., 2010). This results in a stratified epithelium consisting of suprabasal luminal cells sitting on top of basal cells. p38-MAPK is a known downstream target of KGF-to-FGFR2 signaling and is implicated in epithelial differentiation in several tissue types, including prostate (Belleudi et al., 2011; Lamb et al., 2010). Four different genes encode p38-MAPK isoforms: *MAPK14* (p38α), *MAPK11* (p38β), *MAPK12* (p38γ) and *MAPK13* (p38δ). p38α is ubiquitously expressed, while the other isoforms are typically more tissue specific (Cuadrado and Nebreda, 2010). RNA-seq and immunoblotting identified p38α and p38δ to be the predominantly expressed isoforms in basal PrECs (Fig. 1A,B).

Lysates from differentiating cells were collected over a 2-week time course, and p38α activity was measured by immunoblotting with an antibody specific for its activated phosphorylated form (p-p38α). In primary cells (PrECs), elevated p-p38α was detected at day 4 and remained elevated (Fig. 1C). In immortalized cells (iPrECs), which take 4 days longer to differentiate, p-p38α was elevated at day 8 (Fig. 1D). Semi-quantification of a set of biological triplicate experiments indicates that both total p38α and p-p38α levels increase ∼2-fold at day 4 and ∼3-fold by day 12 (Fig. S1A,B).

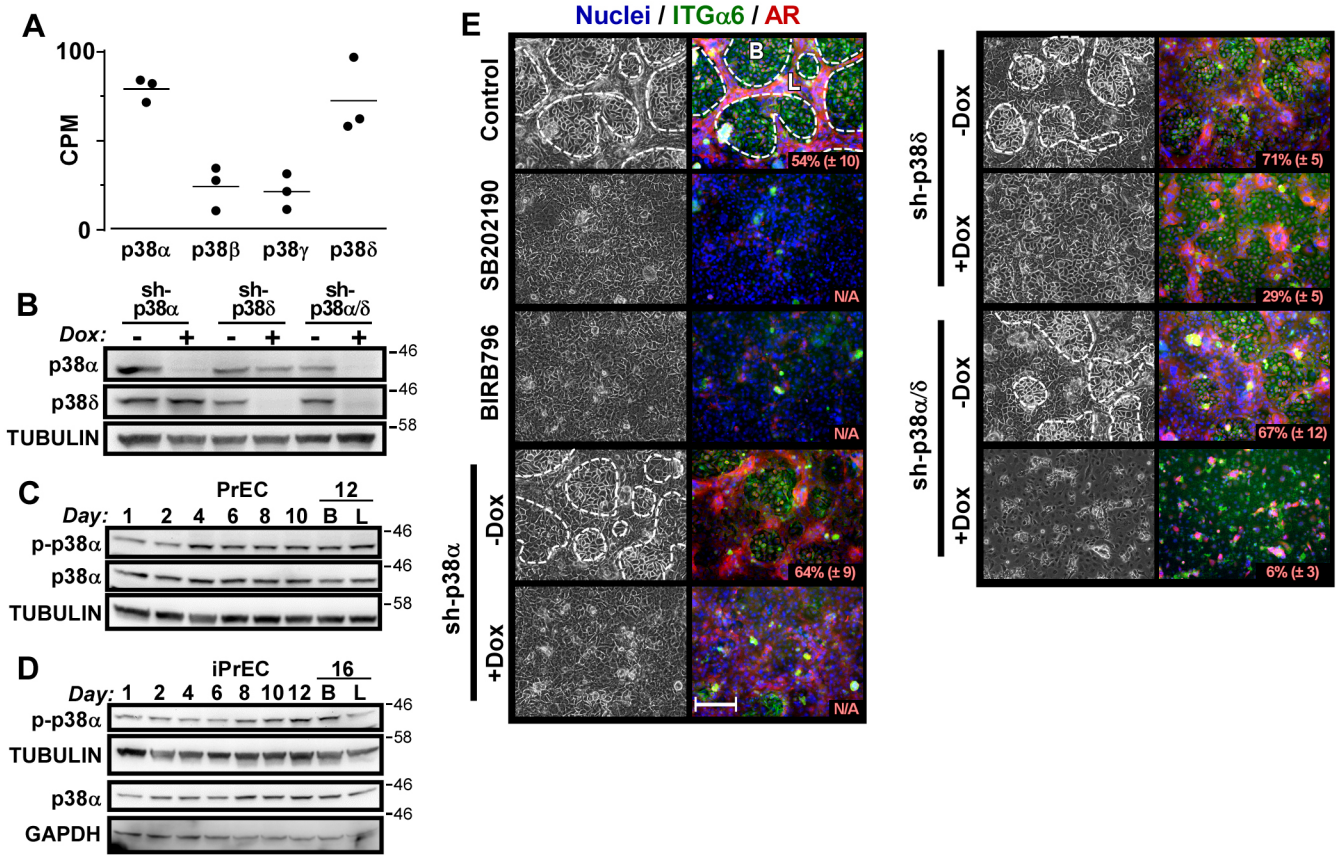

Fig. 1. p38α- and p38δ-MAPK are required for differentiation. (A) Plot of counts per million (CPM) reads for the four p38-MAPK isoforms taken from RNA-seq data of basal iPrECs. Line indicates mean of biological triplicates. (B) Lysates from stable pools of iPrECs expressing Tet-inducible p38α and/or p38δ shRNAs differentiated for 16 days with or without Dox and probed by immunoblotting. Numbers on right indicate the position of molecular mass markers (kDa). (C,D) Primary (PrECs) and immortalized (iPrECs) cells differentiated with KGF and R1881, and lysates collected at indicated time points for immunoblotting. Luminal cells (L) were separated from the basal cells (B) at the final time point before lysis. Note that the same lysates were run on multiple gels for Fig. 1D and Fig. 2A. (E) iPrECs were differentiated for 16 days with DMSO and Dox (control), 1 µM SB202190 or 0.1 µM BIRB796, while inducible shRNA lines were treated with or without Dox. Left columns, phase-contrast images. Right columns: merged epifluorescence images (10× objective) of Hoescht-33258-stained nuclei (blue), immunostaining for androgen receptor (AR, red) and integrin α6 (ITGα6, green). AR is luminal (L) and ITGα6 is basal (B). The upper layer is outlined (dashed line). The percentage in the lower right corner is the mean±s.d. area of coverage by suprabasal cells from three fields. N/A, no clearly defined suprabasal layer. Scale bar: 200 µm.

Journal of Cell Science

Journal of Cell Science (2017) 130, 1952-1964 doi:10.1242/jcs.197152

To determine whether p38-MAPK is necessary for differentiation, iPrECs were differentiated in the presence of two p38-MAPK inhibitors (SB202190 and BIRB796) or Dox-induced shRNA against p38α (sh-p38α), p38δ (sh-p38δ) or both (sh-p38α/δ). Inhibitor concentrations were selected based on their ability to block CREB1 phosphorylation mediated by constitutively active MKK6 [MKK6(CA); MKK6 is also known as MAP2K6] (Fig. S1C). Effective knockdown of p38α and/or p38δ by shRNA was verified by immunoblotting (Fig. 1B). After 16 days of differentiation, control cells (Dox plus DMSO) differentiated normally, as measured by loss of integrin α6 and gain in AR, with a 54% coverage of the culture by suprabasal cells (averaged from three fields) (Fig. 1E). Treatment with 1 µM SB202190 or 0.1 µM BIRB796 completely prevented formation of an AR-positive suprabasal layer. Unexpectedly, integrin α6 (ITGα6) expression was also decreased by these inhibitors. However, this was not due to basal cell toxicity (as judged by the lack of cleaved caspase 3) nor decreased proliferation (as demonstrated by measuring BrdU incorporation) (Fig. S1D,E). Dox-induced shRNA knockdown of p38α did not prevent AR-positive cells from appearing, but it did prevent formation of a distinct suprabasal layer. On the other hand, knockdown of p38δ reduced the production of cells that were both AR^+ and $ITG\alpha6^-$ (29% suprabasal coverage, reduced from 71%), but did not completely block it. However, double p38α/δ knockdown drastically prevented suprabasal layer formation (6% suprabasal coverage, reduced from 67%) (Fig. 1E). Thus, both p38α and p38δ are required for normal luminal cell differentiation, and the differing effects of their loss suggests they may control different steps in suprabasal layer formation.

NOTCH3 is induced during differentiation

A hallmark of normal luminal cell differentiation is the downregulation of integrins including α6, α3, β4 and β1. NOTCH can negatively regulate integrin expression and is generally required for epithelial differentiation (Frank and Miranti, 2013; Koh et al., 2010; Mazzone et al., 2010). Additionally, MYC suppresses integrin α6 and β1 expression (Gebhardt et al., 2006), and was previously demonstrated to be required for prostate differentiation (Berger et al., 2014). In some contexts, MYC is a direct downstream target of NOTCH (Weng et al., 2006). To decipher the roles of MYC and NOTCH, lysates from differentiating iPrECs (Fig. 2A) or primary PrECs (Fig. S2A) were collected over a 2-week time course and protein expression measured by immunoblotting. MYC expression and activation (phosphorylation; denoted p-MYC) was initially elevated but waned as basal cell proliferation subsided and transiently elevated again at around day 8 (Fig. 2A). A similar response was observed in primary cells but it occurred 4 days earlier, as expected due to their faster differentiation (Fig. S2A).

Of the four NOTCH receptors, we were only able to detect significant expression of NOTCH1, NOTCH2 and NOTCH3 (Fig. 2A). Expression of NOTCH2 remained essentially unchanged during differentiation. NOTCH1 protein was initially high, then decreased slightly. In contrast, NOTCH3 protein expression was very low in basal cells, then increased with time during differentiation; moreover, a marked increase occurred at around day 8, when p38α and MYC activity were also maximal (Fig. 2A). A similar pattern was observed in primary PrECs at day 4 (Fig. S2A).

NOTCH1 and *NOTCH3* mRNA expression, as measured by quantitative real-time PCR (qRT-PCR), paralleled protein expression; *NOTCH1* dipped and recovered to baseline levels, while *NOTCH3* increased dramatically and remained higher in the suprabasal layer (Fig. 2B). *NOTCH3* mRNA appeared to increase in two phases; a steady climb increasing ∼10-fold over the first 8 days followed by a more dramatic spike, up ∼220-fold by day 14 in the suprabasal cells (Fig. 2B). NOTCH ligands also displayed two distinct expression profiles; *JAG1* (Fig. 2B) and *DLL4* (Fig. S2B) showed initial decreases but then recovered by day 10, following the pattern of *NOTCH1* expression. Meanwhile, *DLL3* remained flat and began to increase after day 10, paralleling the increase in *NOTCH3* mRNA expression (Fig. 2B). *HEY2*, *HEYL* (Fig. 2B), *HES1*, *HES6* and *HEY1* (Fig. S2B) all increased during differentiation, with day 8 being a key inflection point. *HEY2* mRNA was unique in that it segregated into the suprabasal population (up 45-fold versus day 1) similar to *NOTCH3*. These data indicate that the day 8–10 window is critical for activation of the NOTCH pathway, and correlates with the appearance of an emerging suprabasal layer and integrin α6β1 mRNA downregulation (Fig. S2B).

NOTCH1 and NOTCH3 are required for differentiation

To examine the requirement of NOTCH1 and/or NOTCH3 for differentiation, iPrECs were differentiated and treated with either a γ-secretase inhibitor (RO4929097) or Dox to induce expression of NOTCH1 and/or NOTCH3 shRNA. Efficient knockdown of *NOTCH1* and/or *NOTCH3* mRNA was achieved by 48 h (Fig. S2C) and protein at 96 h (Fig. S2D). NOTCH3 loss also led to a slight decrease in NOTCH1 protein; however, this was not due to an off-target shRNA effect on NOTCH1 since NOTCH1 mRNA was not affected (Fig. S2C,D). Control and non-Dox-treated cells differentiated normally as indicated by formation of a suprabasal layer of cells (both AR^+ and $ITG\alpha6^-$; 44–53% coverage), while treatment with RO4929097 ablated differentiation (Fig. 2C). Induced knockdown of NOTCH1 or NOTCH3 by means of shRNA each led to disruption of the suprabasal layer, with 16% and 31% coverage respectively, compared to 53% and 44% for control cells. Double knockdown of NOTCH1 and NOTCH3 more severely disrupted differentiation, giving a similar appearance to that seen upon treatment with RO4929097 (Fig. 2D). Furthermore, propidium iodide staining indicated that the suprabasal cell clumps observed upon NOTCH inhibition or knockdown were mostly dead cells (Fig. S2E). Thus, NOTCH1 and NOTCH3 are both required for survival of the suprabasal cells during luminal cell differentiation.

p-p38 and NOTCH3 are expressed and active in early differentiating cells

iPrECs were immunostained for p-p38 (all p38-MAPK isoforms) and NOTCH3 at key times during differentiation to observe expression levels and localization (Fig. 2E). Nuclear p-p38 was detected in all basal cells at day 4, when very little NOTCH3 expression was detected, except for in a few cells where it was nuclear localized. By day 8, patches of more intense p-p38 nuclear staining were detected, which corresponded to cells in which NOTCH3 levels were dramatically increased (white arrow). NOTCH3 localization was primarily nuclear in the basal cells, but both nuclear and cytoplasmic staining was apparent at days 8 and 12, when suprabasal layer formation is maximal. By day 21, more membrane and less nuclear staining was observed, with staining occurring primarily in the suprabasal cells with very low levels in the basal cells. p-p38 nuclear localization was lost as suprabasal cells became established. Thus, p-p38 nuclear activity peaks around day 8, just as NOTCH3 expression and downstream signaling

Journal of Cell Science (2017) 130, 1952-1964 doi:10.1242/jcs.197152

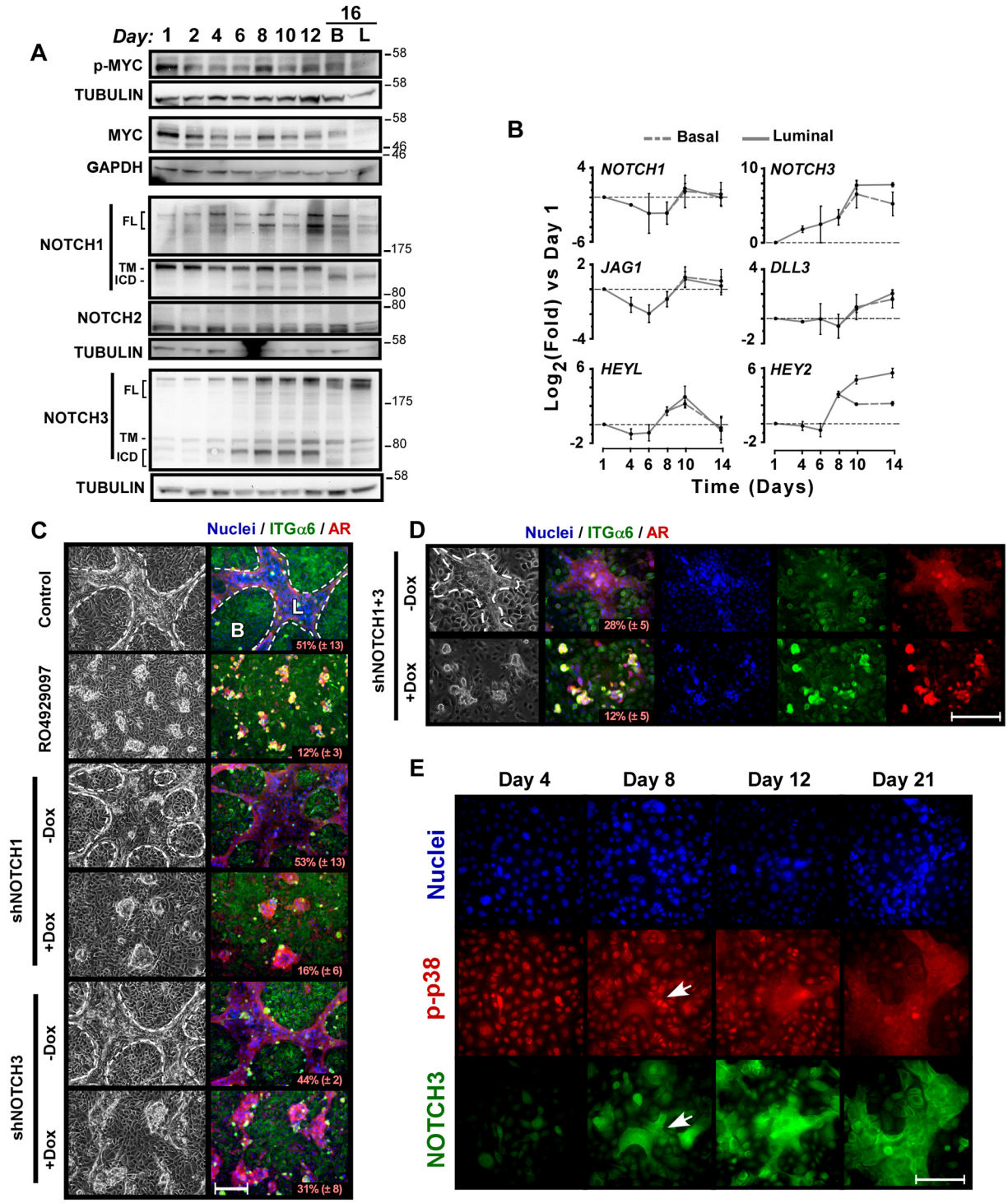

Fig. 2. NOTCH1 and NOTCH3 are required for differentiation. (A) iPrECs were differentiated and analyzed by immunoblotting as in Fig. 1D. Note that the antibody used in the p-MYC row recognizes MYC phosphorylation at T58 and S62, and the antibody used in the NOTCH2 row is specific to the ICD. The antibody used for NOTCH1 and NOTCH3 recognize full-length (FL), transmembrane (TM) and intracellular domain (ICD) forms. Also note that the same lysates were run on multiple gels for Fig. 1D and Fig. 2A. (B) RNA was collected for qRT-PCR to analyze ligands and downstream targets of NOTCH during differentiation. Luminal (L, solid line) cells were separated from basal (B, dashed line) cells at days 10 and 14. Data were normalized to values at day 1. Graph shows mean±s.d. of biological triplicates. (C) iPrECs were differentiated for 12 days with DMSO and Dox (control) or 1 µM RO4929097, while shRNA lines were treated with or without Dox. The percentage in the lower right corner is mean±s.d. area of coverage by suprabasal cells from three fields. Left column, phase-contrast iamges. Right column, merged epifluorescence images (10× objective) of Hoescht-33258-stained nuclei (blue), immunostaining for AR (red) and ITGα6 (green). The upper layer is outlined (dashed line). The percentage in the lower right corner is mean±s.d. area of coverage by suprabasal cells from three fields. (D) iPrECs with shRNAs against NOTCH1 and NOTCH3 were differentiated with KGF and 1 nM R1881 for 21 days and imaged with a 20× objective. (E) iPrECs were differentiated for various times and immunostained for p-p38 (red) and NOTCH3 (green). Note that the anti-p-p38 antibody is not specific for an isoform. The arrows indicate cell clusters co-expressing elevated p-p38 and NOTCH3. Scale bars: 200 µm.

Journal of Cell Science (2017) 130, 1952-1964 doi:10.1242/jcs.197152

increases in the suprabasal layers. Once established, NOTCH3 expression remains high in the suprabasal layer and p-p38 is lost from the nucleus.

MKK6-induced p38-MAPK activation recapitulates differentiation-induced MYC and NOTCH3 expression

To determine the relationship between p38-MAPK and NOTCH3, we engineered an iPrEC line with a Dox-inducible constitutively active MKK6 mutant, MKK6(CA), which directly phosphorylates and activates p38-MAPK (Alonso et al., 2000). During differentiation, p38-MAPK activation is moderately elevated over several days (Fig. S1A,B), but when MKK6(CA) is induced, the signaling events that naturally occur over days are condensed into hours (Fig. 3A). Although prolonged constitutive p38-MAPK activation leads to stress and cell death, the Dox-inducible system allows us to tightly control induction and measure downstream signaling over a short time period. A 16 h treatment of iPrEC-TetON-MKK6(CA) cells with Dox led to an ∼18-fold increase in *NOTCH3* mRNA (Fig. 3B). Conversely, MKK6(CA) induction decreased *NOTCH1* by ∼2.5-fold. Inhibition of p38-MAPK blocked these effects (Fig. 3B).

To establish a temporal order of events, iPrEC-TetON-MKK6 (CA) cells were treated with Dox and lysates collected over time (Fig. 3C). MKK6(CA) was detectable as early as 4 h, at which time a corresponding increase in active p-p38α and MYC was observed, peaking at ∼7–8 h. NOTCH3 levels began to increase around 6 h and continued to climb. At the mRNA level, *MYC* induction also preceded an increase in *NOTCH3* and decrease in *NOTCH1* (Fig. 3D). Furthermore, a short pulse of Dox was sufficient to induce NOTCH3 to higher levels than normally seen at day 4 of differentiation (Fig. 3E); meanwhile, expression of NOTCH1 was decreased. These results show that constitutive activation of MKK6 is sufficient to induce p38α, MYC, MYC phosphorylation and NOTCH3, while downregulating NOTCH1. Thus, the MKK6(CA) model mimics the regulation of these genes observed in the standard differentiation assay. Moreover, differentiation of iPrECs for 4 days in the presence of a p38-MAPK inhibitor suppressed *MYC* induction and dampened *NOTCH3* upregulation (∼7- vs ∼28-fold),

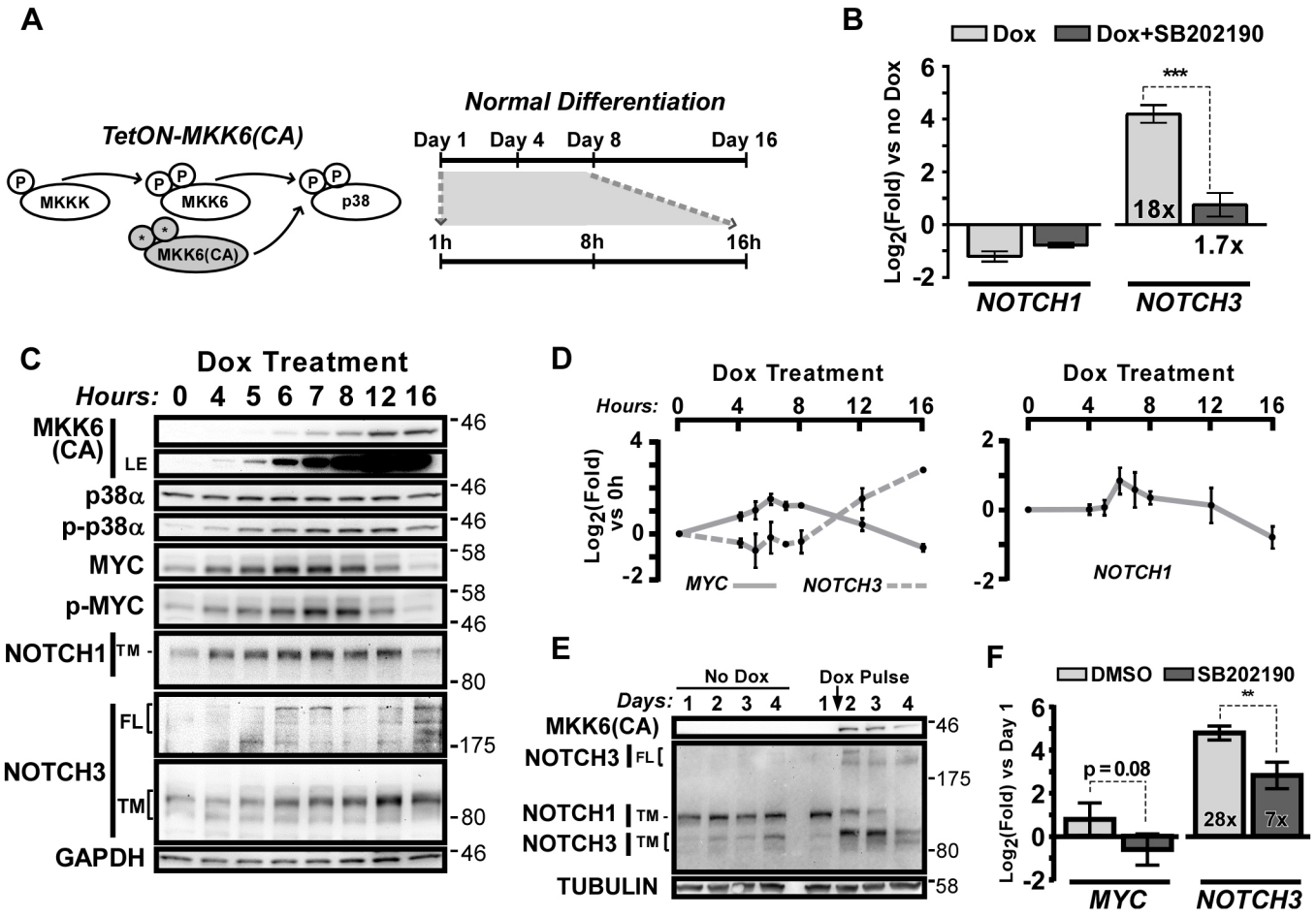

Fig. 3. p38-MAPK induces NOTCH3. (A) Diagram of the Tet-inducible MKK6(CA) model. iPrECs were engineered to stably express a Dox-inducible constitutively active MKK6 mutant, MKK6(CA), which phosphorylates and activates all p38 isoforms. Acute p38-MAPK activation condenses early differentiation signaling events from days into hours. (B) iPrEC-TetON-MKK6(CA) cells were treated with or without Dox for 16 h with DMSO or 5 µM SB202190, and analyzed by qRT-PCR. Data were normalized to cells without Dox (DMSO-only). Graph shows mean±s.d. of biological triplicates. Numbers in bars indicate fold change. (C) iPrEC-TetOn-MKK6(CA) cells were treated with Dox for up to 16 h and harvested at indicated times for immunoblotting. LE, long exposure; FL, full length; TM, transmembrane. (D) iPrEC-TetON-MKK6(CA) cells were treated as in C and analyzed by qRT-PCR. Data were normalized to 0 h samples. Graph shows mean±s.d. of biological triplicates. (E) iPrEC-TetON-MKK6(CA) cells were differentiated for 1–4 days with or without a 4 h pulse of Dox after day 1 (arrow), and analyzed by immunoblotting. Note: NOTCH1 was probed after NOTCH3 and both are shown on the same blot. (F) iPrECs were differentiated for 4 days with DMSO or 5 µM SB202190, and analyzed by qRT-PCR. Data were normalized to the value at day 1. Graph shows mean±s.d. of biological triplicates. Numbers in bars indicate fold change. $^{**}P \leq 0.01$, $^{***}P \leq 0.001$.

Journal of Cell Science (2017) 130, 1952-1964 doi:10.1242/jcs.197152

thus confirming their roles downstream of p38-MAPK in this model (Fig. 3F).

MYC is required for p38-MAPK regulation of NOTCH3

Induction of *NOTCH3* mRNA by p38-MAPK could be due to direct activation of an existing transcription factor or indirect, requiring synthesis of a new factor. iPrEC-TetON-MKK6(CA) cells were treated with Dox for 12 h and cyclohexamide (CHX) was added at 6, 8 or 10 h to measure the requirement for new protein synthesis. Addition of CHX at 6 h blocked *NOTCH3* mRNA upregulation, while addition at 8 h or later did not (Fig. 4A; Fig. S3A). Thus, there is a requirement for the synthesis of an intermediate, which must be translated between 6 and 8 h after Dox; this matches the time of maximal MYC induction and activation (see Fig. 3C).

To test whether *NOTCH3* induction requires MYC, iPrEC-TetON-MKK6(CA) cells were transfected with siRNA against MYC (denoted si.MYC) or a non-targeting control sequence and induced with Dox for 12 h. *MYC* mRNA was knocked down ∼80% and *NOTCH3* mRNA induction was half that seen in the control cells (5- vs 10-fold) (Fig. 4B). Similar results were observed at the protein level as assessed by immunoblotting (Fig. 4C). To further address the dependency of *NOTCH3* induction on MYC, we utilized an antagonist of the MYC–MAX complex, 10058-F4 (Huang et al., 2006). iPrEC-TetON-MKK6(CA) cells were treated with Dox and increasing concentrations of 10058-F4 for 16 h. Treatment with as little as 5 µM 10058-F4 suppressed the induction of NOTCH3 protein (Fig. 4D), whereas 20 µM was required to suppress *NOTCH3* mRNA (Fig. S3B). These doses are at or below common usage for 10058-F4 (Guo et al., 2009; Wang et al., 2014). As an alternative approach, we used JQ-1, a BET bromodomain inhibitor, to block transcription of MYC (Delmore et al., 2011). JQ-1 prevented MKK6(CA)-induced MYC and NOTCH3 expression at 100–500 nM (Fig. 4E). Taken together, these results demonstrate that MYC is required for maximal p38-MAPK-mediated induction of NOTCH3.

To determine whether MYC is sufficient for NOTCH3 induction, we generated a Tet-inducible MYC-expressing cell line: iPrEC-TetON-MYC. MYC induction occurred within 2 h of Dox treatment and NOTCH3 protein increased slightly by 6 h (Fig. 4F). However, there was no change in *NOTCH3* mRNA (Fig. S3C). We also induced MYC after first differentiating cells for 5 days and still observed only a slight increase in NOTCH3 protein expression (Fig. S3D). Thus, MYC is not sufficient in this context to transcriptionally induce *NOTCH3*, although it may have some slight effect on NOTCH3 protein expression.

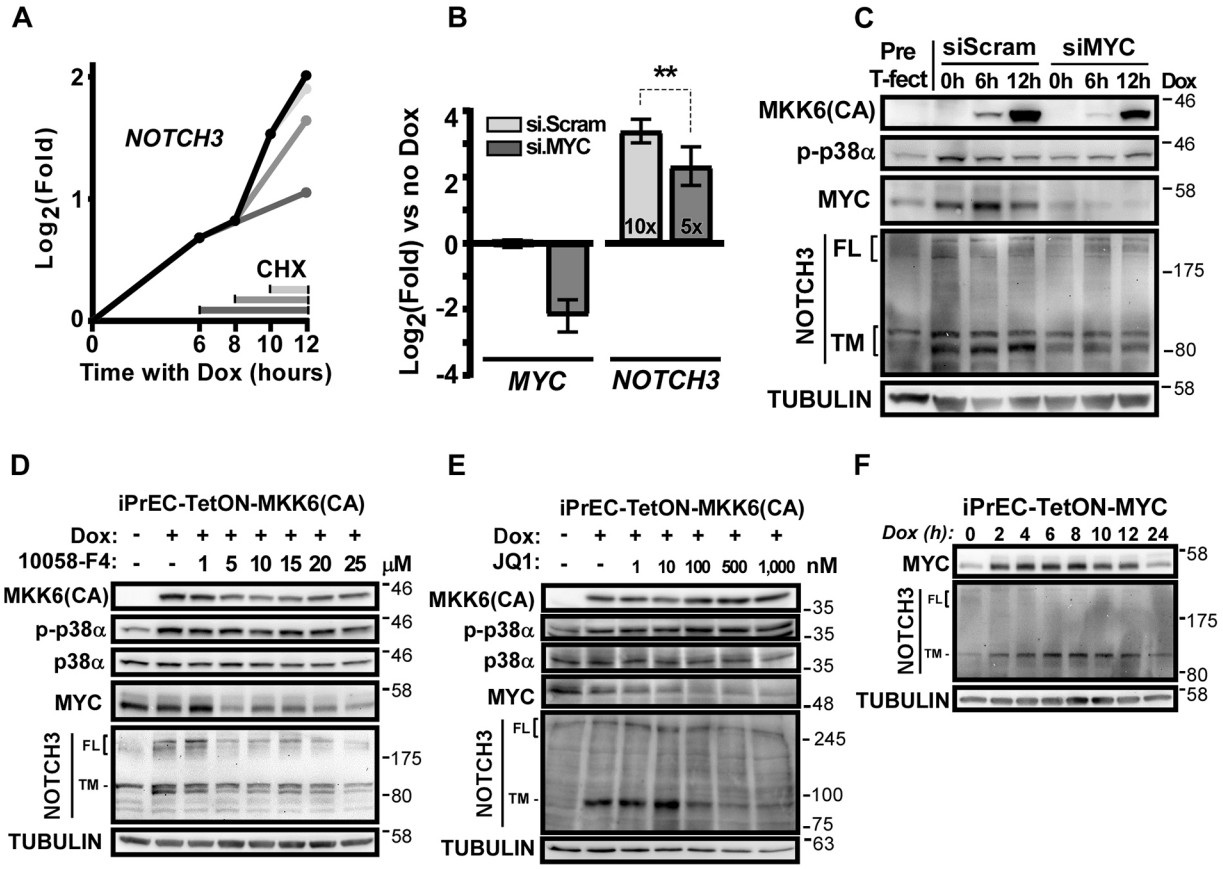

Fig. 4. MYC is an intermediate for p38-MAPK induction of NOTCH3. (A) iPrEC-TetON-MKK6(CA) cells were induced with Dox for a total of 12 h with cyclohexamide (CHX) added at 6, 8 or 10 h. *NOTCH3* mRNA was measured by qRT-PCR. Data were normalized to the value at 0 h. (B) iPrEC-TetON-MKK6(CA) cells were transfected with siMYC or siScram for 24 h, then treated with Dox for 12 h and analyzed by qRT-PCR. Data were normalized to non-transfected untreated controls. Graph shows mean±s.d. of biological triplicates. Numbers in bars indicate fold change. $^{**}P \leq 0.01$. (C) Same experiment set-up as B, except lysates were harvested at 0, 6 or 12 h after Dox treatment and used for immunoblotting. FL, full length; TM, transmembrane. (D) iPrEC-TetON-MKK6(CA) cells were treated for 16 h with Dox plus DMSO or increasing doses of MYC inhibitor 10058-F4. Protein was analyzed by immunoblotting. (E) Same experimental set-up as D, but using a different MYC inhibitor, JQ1. (F) iPrECs expressing Dox-inducible MYC (iPrEC-TetON-MYC) were treated with Dox for 0–24 h and analyzed by immunoblotting.

Journal of Cell Science (2017) 130, 1952-1964 doi:10.1242/jcs.197152

NOTCH3 is transcriptionally regulated via a MYC-dependent enhancer

The *NOTCH3* 2 kb upstream proximal promoter contains a CpG island and no TATA sequence (Kent et al., 2002). The 2 kb region of the *NOTCH3* promoter was not sufficient to induce a luciferase reporter after 6 days of differentiation (Fig. 5A), a time when endogenous *NOTCH3* was elevated over 16-fold. We used two approaches to identify candidate enhancer regions. First, we labeled newly initiated transcripts at the *NOTCH3* transcriptional start site and enhancer elements by using BruUV-Seq (Magnuson et al., 2015). Dox induction in iPrEC-TetON-MKK6(CA) cells dramatically increased *NOTCH3* reads from the coding (−) strand accumulating near the transcription start site (Fig. 5B). Strikingly, there was also a peak of reads from the non-coding (+) strand within the second intron, a locus previously reported to contain a *NOTCH3* enhancer (Gagan et al., 2012; Romano et al., 2012). The gene for MKK6 (*MAP2K6*) served as a positive control; it was induced only upon Dox treatment and with reads mapping only to the exons generated from the cDNA construct (Fig. S4A). Other controls included *CALB1* and *TRIM22*, which were increased and decreased, respectively, upon MKK6 induction (Fig. S4A).

Our second approach used a combination of DNase hypersensitivity, histone acetylation and methylation patterns (H3K27Ac+H3K4me1/2), and ChIP-seq data from ENCODE to identify potential enhancer elements (The ENCODE Project Consortium, 2012; Kent et al., 2002). Five different elements were cloned into a pNL1.1-miniTK luciferase reporter (Fig. S4B). En2.1, En2.2 and the *NOTCH3* promoter showed no induction by Dox in the MKK6(CA) model (Fig. 5C). However, two elements (En1 and En3) were upregulated by 5- and 3-fold, respectively. En1 is ∼10 kb upstream while En3 is in the second intron and corresponds to the site with bidirectional transcripts identified by BruUV-seq. A deletion in En1, Δ1–360, that eliminated most of the predicted MYC-binding sites (Fig. S4C) completely ablated the ability of the En1 reporter to be induced by MKK6(CA) (Fig. 5D). A small En3 deletion, Δ1–350, that removed two-thirds of the predicted MYC sites did not significantly decrease expression of the reporter while a larger deletion, Δ1–655, that removed all three predicted MYC sites significantly blocked induction (Fig. 5E).

To further determine whether MYC is required for induction of these enhancer elements, MKK6(CA) cells were induced in the presence of the MYC inhibitor 10058-F4. Both En1 and En3 (Δ1–350) (the core En3 responsive element) were sensitive to MYC inhibition (Fig. 5F). Induction mediated by En1 was partially decreased (2.7- vs 4.5-fold) while En3(Δ1–350) induction was more thoroughly blocked (0.7- vs 1.7-fold). Thus, both En1 and En3 are

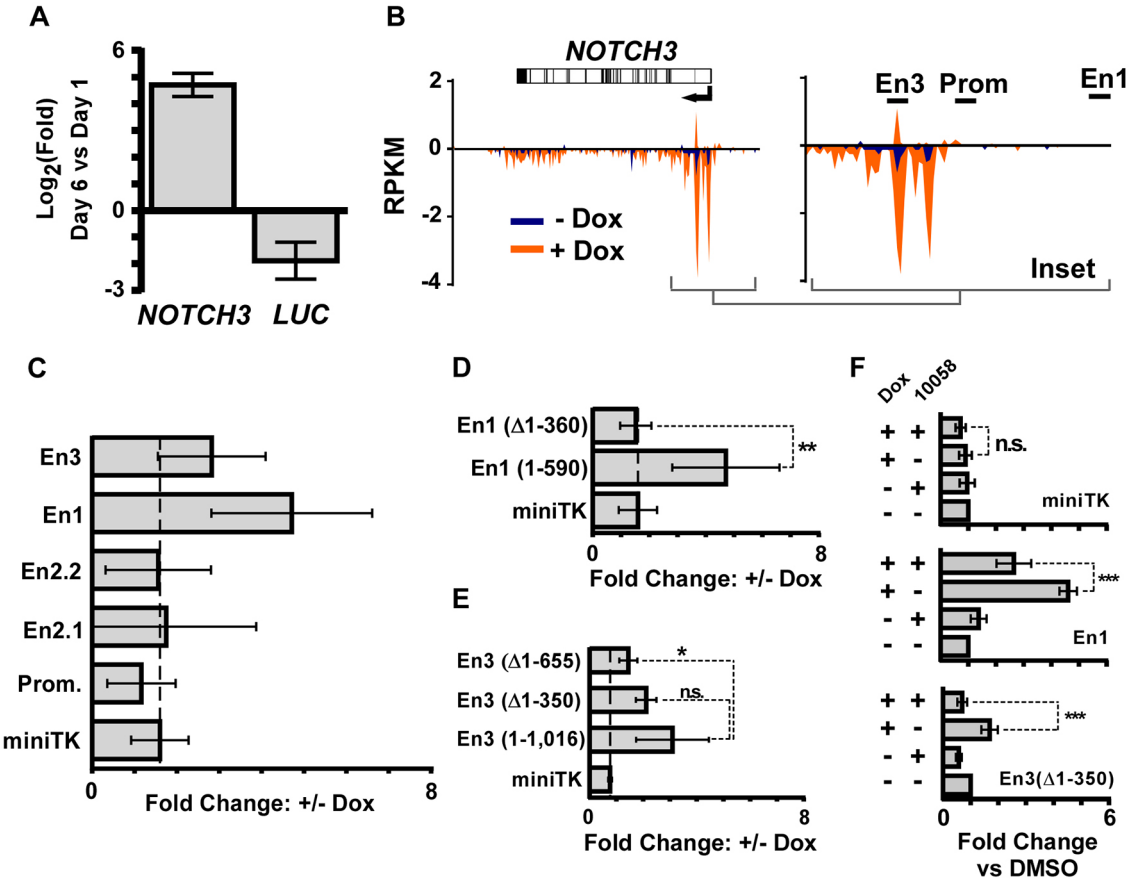

Fig. 5. *NOTCH3* transcription requires a MYC-driven enhancer element. (A) iPrECs were stably transfected with a luciferase reporter driven by 2 kb of *NOTCH3* upstream sequence. A stable pool was differentiated for 1 or 6 days, and analyzed by qRT-PCR. Data were standardized to *18S* and *ACTB* and normalized to the value at day 1. Graph shows mean±s.d. of biological triplicates. (B) iPrEC-TetON-MKK6(CA) cells were treated with or without Dox for 10 h and processed for BruUV-Seq. The *y*-axis is RPKM (reads per kilobase of transcript per million mapped reads). Plus-strand reads are given above the *x*-axis, minus-strand reads are below the x-axis. Blue, without Dox; orange, with Dox. A *NOTCH3* gene diagram shows orientation (arrow) and exons (black lines). (C–F) iPrEC-TetON-MKK6(CA) cells were transfected with indicated luciferase reporter constructs (see Fig. S4B), split, and then treated with or without Dox for 16 h. Graphs show mean±95% c.i. In C, n=8 from two experiments; in D,E n=6 from one experiment. (F) In addition to Dox, cells were treated with DMSO or 10058-F4 (20 µM). n=8 from one experiment, normalized to without Dox (DMSO control). *P≤0.05; **P≤0.01; ***P≤0.001; n.s., not significant.

Journal of Cell Science (2017) 130, 1952-1964 doi:10.1242/jcs.197152

sensitive to MYC inhibition and both contain MYC-binding sites, which when deleted significantly reduced reporter induction in response to MKK6(CA).

NOTCH3 expression is controlled by mRNA stability

NOTCH3 contains an AU-rich element in its 3′ UTR and p38-MAPK is known to regulate RNA-binding proteins (Cuadrado and Nebreda, 2010). Actinomycin D was used to halt transcription, and measurements of mRNA decay were taken at nine time points (Harrold et al., 1991) at day 1 and day 4 of differentiation (Fig. 6A; Table 1). The *MYC* half-life, of 0.8 h, was similar to that found in previous reports (Herrick and Ross, 1994). *MYC* and *NOTCH1* half-lives remained essentially the same at day 4 (P>0.2). However, *NOTCH3* mRNA half-life nearly doubled (11.5 vs 5.9 h), along with an 8.5-fold increase in total mRNA levels. We similarly compared iPrEC-TetON-MKK6(CA) cells stimulated with Dox for 16 h to non-Dox-treated cells (Fig. 6B; Table 2). Both *NOTCH1* and *NOTCH3* mRNA half-lives more than doubled: 3.3 to 8.8 h for *NOTCH1*, and 7.6 to 17.6 h for *NOTCH3*. However, the overall mRNA level of *NOTCH1* decreased ∼4-fold while *NOTCH3* increased ∼9-fold (Table 2). Thus, differentiation and acute p38-MAPK activation both lead to increased *NOTCH3* mRNA half-life, indicating that *NOTCH3* is regulated post-transcriptionally through mRNA stabilization.

DISCUSSION

Differential regulation of NOTCH1 and NOTCH3 during differentiation

NOTCH1 expression has been reported to primarily be present in basal cells of mouse and human prostate, while NOTCH3 has been reported (with some disagreement) to be more luminal (Pedrosa et al., 2016; Shou et al., 2001; Valdez et al., 2012). We detected abundant NOTCH1 and NOTCH2 and very low NOTCH3 in undifferentiated human basal cells. NOTCH4 protein was detectable but at a very low level and did not increase during differentiation (not shown). Owing to their dynamic regulation during differentiation, we focused on NOTCH1 and NOTCH3. We observed a dramatic induction of *NOTCH3* mRNA and protein during differentiation, which coincided with the appearance of suprabasal cells. Therefore, NOTCH3 appears to be a primary driver of luminal cell differentiation, while NOTCH1 serves its previously described role in maintaining the basal population (Pedrosa et al., 2016; Shou et al., 2001; Valdez et al., 2012).

Previous studies have shown that low-Ca^{2+} medium, such as the KSFM in which we culture our cells, selects for basal transit-amplifying prostate epithelial cells and promotes their survival via constitutive activation of NOTCH1 (Dalrymple et al., 2005; Litvinov et al., 2006). However, inhibition or knockdown of NOTCH1 or NOTCH3 did not affect basal cell survival in our assays (Fig. S2E). In the previous studies, constitutive NOTCH1 signaling was most important in subconfluent cultures. We only inhibited NOTCH in completely confluent cells, which may account for the observed differences.

The function of NOTCH3 has been controversial, but recent reports show that it drives luminal differentiation of airway basal cells and mammary epithelium (Baeten and Lilly, 2015; Bhat et al., 2016; Gomi et al., 2015; Mori et al., 2015; Ohashi et al., 2010). Moreover, of the four NOTCH receptors only NOTCH3 is sufficient to drive hepatocyte differentiation in embryonic mouse liver cells (Ortica et al., 2014). Though NOTCH1 seems to drive prostate basal cell commitment, our data supports the idea that NOTCH3 is required to generate the suprabasal cell layer required for prostate luminal cell differentiation.

Transcriptional regulation of *NOTCH3* by p38-MAPK

Part of the mechanistic insight from this work demonstrates that p38-MAPK can regulate *NOTCH3* transcription in part via MYC. Although a relationship between p38-MAPK and NOTCH has previously been suggested, mechanistic details were not clearly established (Brown et al., 2009; Gonsalves and Weisblat, 2007; Kiec-Wilk et al., 2010; Park et al., 2009). We found that the full ability of p38-MAPK to induce NOTCH3 is dependent on MYC. We previously demonstrated MYC is required for PrEC differentiation (Berger et al., 2014; Marderosian et al., 2006). Thus, NOTCH3 appears to be one of the MYC targets downstream of p38-MAPK. MYC has typically been considered a downstream target of NOTCH (Weng et al., 2006), whereas we found that it is upstream of NOTCH3. Although MYC was required for full NOTCH3 induction, blocking its activity did not fully block NOTCH3 induction suggesting that there are likely other factors involved. Furthermore, overexpression of MYC was not sufficient to induce *NOTCH3* mRNA. Thus, p38-MAPK is likely activating

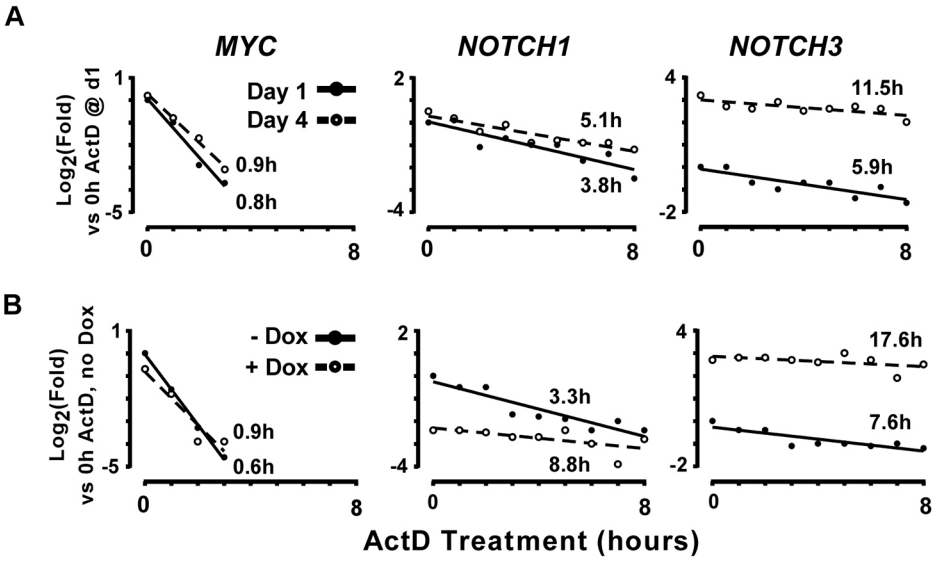

Fig. 6. p38-MAPK upregulates *NOTCH3* mRNA stability. (A) iPrECs were differentiated for 1 or 4 days and at each time treated with actinomycin D (ActD) for 0–8 h. RNA was harvested for qRT-PCR analysis. Samples were standardized to *18S* rRNA and normalized to the day 1, 0 h sample. (B) Same as in A except using the iPrEC-TetON-MKK6(CA) model. Cells were treated with or without Dox for 16 h prior to ActD treatment. Samples were normalized to the 0 h sample without Dox. The numbers given are the calculated half-life in hours.

Journal of Cell Science (2017) 130, 1952-1964 doi:10.1242/jcs.197152

Table 1. Day 4 vs Day 1 mRNA half-life calculations

		Line equation ($y=mx+b$)	r^2	Half-life (1/m)	*P*-value (m1 vs m2)	Overall expression
MYC	*Day1*	$y=-1.30x+0.05$	0.98	0.8 h	0.25	+1.2 fold
	Day4	$y=-1.08x+0.27$	0.99	0.9 h		
NOTCH1	*Day1*	$y=-0.267x+0.03$	0.82	3.8 h	0.23	+1.2 fold
	Day4	$y=-0.197x+0.29$	0.85	5.1 h		
NOTCH3	*Day1*	$y=-0.170x-0.10$	0.74	5.9 h	0.11	+8.5 fold
	Day4	$y=-0.0867x+2.99$	0.55	11.5 h		

r^2 values indicate how well the nine data points fit each linear regression line. *P*-values compare slopes between lines using ANCOVA analysis.

additional unidentified factors that are also required for *NOTCH3* mRNA induction.

Identification and validation of a novel *NOTCH3* enhancer

We investigated potential regulatory regions of the *NOTCH3* gene and found two elements capable of inducing a luciferase reporter upon MKK6(CA) induction that are sensitive to MYC inhibition. One element lies ∼10 kb upstream, denoted En1, and has not previously been linked to *NOTCH3*. A 5′ deletion that eliminates most of the predicted MYC-binding sites in En1 severely compromises its induction; however, it is only partially sensitive to inhibition of MYC. Thus, there are likely to be other factors that cooperate with MYC to fully activate this enhancer. A second element, En3, lies in a previously implicated locus within the second intron (Gagan et al., 2012; Romano et al., 2012). Our report is the first to show functional validation of En3 in human cells. Furthermore, we identified bi-directional eRNA from En3 upon p38-MAPK stimulation, as measured by BruUV-Seq (Kim et al., 2010; Lam et al., 2014; Magnuson et al., 2015). A small deletion (En3Δ1–350) that removed two-thirds of the predicted MYC sites retained reporter activity, thus narrowing down the core regulatory region. Likewise, a second larger deletion (En3Δ1–655) that removed all the predicted MYC-binding sites greatly diminished induction of the reporter. Both elements contain numerous other potential transcription factor-binding sites (The ENCODE Project Consortium, 2012; Mathelier et al., 2016) that may be required for *NOTCH3* to cooperate with MYC. Further detailed analysis will be required to completely define all possible mechanisms of *NOTCH3* transcriptional regulation.

NOTCH3 regulation via mRNA stability

We also demonstrate that *NOTCH3* is post-transcriptionally regulated through mRNA stability during differentiation mediated by p38-MAPK. *NOTCH1* expression is affected by RNA stability, which is known to be modulated through AU-rich elements in its 3′ untranslated region (UTR) and by p38-MAPK (Cisneros et al., 2008; Gonsalves and Weisblat, 2007). p38-MAPK regulates mRNA stability through phosphorylation of mRNA-binding proteins (Cuadrado and Nebreda, 2010). *NOTCH3* also has predicted AU-rich elements in its 3′ UTR (Gruber et al., 2011). Interestingly, p38-MAPK activation via MKK6(CA) for 16 h increased both *NOTCH1* and *NOTCH3* mRNA half-life, but only *NOTCH3* stability was increased after 6 days of differentiation. This may reflect differences in the extent of p38-MAPK activation in the two models or may suggest that other modes of stabilization are involved. There are reports of post-transcriptional NOTCH regulation by micro (mi) RNAs, which may also contribute to long-term stability (Furukawa et al., 2013; Gagan et al., 2012; Liu et al., 2015).

Table 2. MKK6(CA) mRNA half-life calculations

		Line equation ($y=mx+b$)	r^2	Half-life (1/m)	*P*-value (m1 vs m2)	Overall expression
MYC	*−Dox*	$y=-1.55x-0.05$	1.00	0.6 h	0.50	+1.7 fold
	+Dox	$y=-1.17x-0.82$	0.90	0.9 h		
NOTCH1	*−Dox*	$y=-0.302x-0.26$	0.85	3.3 h	0.02	−4.1 fold
	+Dox	$y=-0.113x-2.30$	0.42	8.8 h		
NOTCH3	*−Dox*	$y=-0.132x-0.27$	0.73	7.6 h	0.14	+8.8 fold
	+Dox	$y=-0.057x+2.86$	0.25	17.6 h		

r^2 values indicate how well the nine data points fit each linear regression line. *P*-values compare slopes between lines using ANCOVA analysis.

We also found that MYC enhances NOTCH3 expression independently of mRNA. For instance, it took 20 µM of MYC inhibitor (10058-F4) to suppress *NOTCH3* mRNA expression, yet there were effects on NOTCH3 protein at 5 µM. Similarly, overexpression of MYC did not alter *NOTCH3* mRNA, but it did increase NOTCH3 protein, suggesting that there may be a mechanism for stabilizing NOTCH3 protein or increasing its translation rate. In addition, shRNA against NOTCH3 resulted in partial loss of NOTCH1 protein, but not mRNA. Thus, there are several mechanisms that regulate both NOTCH1 and NOTCH3 during luminal cell differentiation, and further research will be required to define them all.

Role for AR in differentiation

One of the key roles for AR in normal luminal differentiation is to inhibit proliferation, which is the opposite of its role in tumors. Previous reports have shown that AR overexpression in basal PrECs can induce growth arrest and that this requires AR (in cooperation with β-catenin/TCF-4), which transcriptionally represses MYC (Antony et al., 2014; Vander Griend et al., 2014). This is opposite to what is seen in tumors, where AR can drive MYC expression (Antony et al., 2014). Our data showed that p38-MAPK can upregulate MYC expression, which is transient in our differentiation model. Although we have not investigated it, AR may help suppress MYC expression once the suprabasal layer is established. Likewise, it may be that full luminal commitment and increased AR activity may provide a brake for NOTCH3 induction by antagonizing MYC.

Day 8 is a critical transition point in differentiation

Temporal regulation of NOTCH3 throughout differentiation is dynamic. We observed two phases of *NOTCH3* mRNA induction: an early steady increase up to day 8 (day 4 in primary cells) followed by a more dramatic increase. Considering that *NOTCH3* mRNA is stabilized by day 6, it could be that early upregulation is less dependent on transcriptional mechanisms and more on message stability. The suprabasal layer is visible at around day 8, coinciding with induction of downstream target *HES* and *HEY* genes. Additionally, it is at this transition point that p38-MAPK and MYC are activated. Thus, robust transcriptional induction of *NOTCH3* appears to peak at around this time and may drive the secondary phase of *NOTCH3* induction. It is also at this time that *NOTCH1* mRNA begins to increase following an initial dip. Thus, day 8 is a key point for NOTCH1 and NOTCH3 induction and cell commitment to the luminal transition.

Potential downstream effects of NOTCH activity

The direct effectors of NOTCH signaling include the canonical *HES* and *HEY* transcriptional repressor family. Indeed, we observed differential induction of several family members during differentiation. In ongoing studies, we are determining which of these are critical for luminal cell differentiation. Previous findings have reported that AR and GATA cooperate

Journal of Cell Science (2017) 130, 1952-1964 doi:10.1242/jcs.197152

to regulate a set of target genes, and HEY transcriptional repressors can prevent GATA-mediated induction of AR target genes (Belandia et al., 2005; Fischer et al., 2005; Litvinov et al., 2006; Xiao et al., 2016). This would support downstream HEY activity in maintaining a basal commitment. With the NOTCH pathway, timing and dose are critical. Our attempts to drive differentiation with inducible NOTCH ICD (NICD) constructs led to cell stress and death within 24–48 h (data not shown). It may be that a low or moderate amount of NOTCH activity is needed for survival and initial differentiation but too much activity can block terminal differentiation. Whether the functional role of NOTCH3 is via HES and HEY or non-canonical downstream targets will require further investigation.

Some of the reported non-canonical NOTCH targets include PTEN and CDH1 (also known as E-cadherin), both of which are critical for luminal cell survival (Bertrand et al., 2014; Lamb et al., 2010). Furthermore, NOTCH downregulates adhesion genes, including integrins such as β4, which is required for basal cell detachment from the extracellular matrix (Cress et al., 1995; Mazzone et al., 2010; Nguyen et al., 2006). We also see loss of integrin expression during differentiation. There are also reports that NOTCH can upregulate MKP1 (also known as DUSP1), a phosphatase that targets p38-MAPK, thus providing a potential feedback mechanism in terminally differentiated cells to balance p38-MAPK activity (Gagan et al., 2012; Yoshida et al., 2014). The balance of downstream NOTCH targets (both canonical and non-canonical) could help explain the conflicting roles for the pathway in promoting both basal and luminal commitments.

Previous studies suggested that the ICD from NOTCH3 is a weaker activator than other NICDs (Beatus et al., 1999; Ong et al., 2006). However, our findings and other recent reports have begun to reveal novel signaling effects and preferential targets for NOTCH3 (Baeten and Lilly, 2015; Cui et al., 2013; Wang et al., 2016). As it stands, NOTCH3 appears to be unique among the receptors. Further research will be needed to validate which downstream NOTCH3-specific targets are most relevant to luminal cell differentiation.

Conclusion

In this study, we report on a novel mechanism for crosstalk between p38-MAPK, MYC and NOTCH. Moreover, we identify two distinct regulatory mechanisms for *NOTCH3* in the prostate: a coordination of elevated mRNA stability and increased transcription from multiple enhancers. These findings provide a better understanding for how these differentiation pathways are connected in normal prostate epithelium and opens the door to investigating how their dysregulation may impact prostate cancer development and progression.

MATERIALS AND METHODS

Cell culture

Primary and immortalized PrECs (Berger et al., 2014) were grown in KSFM medium (Gibco) plus penicillin-streptomycin at 30 units/ml (Gibco). Differentiation was induced as previously reported with 2.5 ng/ml recombinant KGF (Cell Sciences) and 1–10 nM R1881 (Perkin Elmer) (10 nM unless otherwise specified) with fresh medium added every 24 h (Lamb et al., 2010). Suprabasal layer separation was achieved by using Ca^{2+} and Mg^{2+}-free PBS with 1 mM EDTA as previously described (Lamb et al., 2010). HEK 293FT cells were used for lentivirus production (ViraPower, Invitrogen) and grown in Dulbecco's modified Eagle's medium (DMEM; 11995, Gibco) with 10% fetal bovine serum (FBS; Gemini) and 2 mM L-glutamine (Gibco). Cell lines were tested via a MycoAlert PLUS kit (Lonza) and confirmed to be mycoplasma free.

Molecular cloning and stable cell line construction

Immortalized PrECs (iPrECs) were engineered with Dox-inducible shRNAs using the EZ-Tet-pLKO-Puro and EZ-Tet-pLKO-Hygro vectors (Addgene plasmids 85966, 85972) (Frank et al., 2017). shRNA sequences are listed in Table S1. Expression cDNAs were subcloned, via PCR with Q5 polymerase (NEB), into the pENTR3C gateway vector (Invitrogen) between the SalI and NotI sites and then recombined with LR Clonase II (Invitrogen) into pLenti-CMV/TO-Puro-DEST (Addgene plasmid 17293) (Campeau et al., 2009). The constitutively active MKK6 mutant (MKK6-DD) was a gift from Angel Nebreda (Oncology Unit, Institute for Research in Biomedicine, Spain) (Alonso et al., 2000). The MYC cDNA, subcloned from pBabe-Myc, was a gift from Beatrice Knudsen (Biomedical Sciences and Pathology, Cedars Sinai, USA). TetR lines were established by using pLenti-CMV-TetR-Blast (Addgene plasmid 17492) (Campeau et al., 2009). iPrECs antibiotic selection doses were as follows: 50 µg/ml hygromycin, 5 µg/ml blasticidin and 2 µg/ml puromycin. Doxycycline (Sigma) was used at 50 ng/ml to induce shRNAs and 2–10 ng/ml to induce cDNA expression.

siRNA and inhibitors

A mixed siRNA pool against *MYC* and non-targeting siRNA (siScram) were purchased from Origene (SR303025). Cells were transfected by using siLentfect reagent (Bio-Rad). Cyclohexamide was used at 10 µg/ml, and actinomycin D at 5 µg/ml (Calbiochem). SB202190, BIRB796/Doramapimod, 10058-F4, JQ-1, BrdU and staurosporine were purchased from Cayman Chemical. RO4929097 was purchased from Apex Bio.

Immunoblotting

Cell lysates were prepared in RIPA as previously described (Edick et al., 2007). Protein loading was standardized by use of the BCA assay (Pierce). 20–50 µg of denatured protein was run on Novex SDS polyacrylamide Tris-glycine gels (Life Technologies) and transferred onto PVDF membrane (Fisher). Chemiluminescence was used to image blots with a Bio-Rad Chemi-Doc imaging system with CCD camera. The quantification shown in Fig. S1A,B was performed with ImageJ software. Data were first normalized to tubulin, then to day 1 'i' samples and plotted as mean±s.d. *P*-values were determined by paired one-way ANOVA with Turkey's multiple testing correction. Antibodies are listed in Table S2. The protein ladder was from Cell Signaling Technology (7720) or GoldBio (P007).

qRT-PCR

RNA was harvested and extracted with Trizol following the manufacturer's protocol (Invitrogen). cDNA was synthesized with M-MuLV reverse transcriptase (NEB) using a 4:1 mix of poly-d(16)T and random hexamer primers. qRT-PCR was performed using SYBR Green Master Mix (Roche) and an ABI 7500 thermal cycler (Applied Biosystems). Data were standardized to *18S* plus *GAPDH* unless otherwise stated and were normalized (ΔΔCT) and plotted as Log_2(Fold). Primers were synthesized by Integrated DNA Technologies. Primers are in Table S3.

Immunostaining

Cells were fixed, permeabilized, and stained as previously described (Berger et al., 2014). Antibodies against ITGα6 (555734, BD) and AR (sc-815, Santa Cruz Biotechnology) were used at 1:200 dilution. Suprabasal coverage of the underlying basal layer was determined by tracing the clusters that were both AR^+ and $ITG\alpha6^-$ by hand using ImageJ software, and calculating the percentage area of suprabasal regions versus total image area. Three fields of view were measured for each condition. For propidum iodide staining, cells were fixed with 4% paraformaldahyde, treated with 100 ng/ml RNaseA (Thermo) for 10 min, then stained with 100 ng/ml propidum iodide (Sigma) for 5 min. Nuclei were stained with 10 µg/ml Hoescht 33258 (Sigma) for 10 min. Epifluorescence microscopy was performed on a Nikon TE300 using Nikon Elements software (v4.11.00). Fig. 2E was captured on a DeltaVision (GE) epifluorescence scope with SoftWoRx software, with processing by deconvolution and maximum intensity projection from a *z*-stack capture.

Luciferase assay and constructs

Putative *NOTCH3* regulatory elements were PCR subcloned from the RP11-937H1 BAC library (Life Technologies) using Q5 or LongAmp polymerase

(NEB). The *NOTCH3* 2 kb promoter element was ligated into pGL4.15-Hygro (Promega). Candidate regulatory elements were ligated into pNL1.1 (Promega) after first cloning in a miniTK promoter at the HindIII site. Deletion mutants were made using the QuickChange II Mutagenesis kit (200524, Stratagene). Cloning primers, miniTK sequence, and mutagenesis primers are in Table S4.

En1 and En3 maps in Fig. S4C were generated using SnapGene and modified with Canvas software. MYC-binding sites were determined by using the JASPAR online database (http://jaspar.genereg.net/) (Mathelier et al., 2016), with a threshold of 80% using the MA0147.2 matrix model for MYC-binding sites (Chen et al., 2008).

Luciferase assays were performed by using the NanoGlo kit (Promega) and a Synergy Neo II (Bio Tek) plate reader with Gen5 software (v2.04). Cells were transfected as a pool with XtremeGeneHP reagent (Roche) and then split for different treatments. pNL1.1-miniTK served as the negative control. Luciferase assays were run 16 h after Dox treatment and 48 h after transfection.

mRNA half-life measurement

Cells were treated with 5 µg/ml Actinomycin D for 0–8 h. RNA and cDNA were prepared as described above. Data were standardized to *18S* rRNA and normalized as ΔΔCT values versus the Day 1 or 'no Dox' samples at 0 h. 18S rRNA has a very long half-life (1–7 days) and thus is suitable for standardization (Defoiche et al., 2009). Linear regression curves, line equations, r^2 values, and *P*-values were calculated with GraphPad PRISM software. Half-life was calculated as 1/m, where m is the slope. Overall expression change was calculated as $2^{(b2-b1)}$, where b=y-intercept; b1 is intercept 1 and b2 is intercept 2. AU-rich elements were identified using the ARE site (v1) online tool (http://nibiru.tbi.univie.ac.at/cgi-bin/AREsite/AREsite.cgi) (Gruber et al., 2011).

BruUV-Seq

iPrEC-TetON-MKK6(CA) cells were treated with 5 ng/ml Dox for 10 h or left untreated, then exposed to UV (100 J/m^2) using a Stratalinker UV Crosslinker 1800 (Stratagene) and labeled with 2 mM 5-bromo-deoxyuridine (sc-256904, Santa Cruz Biotechnology) for 30 min before washing with PBS and collecting RNA with Trizol (Life Technologies). BrU isolation, library prep, sequencing and mapping was performed as previously described (Andrade-Lima et al., 2015; Paulsen et al., 2014). Data were exported (bin size=300 bp) and graphed using GraphPad PRISM software.

Statistical analysis

Unless otherwise specified, *P*-values were calculated using paired, one-tailed *t*-tests on biological triplicates, with $*P \leq 0.05$, $**P \leq 0.01$, $***P \leq 0.001$ and n. s., not significant ($P > 0.05$). For Tables 1 and 2, *P*-values were calculated by ANCOVA analysis using PRISM GraphPad software. Fig. 5D,E used one-way ANOVA with Greenhouse–Geisser correction. Fig. 5F used two-way ANOVA with Turkey's multiple testing correction.

Acknowledgements

We acknowledge Mary Winn and the VARI Bioinformatics and Biostatistics Core for assistance with statistical and RNA-Seq analysis. We thank Michelle Paulsen for technical consolation on BruUV-Seq. Additional thanks to the VARI Program for Skeletal Disease and Tumor Metastasis for feedback and suggestions. The TetON cDNA and TetR vectors were gifts from Eric Campeau, the MMK6(CA) (MKK6-DD) construct was a gift from Dr. Angel Nebreda, and pBabe-MYC a gift from Dr. Beatrice Knudsen.

Competing interests

The authors declare no competing or financial interests.

Author contributions

Conceptualization: S.B.F., M.L., C.K.M.; Methodology: S.B.F., P.L.B., M.L.; Software: M.L.; Validation: S.B.F., P.L.B.; Formal analysis: S.B.F., M.L., C.K.M.; Investigation: P.L.B.; Resources: C.K.M.; Data curation: P.L.B.; Writing - original draft: S.B.F., C.K.M.; Writing - review & editing: S.B.F., C.K.M.; Supervision: C.K.M.; Project administration: C.K.M.; Funding acquisition: C.K.M.

Funding

These studies were supported by funding from the U.S. Department of Defense Prostate Cancer Research Program W81XWH-14-1-0479 (to C.K.M., S.B.F. and P.L.B.), Association for International Cancer Research (Worldwide Cancer Research) (11-0082 to S.B.F.), the Van Andel Research Institute and the University of Arizona.

Supplementary information

Supplementary information available online at
http://jcs.biologists.org/lookup/doi/10.1242/jcs.197152.supplemental

References

Alonso, G., Ambrosino, C., Jones, M. and Nebreda, A. R. (2000). Differential activation of p38 mitogen-activated protein kinase isoforms depending on signal strength. *J. Biol. Chem.* **275**, 40641-40648.

Andrade-Lima, L. C., Veloso, A., Paulsen, M. T., Menck, C. F. M. and Ljungman, M. (2015). DNA repair and recovery of RNA synthesis following exposure to ultraviolet light are delayed in long genes. *Nucleic Acids Res.* **43**, 2744-2756.

Antony, L., van der Schoor, F., Dalrymple, S. L. and Isaacs, J. T. (2014). Androgen receptor (AR) suppresses normal human prostate epithelial cell proliferation via AR/beta-catenin/TCF-4 complex inhibition of c-MYC transcription. *Prostate* **74**, 1118-1131.

Baeten, J. T. and Lilly, B. (2015). Differential regulation of NOTCH2 and NOTCH3 contribute to their unique functions in vascular smooth muscle cells. *J. Biol. Chem.* **290**, 16226-16237.

Beatus, P., Lundkvist, J., Oberg, C. and Lendahl, U. (1999). The notch 3 intracellular domain represses notch 1-mediated activation through Hairy/Enhancer of split (HES) promoters. *Development* **126**, 3925-3935.

Belandia, B., Powell, S. M., Garcia-Pedrero, J. M., Walker, M. M., Bevan, C. L. and Parker, M. G. (2005). Hey1, a mediator of notch signaling, is an androgen receptor corepressor. *Mol. Cell. Biol.* **25**, 1425-1436.

Belleudi, F., Purpura, V. and Torrisi, M. R. (2011). The receptor tyrosine kinase FGFR2b/KGFR controls early differentiation of human keratinocytes. *PLoS ONE* **6**, e24194.

Berger, P. L., Frank, S. B., Schulz, V. V., Nollet, E. A., Edick, M. J., Holly, B., Chang, T.-T. A., Hostetter, G., Kim, S. and Miranti, C. K. (2014). Transient induction of ING4 by Myc drives prostate epithelial cell differentiation and its disruption drives prostate tumorigenesis. *Cancer Res.* **74**, 3357-3368.

Berger, P. L., Winn, M. E. and Miranti, C. K. (2017). Miz1, a novel target of ING4, can drive prostate luminal epithelial cell differentiation. *Prostate* **77**, 49-59.

Bertrand, F. E., McCubrey, J. A., Angus, C. W., Nutter, J. M. and Sigounas, G. (2014). NOTCH and PTEN in prostate cancer. *Adv. Biol. Regul.* **56**, 51-65.

Bhat, V., Sun, Y. J., Weger, S. and Raouf, A. (2016). Notch-induced expression of FZD7 requires noncanonical NOTCH3 signaling in human breast epithelial cells. *Stem Cells Dev.* **25**, 522-529.

Brown, D., Hikim, A. P. S., Kovacheva, E. L. and Sinha-Hikim, I. (2009). Mouse model of testosterone-induced muscle fiber hypertrophy: involvement of p38 mitogen-activated protein kinase-mediated Notch signaling. *J. Endocrinol.* **201**, 129-139.

Campeau, E., Ruhl, V. E., Rodier, F., Smith, C. L., Rahmberg, B. L., Fuss, J. O., Campisi, J., Yaswen, P., Cooper, P. K. and Kaufman, P. D. (2009). A versatile viral system for expression and depletion of proteins in mammalian cells. *PLoS ONE* **4**, e6529.

Carvalho, F. L. F., Simons, B. W., Eberhart, C. G. and Berman, D. M. (2014). Notch signaling in prostate cancer: a moving target. *Prostate* **74**, 933-945.

Chen, X., Xu, H., Yuan, P., Fang, F., Huss, M., Vega, V. B., Wong, E., Orlov, Y. L., Zhang, W., Jiang, J. et al. (2008). Integration of external signaling pathways with the core transcriptional network in embryonic stem cells. *Cell* **133**, 1106-1117.

Cisneros, E., Latasa, M. J., García-Flores, M. and Frade, J. M. (2008). Instability of Notch1 and Delta1 mRNAs and reduced Notch activity in vertebrate neuroepithelial cells undergoing S-phase. *Mol. Cell. Neurosci.* **37**, 820-831.

Conacci-Sorrell, M., McFerrin, L. and Eisenman, R. N. (2014). An overview of MYC and its interactome. *Cold Spring Harb. Perspect. Med.* **4**, a014357.

Cress, A. E., Rabinovitz, I., Zhu, W. and Nagle, R. B. (1995). The alpha 6 beta 1 and alpha 6 beta 4 integrins in human prostate cancer progression. *Cancer Metastasis Rev.* **14**, 219-228.

Cuadrado, A. and Nebreda, A. R. (2010). Mechanisms and functions of p38 MAPK signalling. *Biochem. J.* **429**, 403-417.

Cui, H., Kong, Y., Xu, M. and Zhang, H. (2013). Notch3 functions as a tumor suppressor by controlling cellular senescence. *Cancer Res.* **73**, 3451-3459.

Dalrymple, S., Antony, L., Xu, Y., Uzgare, A. R., Arnold, J. T., Savaugeot, J., Sokoll, L. J., De Marzo, A. M. and Isaacs, J. T. (2005). Role of notch-1 and E-cadherin in the differential response to calcium in culturing normal versus malignant prostate cells. *Cancer Res.* **65**, 9269-9279.

Defoiche, J., Zhang, Y., Lagneaux, L., Pettengell, R., Hegedus, A., Willems, L. and Macallan, D. C. (2009). Measurement of ribosomal RNA turnover in vivo by use of deuterium-labeled glucose. *Clin. Chem.* **55**, 1824-1833.

Delmore, J. E., Issa, G. C., Lemieux, M. E., Rahl, P. B., Shi, J., Jacobs, H. M., Kastritis, E., Gilpatrick, T., Paranal, R. M., Qi, J. et al. (2011). BET bromodomain inhibition as a therapeutic strategy to target c-Myc. *Cell* **146**, 904-917.

Journal of Cell Science

Deng, G., Ma, L., Meng, Q., Ju, X., Jiang, K., Jiang, P. and Yu, Z. (2015). Notch signaling in the prostate: critical roles during development and in the hallmarks of prostate cancer biology. *J. Cancer Res. Clin. Oncol.* **142**, 531-47.

Edick, M. J., Tesfay, L., Lamb, L. E., Knudsen, B. S. and Miranti, C. K. (2007). Inhibition of integrin-mediated crosstalk with epidermal growth factor receptor/Erk or Src signaling pathways in autophagic prostate epithelial cells induces caspase-independent death. *Mol. Biol. Cell* **18**, 2481-2490.

Fischer, A., Klattig, J., Kneitz, B., Diez, H., Maier, M., Holtmann, B., Englert, C. and Gessler, M. (2005). Hey basic helix-loop-helix transcription factors are repressors of GATA4 and GATA6 and restrict expression of the GATA target gene ANF in fetal hearts. *Mol. Cell. Biol.* **25**, 8960-8970.

Frank, S. B. and Miranti, C. K. (2013). Disruption of prostate epithelial differentiation pathways and prostate cancer development. *Front. Oncol.* **3**, 273.

Frank, S. B., Schulz, V. V. and Miranti, C. K. (2017). A streamlined method for the design and cloning of shRNAs into an optimized Dox-inducible lentiviral vector. *BMC Biotechnol.* **17**, 24.

Furukawa, S., Kawasaki, Y., Miyamoto, M., Hiyoshi, M., Kitayama, J. and Akiyama, T. (2013). The miR-1-NOTCH3-Asef pathway is important for colorectal tumor cell migration. *PLoS ONE* **8**, e80609.

Gagan, J., Dey, B. K., Layer, R., Yan, Z. and Dutta, A. (2012). Notch3 and Mef2c proteins are mutually antagonistic via Mkp1 protein and miR-1/206 microRNAs in differentiating myoblasts. *J. Biol. Chem.* **287**, 40360-40370.

Gebhardt, A., Frye, M., Herold, S., Benitah, S. A., Braun, K., Samans, B., Watt, F. M., Elsässer, H. P. and Eilers, M. (2006). Myc regulates keratinocyte adhesion and differentiation via complex formation with Miz1. *J. Cell Biol.* **172**, 139-149.

Gomi, K., Arbelaez, V., Crystal, R. G. and Walters, M. S. (2015). Activation of NOTCH1 or NOTCH3 signaling skews human airway basal cell differentiation toward a secretory pathway. *PLoS ONE* **10**, e0116507.

Gonsalves, F. C. and Weisblat, D. A. (2007). MAPK regulation of maternal and zygotic Notch transcript stability in early development. *Proc. Natl. Acad. Sci. USA* **104**, 531-536.

Gruber, A. R., Fallmann, J., Kratochvill, F., Kovarik, P. and Hofacker, I. L. (2011). AREsite: a database for the comprehensive investigation of AU-rich elements. *Nucleic Acids Res.* **39**, D66-D69.

Guo, J., Parise, R. A., Joseph, E., Egorin, M. J., Lazo, J. S., Prochownik, E. V. and Eiseman, J. L. (2009). Efficacy, pharmacokinetics, tisssue distribution, and metabolism of the Myc-Max disruptor, 10058-F4 [Z,E]-5-[4-ethylbenzylidine]-2-thioxothiazolidin-4-one, in mice. *Cancer Chemother. Pharmacol.* **63**, 615-625.

Harrold, S., Genovese, C., Kobrin, B., Morrison, S. L. and Milcarek, C. (1991). A comparison of apparent mRNA half-life using kinetic labeling techniques vs decay following administration of transcriptional inhibitors. *Anal. Biochem.* **198**, 19-29.

Heer, R., Collins, A. T., Robson, C. N., Shenton, B. K. and Leung, H. Y. (2006). KGF suppresses alpha2beta1 integrin function and promotes differentiation of the transient amplifying population in human prostatic epithelium. *J. Cell Sci.* **119**, 1416-1424.

Herrick, D. J. and Ross, J. (1994). The half-life of c-myc mRNA in growing and serum-stimulated cells: influence of the coding and 3′ untranslated regions and role of ribosome translocation. *Mol. Cell. Biol.* **14**, 2119-2128.

Hodkinson, P. S., Elliott, P. A., Lad, Y., McHugh, B. J., MacKinnon, A. C., Haslett, C. and Sethi, T. (2007). Mammalian NOTCH-1 activates beta1 integrins via the small GTPase R-Ras. *J. Biol. Chem.* **282**, 28991-29001.

Huang, M.-J., Cheng, Y.-C., Liu, C.-R., Lin, S. and Liu, H. E. (2006). A small-molecule c-Myc inhibitor, 10058-F4, induces cell-cycle arrest, apoptosis, and myeloid differentiation of human acute myeloid leukemia. *Exp. Hematol.* **34**, 1480-1489.

Kent, W. J., Sugnet, C. W., Furey, T. S., Roskin, K. M., Pringle, T. H., Zahler, A. M. and Haussler, D. (2002). The human genome browser at UCSC. *Genome Res.* **12**, 996-1006.

Kiec-Wilk, B., Grzybowska-Galuszka, J., Polus, A., Pryjma, J., Knapp, A. and Kristiansen, K. (2010). The MAPK-dependent regulation of the Jagged/Notch gene expression by VEGF, bFGF or PPAR gamma mediated angiogenesis in HUVEC. *J. Physiol. Pharmacol.* **61**, 217-225.

Kim, T.-K., Hemberg, M., Gray, J. M., Costa, A. M., Bear, D. M., Wu, J., Harmin, D. A., Laptewicz, M., Barbara-Haley, K., Kuersten, S. et al. (2010). Widespread transcription at neuronal activity-regulated enhancers. *Nature* **465**, 182-187.

Koh, C. M., Bieberich, C. J., Dang, C. V., Nelson, W. G., Yegnasubramanian, S. and De Marzo, A. M. (2010). MYC and prostate cancer. *Genes Cancer* **1**, 617-628.

Kopan, R. and Ilagan, M. X. G. (2009). The canonical Notch signaling pathway: unfolding the activation mechanism. *Cell* **137**, 216-233.

Kwon, O.-J., Valdez, J. M., Zhang, L., Zhang, B., Wei, X., Su, Q., Ittmann, M. M., Creighton, C. J. and Xin, L. (2014). Increased Notch signalling inhibits anoikis and stimulates proliferation of prostate luminal epithelial cells. *Nat. Commun.* **5**, 4416.

Kwon, O.-J., Zhang, L. and Xin, L. (2016). Stem cell antigen-1 identifies a distinct androgen-independent murine prostatic luminal cell lineage with bipotent potential. *Stem Cells* **34**, 191-202.

Lam, M. T. Y., Li, W., Rosenfeld, M. G. and Glass, C. K. (2014). Enhancer RNAs and regulated transcriptional programs. *Trends Biochem. Sci.* **39**, 170-182.

Lamb, L. E., Knudsen, B. S. and Miranti, C. K. (2010). E-cadherin-mediated survival of androgen-receptor-expressing secretory prostate epithelial cells derived from a stratified in vitro differentiation model. *J. Cell Sci.* **123**, 266-276.

Litvinov, I. V., Vander Griend, D. J., Xu, Y., Antony, L., Dalrymple, S. L. and Isaacs, J. T. (2006). Low-calcium serum-free defined medium selects for growth of normal prostatic epithelial stem cells. *Cancer Res.* **66**, 8598-8607.

Liu, X. D., Zhang, L. Y., Zhu, T. C., Zhang, R. F., Wang, S. L. and Bao, Y. (2015). Overexpression of miR-34c inhibits high glucose-induced apoptosis in podocytes by targeting Notch signaling pathways. *Int. J. Clin. Exp. Pathol.* **8**, 4525-4534.

Lüscher, B. and Vervoorts, J. (2012). Regulation of gene transcription by the oncoprotein MYC. *Gene* **494**, 145-160.

Magnuson, B., Veloso, A., Kirkconnell, K. S., de Andrade Lima, L. C., Paulsen, M. T., Ljungman, E. A., Bedi, K., Prasad, J., Wilson, T. E. and Ljungman, M. (2015). Identifying transcription start sites and active enhancer elements using BruUV-seq. *Sci. Rep.* **5**, 17978.

Marderosian, M., Sharma, A., Funk, A. P., Vartanian, R., Masri, J., Jo, O. D. and Gera, J. F. (2006). Tristetraprolin regulates Cyclin D1 and c-Myc mRNA stability in response to rapamycin in an Akt-dependent manner via p38 MAPK signaling. *Oncogene* **25**, 6277-6290.

Mathelier, A., Fornes, O., Arenillas, D. J., Chen, C.-Y., Denay, G., Lee, J., Shi, W., Shyr, C., Tan, G., Worsley-Hunt, R. et al. (2016). JASPAR 2016: a major expansion and update of the open-access database of transcription factor binding profiles. *Nucleic Acids Res.* **44**, D110-D115.

Mazzone, M., Selfors, L. M., Albeck, J., Overholtzer, M., Sale, S., Carroll, D. L., Pandya, D., Lu, Y., Mills, G. B., Aster, J. C. et al. (2010). Dose-dependent induction of distinct phenotypic responses to Notch pathway activation in mammary epithelial cells. *Proc. Natl. Acad. Sci. USA* **107**, 5012-5017.

McKeown, M. R. and Bradner, J. E. (2014). Therapeutic strategies to inhibit MYC. *Cold Spring Harb. Perspect. Med.* **4**, a014266.

Mori, M., Mahoney, J. E., Stupnikov, M. R., Paez-Cortez, J. R., Szymaniak, A. D., Varelas, X., Herrick, D. B., Schwob, J., Zhang, H. and Cardoso, W. V. (2015). Notch3-Jagged signaling controls the pool of undifferentiated airway progenitors. *Development* **142**, 258-267.

Nguyen, B.-C., Lefort, K., Mandinova, A., Antonini, D., Devgan, V., Della Gatta, G., Koster, M. I., Zhang, Z., Wang, J., Tommasi di Vignano, A. et al. (2006). Cross-regulation between Notch and p63 in keratinocyte commitment to differentiation. *Genes Dev.* **20**, 1028-1042.

Ohashi, S., Natsuizaka, M., Yashiro-Ohtani, Y., Kalman, R. A., Nakagawa, M., Wu, L., Klein-Szanto, A. J., Herlyn, M., Diehl, J. A., Katz, J. P. et al. (2010). NOTCH1 and NOTCH3 coordinate esophageal squamous differentiation through a CSL-dependent transcriptional network. *Gastroenterology* **139**, 2113-2123.

Ong, C.-T., Cheng, H.-T., Chang, L.-W., Ohtsuka, T., Kageyama, R., Stormo, G. D. and Kopan, R. (2006). Target selectivity of vertebrate notch proteins. Collaboration between discrete domains and CSL-binding site architecture determines activation probability. *J. Biol. Chem.* **281**, 5106-5119.

Ortica, S., Tarantino, N., Aulner, N., Israel, A. and Gupta-Rossi, N. (2014). The 4 Notch receptors play distinct and antagonistic roles in the proliferation and hepatocytic differentiation of liver progenitors. *FASEB J.* **28**, 603-614.

Ousset, M., Van Keymeulen, A., Bouvencourt, G., Sharma, N., Achouri, Y., Simons, B. D. and Blanpain, C. (2012). Multipotent and unipotent progenitors contribute to prostate postnatal development. *Nat. Cell Biol.* **14**, 1131-1138.

Park, J.-S., Kim, Y.-S. and Yoo, M.-A. (2009). The role of p38b MAPK in age-related modulation of intestinal stem cell proliferation and differentiation in Drosophila. *Aging (Albany NY)* **1**, 637-651.

Paulsen, M. T., Veloso, A., Prasad, J., Bedi, K., Ljungman, E. A., Magnuson, B., Wilson, T. E. and Ljungman, M. (2014). Use of Bru-Seq and BruChase-Seq for genome-wide assessment of the synthesis and stability of RNA. *Methods* **67**, 45-54.

Pedrosa, A.-R., Graça, J. L., Carvalho, S., Peleteiro, M. C., Duarte, A. and Trindade, A. (2016). Notch signaling dynamics in the adult healthy prostate and in prostatic tumor development. *Prostate* **76**, 80-96.

Rangarajan, A., Talora, C., Okuyama, R., Nicolas, M., Mammucari, C., Oh, H., Aster, J. C., Krishna, S., Metzger, D., Chambon, P. et al. (2001). Notch signaling is a direct determinant of keratinocyte growth arrest and entry into differentiation. *EMBO J.* **20**, 3427-3436.

Romano, R.-A., Smalley, K., Magraw, C., Serna, V. A., Kurita, T., Raghavan, S. and Sinha, S. (2012). DeltaNp63 knockout mice reveal its indispensable role as a master regulator of epithelial development and differentiation. *Development* **139**, 772-782.

Shou, J., Ross, S., Koeppen, H., de Sauvage, F. J. and Gao, W. Q. (2001). Dynamics of notch expression during murine prostate development and tumorigenesis. *Cancer Res.* **61**, 7291-7297.

The ENCODE Project Consortium (2012). An integrated encyclopedia of DNA elements in the human genome. *Nature* **489**, 57-74.

Tokar, E. J., Ancrile, B. B., Cunha, G. R. and Webber, M. M. (2005). Stem/progenitor and intermediate cell types and the origin of human prostate cancer. *Differentiation* **73**, 463-473.

Uzgare, A. R., Xu, Y. and Isaacs, J. T. (2004). In vitro culturing and characteristics of transit amplifying epithelial cells from human prostate tissue. *J. Cell. Biochem.* **91**, 196-205.

Valdez, J. M., Zhang, L., Su, Q., Dakhova, O., Zhang, Y., Shahi, P., Spencer, D. M., Creighton, C. J., Ittmann, M. M. and Xin, L. (2012). Notch and TGFbeta form a reciprocal positive regulatory loop that suppresses murine prostate basal stem/progenitor cell activity. *Cell Stem Cell* **11**, 676-688.

Vander Griend, D. J., Litvinov, I. V. and Isaacs, J. T. (2014). Conversion of androgen receptor signaling from a growth suppressor in normal prostate epithelial cells to an oncogene in prostate cancer cells involves a gain of function in c-Myc regulation. *Int. J. Biol. Sci.* **10**, 627-642.

Wang, J., Ma, X., Jones, H. M., Chan, L. L.-Y., Song, F., Zhang, W., Bae-Jump, V. L. and Zhou, C. (2014). Evaluation of the antitumor effects of c-Myc-Max heterodimerization inhibitor 100258-F4 in ovarian cancer cells. *J. Transl. Med.* **12**, 226.

Wang, X., Shen, Q. W., Wang, J., Zhang, Z., Feng, F., Chen, T., Zhang, Y., Wei, H., Li, Z., Wang, X. et al. (2016). KLF7 regulates satellite cell quiescence in response to extracellular signaling. *Stem Cells* **34**, 1310-1320.

Weng, A. P., Millholland, J. M., Yashiro-Ohtani, Y., Arcangeli, M. L., Lau, A., Wai, C., Del Bianco, C., Rodriguez, C. G., Sai, H., Tobias, J. et al. (2006). c-Myc is an important direct target of Notch1 in T-cell acute lymphoblastic leukemia/lymphoma. *Genes Dev.* **20**, 2096-2109.

Xiao, L., Feng, Q., Zhang, Z., Wang, F., Lydon, J. P., Ittmann, M. M., Xin, L., Mitsiades, N. and He, B. (2016). The essential role of GATA transcription factors in adult murine prostate. *Oncotarget* **7**, 47891-47903.

Yoshida, Y., Hayashi, Y., Suda, M., Tateno, K., Okada, S., Moriya, J., Yokoyama, M., Nojima, A., Yamashita, M., Kobayashi, Y. et al. (2014). Notch signaling regulates the lifespan of vascular endothelial cells via a p16-dependent pathway. *PLoS ONE* **9**, e100359.

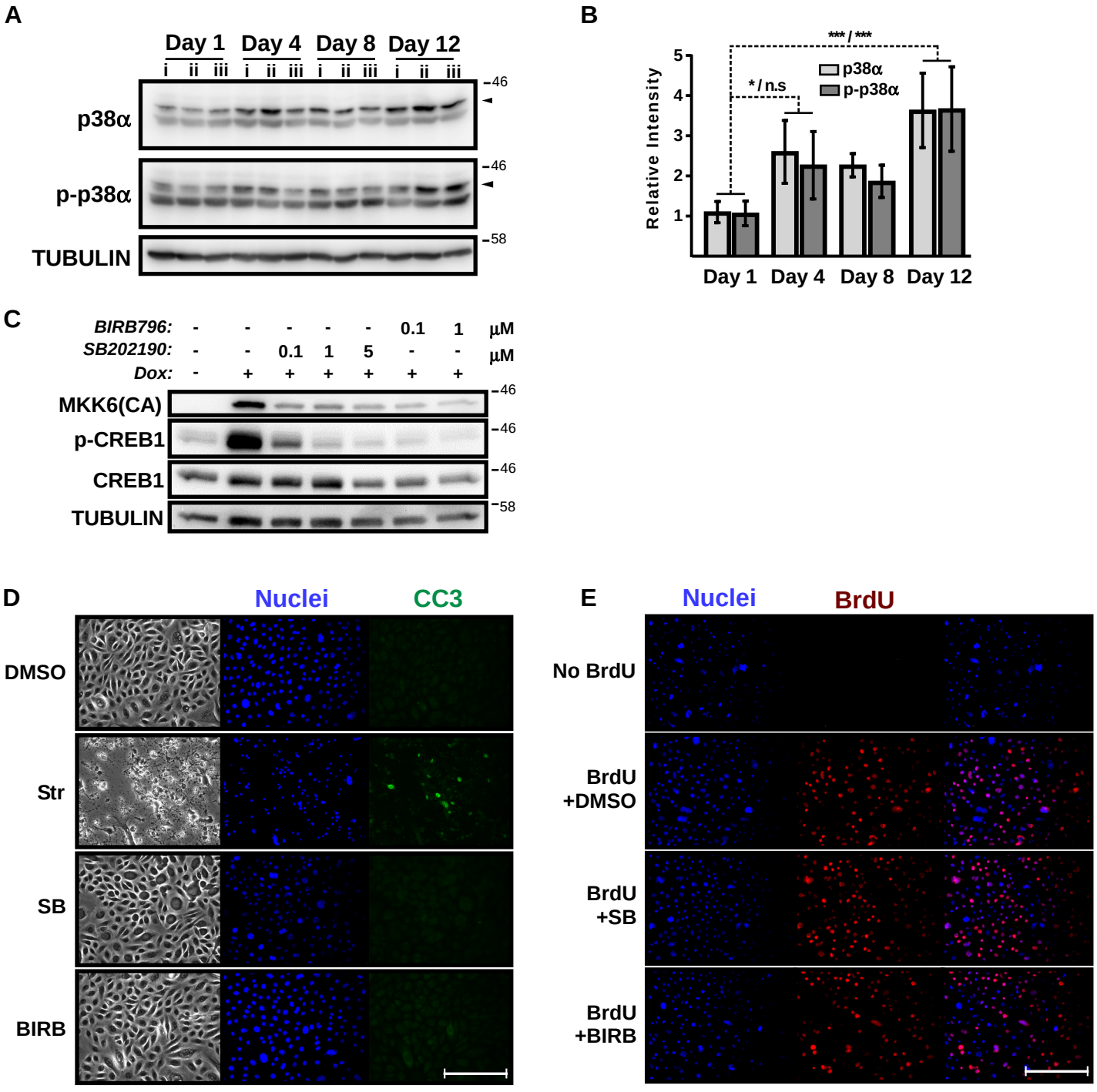

Figure S1: p38-MAPK induction and inhibition. (A) iPrECs were differentiated and lysates harvested in biologic triplicates (i,ii,iii) at different days during differentiation for immunoblotting. Arrows: p38α- and p-p38α-specific bands. **(B)** Quantification of (A). Data were first normalized to TUBULIN, then to Day 1 'i' samples and plotted as mean±sd. p-values were determined by paired one way ANOVA with Turkey's multiple testing correction. *** = p<0.001, * = p<0.05, n.s = not significant (p>0.05). Left p-value is for p38α / right is for p-p38α. **(C)** iPrEC-TetON-MKK6(CA) cells were treated with Dox for 6 h in the presence of increasing concentrations of p38-MAPK inhibitors SB202190 or BIRB796. Levels of total CREB, activated CREB (p-CREB), and TUBULIN protein were analyzed by immunoblotting. **(D)** iPrECs were grown to confluence and treated 24 h with DMSO (control), 200 nM Staurosporine (Str), 1 µM SB202190, or 0.1 µM BIRB796. Cells were immunostained for cleaved caspase 3 (CC3; green) to mark apoptotic cells. **(E)** iPrECs were differentiated 4 days, then treated 24 h with 10 mM BrdU plus p38 inhibitors (as in (D)) to measure proliferation. Scale bar = 200 µm.

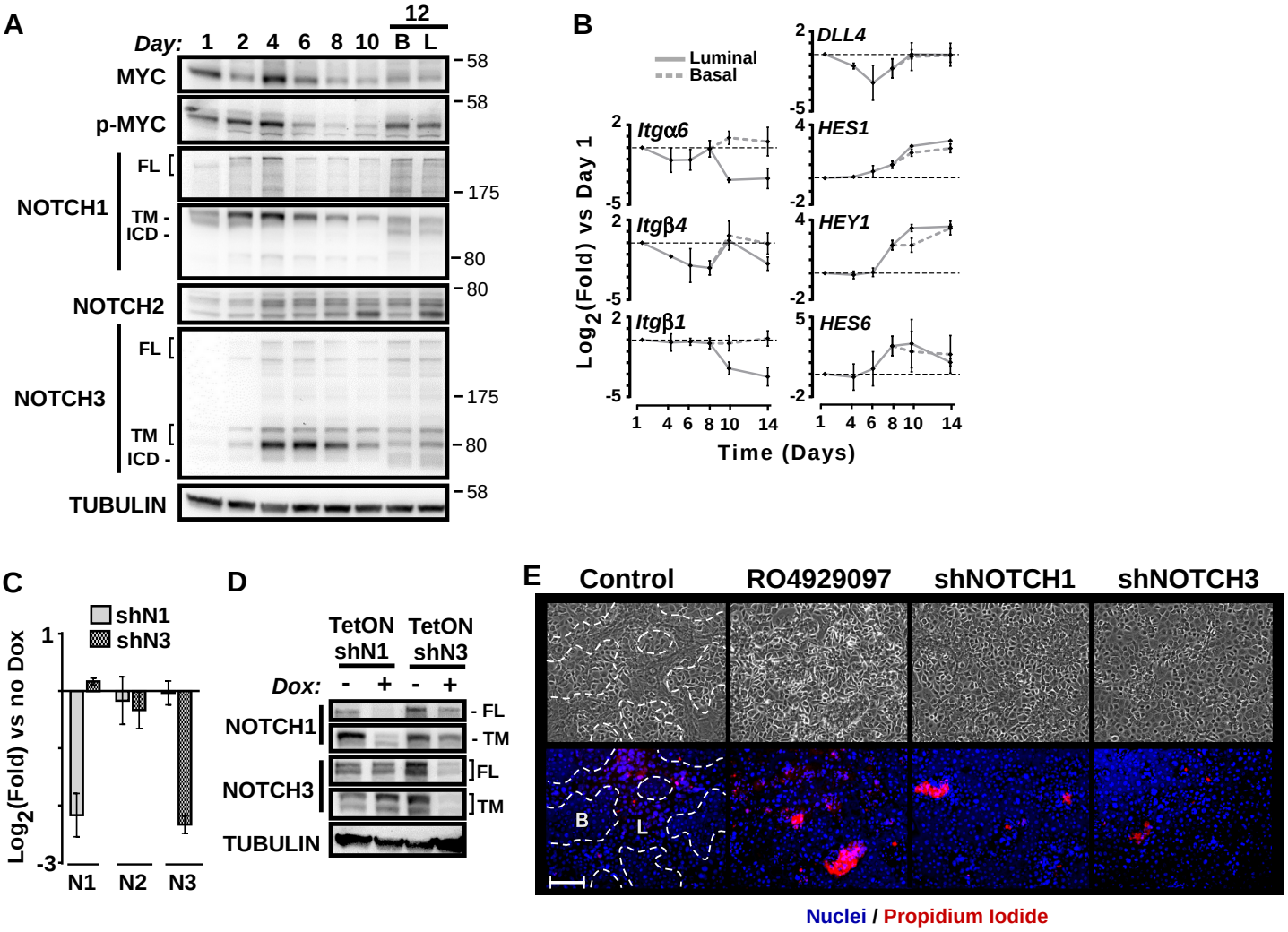

Figure S2: NOTCH induction. (A) Primary PrECs were differentiated for 1-12 days and lysates collected at various times to assess protein expression by immunoblotting. Antibody notes: p-MYC recognizes phosphorylated T58/S62. NOTCH2 is ICD-specific. NOTCH1/3 recognize full length (FL), transmembrane (TM), and intracellular domain (ICD). **(B)** RNA was collected from iPrECs differentiated for the indicated days and indicated genes analyzed by qRT-PCR. Luminal (L, solid line) cells were separated from basal (B, dashed line) cells at days 10 and 14. Graph shows mean±s.d. of biological triplicates. Data were normalized to day 1. **(C)** iPrEC pools expressing TetON shNOTCH1 (shN1) or shNOTCH3 (shN3) were treated 48 h ±Dox and analyzed by qRT-PCR for expression of NOTCH1, NOTCH2, and NOTCH3 mRNA. Data were standardized to 18S and RPL19 and normalized to -Dox. Graph shows mean±s.d. of biological triplicates. **(D)** NOTCH protein knockdown was validated by immunoblotting of cells treated with Dox and differentiated for 4 days. **(E)** iPrECs were differentiated for 16 days in the presence of DMSO+Dox (Control), 1 µM RO4929097 (gamma secretase inhibitor), or Dox on shRNA lines. Top row: phase contrast microscopy. Bottom row: merged epifluorescence images of Hoescht-stained nuclei (blue) and propidium iodide-permeable dead cells (red). Luminal layer (L) is outlined (dashed line) on top of basal (B) cells. Scale bar = 200 µm.

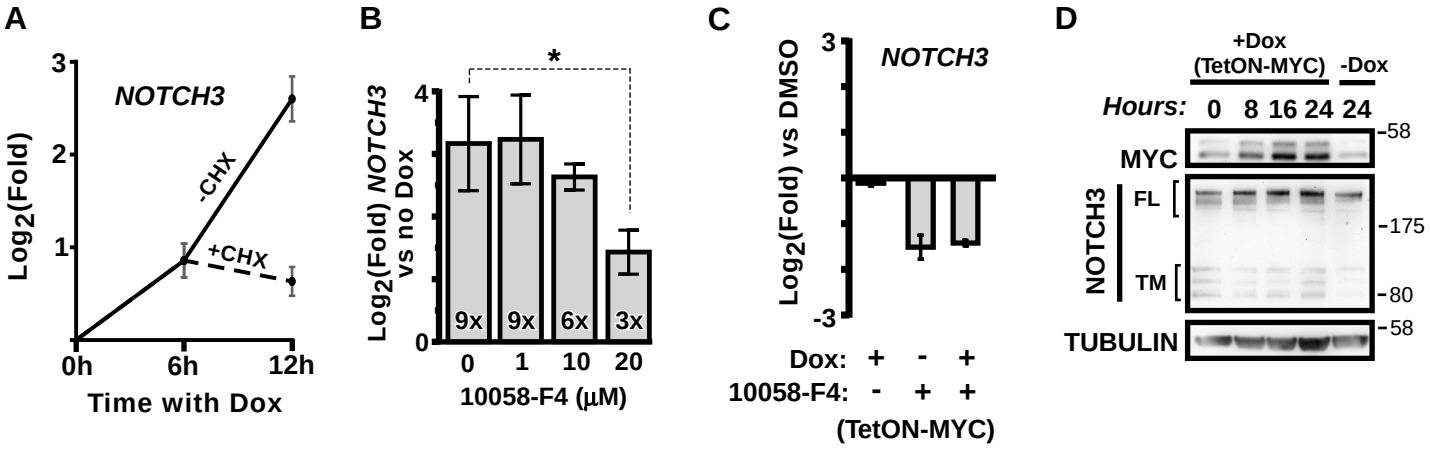

Figure S3: MYC is required but not sufficient for full NOTCH3 induction. (A) iPrEC-TetON-MKK6(CA) cells were treated with Dox ±Cyclohexamide (CHX) for 12 h. NOTCH3 mRNA was measured by qRT-PCR at 6 or 12 h. Samples were normalized to 0 h. Graph shows mean±s.d. of biological triplicates. **(B)** iPrEC-TetON-MKK6(CA) cells were treated with Dox for 16 h in the presence of DMSO or varying amounts of the MYC inhibitor 10058-F4. NOTCH3 mRNA was measured by qRT-PCR. Data were standardized to 18S and RPL19 and normalized to -Dox control. Graph shows mean±s.d. of biological triplicates. Text within bars is rounded fold change. **(C)** Basal, undifferentiated iPrEC-TetON-MYC cells were treated with DMSO, Dox, or 10058-F4 (10 μM) for 8 h and NOTCH3 mRNA was measured by qRT-PCR. Data were standardized to 18S and RPL19 and normalized to untreated controls (DMSO). Graph shows mean±s.d. of biological triplicates. **(D)** iPrEC-TetON-MYC cells were differentiated five days then treated with Dox for up to 24 h. MYC, NOTCH3, and TUBULIN levels were analyzed by immunoblotting. FL=full length, TM=trans-membrane.

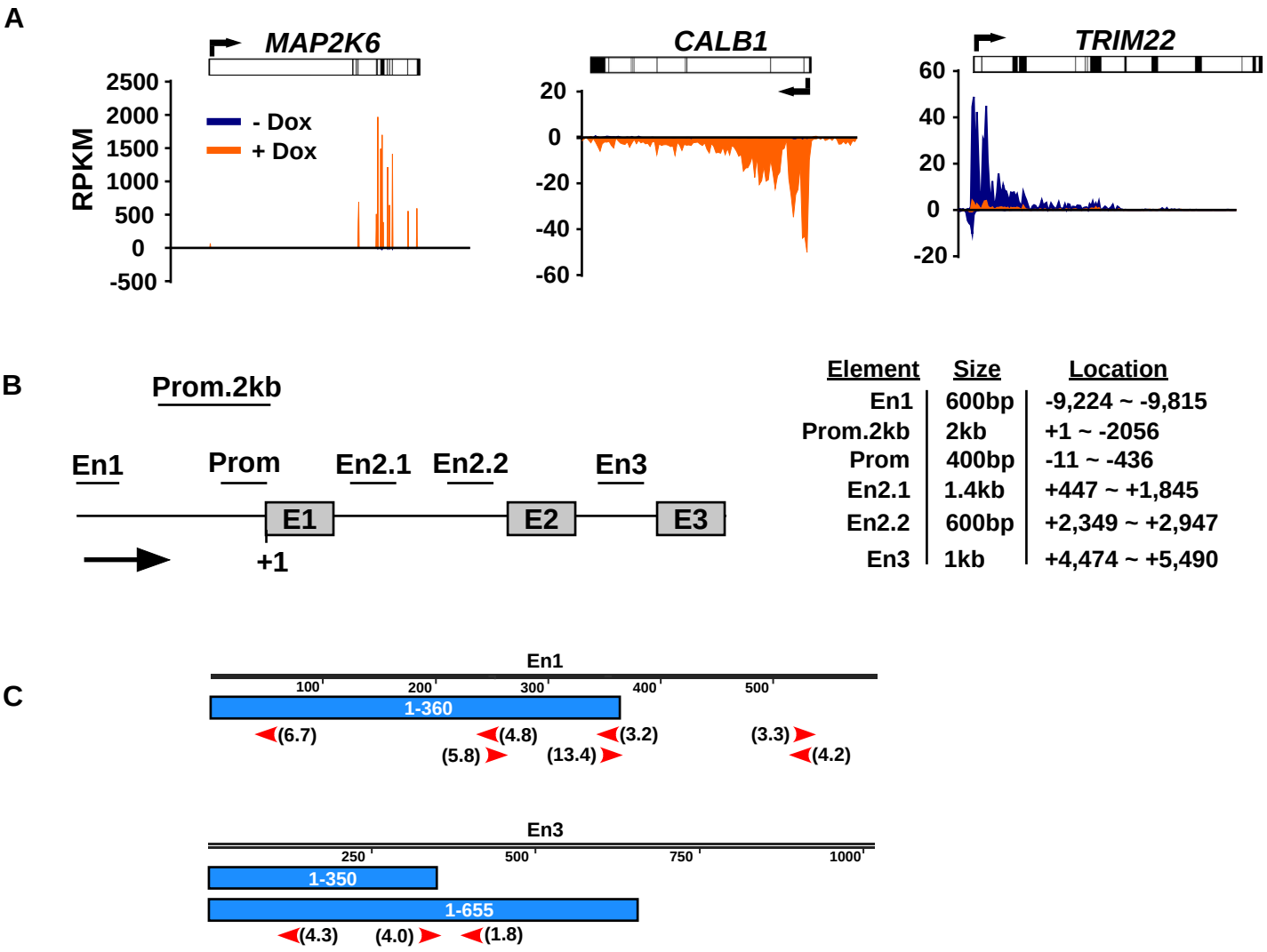

Element	Size	Location
En1	600bp	-9,224 ~ -9,815
Prom.2kb	2kb	+1 ~ -2056
Prom	400bp	-11 ~ -436
En2.1	1.4kb	+447 ~ +1,845
En2.2	600bp	+2,349 ~ +2,947
En3	1kb	+4,474 ~ +5,490

Figure S4: BruUV-Seq and NOTCH3 promoter elements. (A) BruUV-Seq controls. iPrEC-TetON-MKK6(CA) cells were treated with Dox for 10 h and processed for BruUV-Seq. Y-axis is RPKM (reads per kilobase of transcript per million mapped reads). Plus strand reads are above the x-axis, minus strand reads are below the x-axis. Blue = -Dox; Orange = +Dox. Gene diagram shows orientation (arrow) and exons (black lines). **B)** Diagram (not to scale) of the first three exons of NOTCH3 and regions cloned for reporter assays are highlighted. Note: NOTCH3 is on the minus strand but is depicted here in 5'>3' orientation. The table indicates the approximate size of the cloned regions and their location in relation to the NOTCH3 start codon (ATG = +1). **(C)** Maps of En1 and En3 elements (in 5'>3' orientation) with the deleted regions (blue) plus predicted MYC binding sites and orientation (red arrows). Numbers in parenthesis indicate predicted binding score from JASPAR (http://jaspar.genereg.net/) with a threshold of 80% using the MA0147.2 matrix model for MYC binding sites.

Table S1. shRNA information

Target Gene	Target[1] bp	Source[2]		Sequence (sense_loop_antisense)[3]
p38α	1971	TRCN0000196472	5'	GTACTTCCTGTGTACTCTTTA_AACTAGTGA _TAAAGAGTACACAGGAAGTAC
p38δ	993	TRCN0000197043	5'	GAAACTCACAGTGGATGAATG_TACTAGT _CATTCATCCACTGTGAGTTTC
NOTCH1	6258	TRCN0000350330	5'	CCGGGACATCACGGATCATAT_ACTAGT _ATATGATCCGTGATGTCCCGG
NOTCH3	1958	TRCN0000363316	5'	TTTGTAACGTGGAGATCAATG_TACTAGT _CATTGATCTCCACGTTACAAA

[1]Target bp is the first base targeted by the shRNA based on cDNA sequence. [2]Source includes BROAD RNAi Consortium ID used for target sequences. [3]All shRNAs were cloned into the Tet-pLKO-Puro vector and included a terminator sequence (TTTTT).

Table S2. Antibody information

Target	Species	Mono/Poly-clonal	Company	Product no.	Lot no.	Dilution for WB	Dilution for IF	Additional Info
AR	Rabbit	Poly	Santa Cruz	sc-815	B1513		200	
AR	Mouse	Mono	Santa Cruz	sc-7305			800	
BrdU	Mouse	Mono	BD	555627			500	
cleaved-Caspase 3	Rabbit	Mono	CST	9664			400	
CREB1	Rabbit	Mono	CST	4820	3	1,000		
p-CREB1	Rabbit	Mono	CST	9198	10	1,000		pSer133
GAPDH	Mouse	Mono	Millipore	CB1001	NG1780785	10,000		
ITGA6	Rat	Mono	BD	555734	4353644		200	
MYC	Rabbit	Poly	Millipore	06-340	DAM1770290	1,000		
MYC	Mouse	Mono	Santa Cruz	sc-40	G310	1,000		Used for myc-tag
p-MYC	Rabbit	Mono	Millipore	04-217	2433275	5,000		pThr58/pSer62
NOTCH1	Rabbit	Mono	CST	3608	3	1,000		
NOTCH2	Rabbit	Poly	Millipore	07-1234	NG1853763	500		ICD-specific
NOTCH3	Rabbit	Mono	CST	5276	2	1,000		
NOTCH3	Rabbit	Poly	Santa Cruz	sc-5593			400	
p38α	Rabbit	Poly	CST	9218	5	2,000		
p-p38	Mouse	Mono	Millipore	MABS64			400	all isoforms
p-p38α	Rabbit	Mono	Epitomics	1229-1	YH080601C	2,000		pThr180/pTyr182
p38δ	Mouse	Mono	Santa Cruz	sc-136063	G0209	1,000		
TUBULIN	Mouse	Mono	Sigma	T9026	093K4880	10,000		

Table S3. qRT-PCR Primer sequences and source if not self-designed

Gene			Sequence	Source
18S	Fwd	5'	CCGCAGCTAGGAATAATGGA	
	Rev	5'	CGGTCCAAGAATTTCACCTC	
ACTB	Fwd	5'	CCCTCCATCGTGGGGC	
	Rev	5'	GACGATGCCGTGCTCGATG	
DLL3	Fwd	5'	GGCGGCTTGTGTGTCGGG	
	Rev	5'	GCAGTCGTCCAGGTCGTGC	
DLL4	Fwd	5'	AGGCCTGTTTTGTGACCAAG	PMID:
	Rev	5'	CTCCAGCTCACAGTCCACAC	22002304
GAPDH	Fwd	5'	GATCATCAGCAATGCCTCCTGC	
	Rev	5'	CTTCTGGGTGGCAGTGATGGC	
HES1	Fwd	5'	AATGACAGTGAAGCACCTCCG	
	Rev	5'	ATGCACTCGCTGAAGCCG	
HES6	Fwd	5'	GAGGACGGCTGGGAGACG	
	Rev	5'	TCGCTCGCTTCCGCCTGC	
HEY1	Fwd	5'	AGAGTGCGGACGAGAATGGAAACT	PMID:
	Rev	5'	CGTCGGCGCTTCTCAATTATTCCT	18663143
HEY2	Fwd	5'	AAGATGCTTCAGGCAACAGGG	
	Rev	5'	GGATCCGAGGAGTCCAGGC	
HEYL	Fwd	5'	CAGGATTCTTTGATGCCCGAG	PMID:
	Rev	5'	GACAGGGCTGGGCACTCTTC	21834989
ITGA6	Fwd	5'	GCTGGTTATAATCCTTCAATATCAATTGT	PMID:
	Rev	5'	TTGGGCTCAGAACCTTGGTTT	20048343
ITGB1	Fwd	5'	CTGGCAAATTCTGCGAGTGTG	
	Rev	5'	CACTCACACACACGACACTTGC	
ITGB4	Fwd	5'	AACGGCGGTGAGCTGCATC	
	Rev	5'	GAGTGCTCAAAGTGAAGGCGG	
JAG1	Fwd	5'	ATAAGTGCATCCCACACCCG	
	Rev	5'	AGACACGGCTGATGAGTCCC	
LUC	Fwd	5'	GGCCTGACAGAAACAACCAGCG	
	Rev	5'	GGACGCACAGCTCGCCGC	
MYC	Fwd	5'	TTCGGGTAGTGGAAAACCAG	Integrated DNA
	Rev	5'	AGTAGAAATACGGCTGCACC	Technologies
NOTCH1	Fwd	5'	CGCAGATGCCAACATCCAGG	
	Rev	5'	CCCAGGTCATCTACGGCGTTG	
NOTCH3	Fwd	5'	CGTGGCTTCTTTCTACTGTGC	
	Rev	5'	CGTTCACCGGATTTGTGTCAC	
RPL19	Fwd	5'	CGGCTGCTCAGAAGATACCG	
	Rev	5'	TTGTCTGCCTTCAGCTTGTGG	

TableS4. Enhancer element PCR cloning and mutagenesis primers

Element			Flank_Restriction Enzyme_Target
Prom.2kb	Fwd	5'	ATTAT_CTCGAG_CCGGCCCCATGGCGGCC
(2kb)	Rev	5'	ATAAT_GCTAGC_GATACAGGGCTGGAGCCTTAGCC
Prom	Fwd	5'	ATTAT_AAGCTT_TGGGTCCATGAGCCTCTCAGG
(400bp)	Rev	5'	ATTAT_AAGCTT_TCCCTCCTTCCCTGGGC
En1	Fwd	5'	ATTAT_GGTACC_CTGGGTGTCTCAGGCAGAGGG
(600bp)	Rev	5'	ATTAT_GGTACC_GCCTAGAGTTCGAGACCAGCC
En2.1	Fwd	5'	ATTAT_AGATCT_CGCCTGGAGTCCTGGG
(1.4kb)	Rev	5'	ATTAT_AGATCT_CCTGTGGGTGTTCGTGA
En2.2	Fwd	5'	ATTAT_GCTAGC_GCTGGTCTCGAACTCCTGACC
(600bp)	Rev	5'	ATTAT_GCTAGC_TTCAGGGGTAATAGAAGGG
En3	Fwd	5'	ATTAT_CTCGAG_TCTCCCACTCGGGCTCACC
(1kb)	Rev	5'	ATTAT_CTCGAG_CCAGAGAGTCCAAGCTCCGCC
En1Δ1-360		5'	CCTAACTGGCCGGTACCGTCACTGAGACCCAGG
En3Δ1-350		5'	GCTCGCTAGCCTCGAGACGGTCTCAAATACTC
En3Δ1-655		5’	GAGCTCGCTAGCCTCGAGCCTGCCTGGCGGTGGGACC
miniTK		5'	TTCGCATATTAAGGTGACGCGTGTGGCCTCGAACACCGA GCGACCCTGCAGCGACCCGCTTAA